Title
Lysozyme resistance of Listeria monocytogenes

Author
BURKE, THOMAS PATRICK

Publication Date
2015

Peer reviewed|Thesis/dissertation

Lysozyme resistance of *Listeria monocytogenes*

by

Thomas Patrick Burke II

A dissertation submitted in partial satisfaction of the

requirements for the degree of

Doctor of Philosophy

in

Molecular and Cell Biology

in the

Graduate Division

of the

University of California, Berkeley

Committee in Charge:

Professor Daniel A. Portnoy, Chair
Professor Laurent Coscoy
Professor Kathleen Ryan
Professor Russell Vance

Spring 2015

ABSTRACT

Lysozyme resistance of *Listeria monocytogenes*

by

Thomas Patrick Burke II

Doctor of Philosophy in Molecular and Cell Biology

University of California, Berkeley

Professor Daniel A. Portnoy, Chair

Bacterial pathogens must survive exposure to antibacterial molecules of the innate immune system in order to successfully establish infection. Such is the case with *Listeria monocytogenes*, a Gram-positive bacterial pathogen that is the causative agent of listeriosis, a deadly foodborne disease dangerous to pregnant women and immunocompromised individuals. *L. monocytogenes* is highly resistant to antibacterial molecules of the innate immune system such as lysozyme, a potent cell wall-degrading enzyme found throughout the body of all animals. Nearly 100 years ago, Alexander Fleming discovered lysozyme and observed that pathogenic bacteria were lysozyme-resistant, while non-pathogens were lysozyme-sensitive. Curiously, non-pathogenic lysozyme-sensitive bacteria encode the same cell wall enzymes as pathogenic lysozyme-resistant bacteria. It therefore remained unclear what distinguished pathogens from non-pathogens in regards to lysozyme resistance. In this work, a forward genetic screen was performed to identify additional factors required for lysozyme resistance in *L. monocytogenes* and subsequent investigations were made to uncover how these molecules regulated one another.

The screen for lysozyme-sensitive mutants identified a number of cell wall-related enzymes, such as the peptidoglycan deacetylase *pgdA*; however no enzymes were identified that were unique to *L. monocytogenes*. Rather, the screen identified two regulators of gene expression, the non-coding RNA Rli31 and the transcription factor DegU, which upregulated expression of cell wall-modifying enzymes. Mutants of *rli31* and *degU* were similarly sensitive to lysozyme as mutants of *pgdA*, suggesting that the regulators were absolutely required for lysozyme resistance. These data suggested that high lysozyme resistance of *L. monocytogenes* was not due to the acquisition of novel cell wall-modifying enzymes, but was due to upregulation of cell wall enzymes that were distributed among both pathogenic and non-pathogenic bacteria. This logic provides an alternative example of how virulence phenotypes are acquired by bacteria, many of which originate via horizontal gene transfer. We propose that pathogen-specific regulation of broadly distributed genes represents another mechanism by which pathogens acquire virulence.

Non-coding RNAs are an increasingly appreciated class of gene regulators in bacteria, with over 200 non-coding RNAs having been identified to date in *L. monocytogenes*. The mechanism of Rli31 function was investigated and multiple lines of evidence suggested that the

uncharacterized protein SpoVG was as an intimately related, opposing regulator to Rli31. Neither Rli31 nor SpoVG was epistatic with any of the fourteen lysozyme-sensitive mutants, and the data suggested that Rli31 and SpoVG both regulated an unknown lysozyme-resistance gene. The cell wall morphology of the *spoVG* mutant suggested that this unknown gene may be required for producing extracellular polysaccharide. Separately from the lysozyme-resistance phenotypes of these mutants, Rli31 inhibited expression of the carbohydrate import protein Lmo0901, while SpoVG was independently required for Lmo0901 expression. The 5' UTR of SpoVG contained 14/14 nucleotides of perfect complementarity to Rli31, yet Rli31 did not regulate SpoVG mRNA nor protein abundance. This suggested that the SpoVG mRNA may function as an Rli31 decoy target that regulates its activity. In summary, these data described a complex model whereby Rli31 and SpoVG independently and oppositely regulate multiple target genes, but may also regulate one another.

Attempts were made to better characterize SpoVG, whose function remained unclear. SpoVG was required for swarming motility of *L. monocytogenes*, and suppressor mutations of this phenotype mapped to RNAse J1, Rho, and NusG. SpoVG was then described as an RNA-binding protein that interacted with multiple sRNAs *in vitro* but did not bind RNAs with known protein-binding partners such as SRP RNA. Together, these results suggested that SpoVG is a pleiotropic RNA-binding protein that interacts closely with sRNAs, and we propose that SpoVG is similar in function to the well-described RNA chaperone Hfq in Gram-negative bacteria.

In conclusion, this study described the genes required for lysozyme resistance of *L. monocytogenes*, and identified a complex regulatory mechanism required for their expression. From these data, we determined that high lysozyme resistance in pathogens is due to upregulation of common cell wall enzymes. We conclude that the non-coding RNA Rli31 and the RNA binding protein SpoVG are important regulators of lysozyme resistance genes in *L. monocytogenes*. Together, this study provides a comprehensive examination of lysozyme resistance genes in a bacterial pathogen.

Each living creature must be looked upon as a microcosm −
a little universe −formed of a host of self-propagating
organisms, inconceivably minute and
as numerous as the stars of heaven.
Charles Darwin

Dedication

Any laughter that I may enjoy during life
is owed to my father

Any smiles I might share
are shared with Christina

Any competition that I may win
is owed to my sisters

And all of these things
are owed to my mother
to whom I owe everything

Table of Contents

Chapter 1: An introduction to *Listeria monocytogenes* **1**
1.1 *Listeria monocytogenes*, a deadly foodborne pathogen..... 2
1.2 Molecular determinants of infection and the pathogenicity island..... 3
1.3 The cell wall and resistance to lysozyme..... 5
1.4 Small non-coding RNAs, emerging gene regulators in bacteria..... 7
1.5 SpoVG..... 8
1.6 Carbohydrate metabolism in bacteria..... 8

Chapter 2: *Listeria monocytogenes* is resistant to lysozyme through the regulation, not the acquisition, of cell wall-modifying enzymes..... **10**
2.1 Summary of results and introduction..... 11
2.2 Results
2.2.1 A screen for lysozyme-sensitive mutants..... 12
2.2.2 Characterization of the *rli31* mutant phenotype..... 19
2.2.3 How lysozyme-sensitive bacteria are killed during infection..... 24
2.3 Discussion..... 27

Chapter 3: Rli31 and SpoVG are opposing regulators of gene expression..... **32**
3.1 Introduction and summary of results..... 33
3.2 Results
3.2.1 Suppressor mutations that increase lysozyme resistance..... 34
3.2.2 Deletion of *spoVG* increases lysozyme resistance..... 40
3.2.3 Characterization of the *spoVG* mutant cell wall..... 41
3.2.4 Rli31 and SpoVG regulate expression of Lmo0901..... 46
3.3 Discussion..... 48

Chapter 4: SpoVG is an RNA binding protein required for expression of flagellin.... **55**
4.1 Summary of results and introduction..... 56
4.2 Results
4.2.1 *spoVG* mutants are non-motile in soft agar..... 57
4.2.2 Suppressor mutations increase swarming of Δ*spoVG*..... 59
4.2.3 SpoVG is an RNA binding protein..... 62
4.2.4 Post-translational modifications of SpoVG..... 63
4.3 Discussion..... 66

Chapter 5: Concluding remarks and future perspectives..... **70**
5.1 Summary of results and conclusions..... 71
5.2 Remaining questions and future directions..... 71
5.3 Speculation into the future..... 72

Materials and Methods..... **75**
References..... **79**

List of Figures

Chapter 1

Figure 1.1: The intracellular lifecycle of *L. monocytogenes*……..... 4
Figure 1.2: Sir Alexander Fleming……..... 5

Chapter 2

Figure 2.1: A forward-genetic screen for lysozyme-sensitive mutants……. 13
Figure 2.2: Growth in liquid media of lysozyme-sensitive mutants……14
Figure 2.3: Treatment of lysozyme-sensitive strains with CRAMP and antibiotics…… 16
Figure 2.4: Treatment of lysozyme-sensitive strains with other CAMPs……17
Figure 2.5: Rli31 is highly abundant and expressed at all growth phases……..... 18
Figure 2.6: Characterization of the *rli31* mutant phenotype……20
Figure 2.7: Downregulation of *pgdA* and *pbpX* in the *rli31* mutant.....….. 22
Figure 2.8: DegU and Rli31 do not regulate one another…….....23
Figure 2.9: The Δ*rli31* phenotype is additive with Δ*pgdA* and Δ*oatA in vivo*……..... 24
Figure 2.10: Serum kills lysozyme-sensitive *L. monocytogenes*…….. 25
Figure 2.11: Examining the *in vivo* defect of lysozyme-sensitive bacteria……..... 26
Figure 2.12: Addition of lysozyme to bentonite-treated blood restores killing …….....27

Chapter 3

Figure 3.1: Secondary structure of Rli31…….....35
Figure 3.2: Characterization of variants that increase lysozyme resistance……. 39
Figure 3.3: Deletion of *spoVG* increases lysozyme resistance …….....41
Figure 3.4: Characterization of the Δ*spoVG* cell wall…….…. 43
Figure 3.5: Deletion of *rli31* does not affect mRNA nor protein abundance of *spoVG* ….. 45
Figure 3.6: Lmo0901 is regulated by Rli31 and SpoVG…….....47
Figure 3.7: A model for SpoVG and Rli31 mediated gene regulation……. 48

Chapter 4

Figure 4.1: *spoVG* mutant bacteria are non-motile in semisolid agar……...58
Figure 4.2: Swarming mutations do not alter the lysozyme resistance phenotype……..... 60
Figure 4.3: SpoVG binds weakly and non-specifically to single-stranded DNA ……..... 61
Figure 4.4: SpoVG interacts with RNA *in vitro*…….....63
Figure 4.5: Purification of SpoVG and identification of post-translational modifications.. 64
Figure 4.6: Two positively-charged grooves in the SpoVG dimer……...65

List of Tables

Chapter 2

2.1: Lysozyme-sensitive mutants identified in *L. monocytogenes*……..... 14
2.2: Cell wall analysis of the *rli31* mutant……....19
2.3: Variants identified in *rli31* mutant suppressor strains…….. 21
2.4: List of strains used in Chapter 2……..... 30
2.5: List of DNA oligonucleotides used in Chapter 2……...31

Chapter 3

3.1: Variants identified by whole-genome sequencing of lysozyme-resistant strains….....37
3.2: Predicted targets of Rli31…….. 38
3.3: Strains used in Chapter 3……... 51
3.4: Oligonucleotides used in Chapter 3……...53

Chapter 4

4.1: Variants identified in Δ*spoVG* swarming suppressors..... 59
4.2: Strains used in Chapter 4……... 68
4.3: Oligonucleotides used in Chapter 4……...68

Acknowledgements

Dan, I've truly enjoyed my time in your lab and will miss our scientific conversations together. Thank you for your fairness, your professionalism, and your curiosity. I'm grateful to have spent the past six years training under you (insert joke here) and will miss the humor that you bring to the lab. I have learned an incredible amount of science and we have made some exciting discoveries together. Your sincere passion for science is truly something to strive for.

To those who originally got me interested in doing research, Brody and Roger, I'll always be indebted to you for the opportunities that you provided me. I was so fortunate to have landed in your lab and had such a positive experience, it literally changed my life. As Roger said at the Gordon, "Dan, if Thomas goes on to do great things, I get the credit for originally training him." I hope that Brody and I can return to Bloomington for a pontoon boat party (no habañeros).

To JD, thank you, sincerely, for believing in me and for being such a badass mentor to me in the lab. I learned so much from your leadership, your dedication, and your charisma. I miss putting the projector on your bench before you arrived to lab. Josh, thanks for imparting so much wisdom on me, baymates forever (emphasis on the mates). To JD, Josh, Ben, and Matthieu, I wish we could go back to 2011 and party on Matt's roof again. I'm grateful for your friendship and will always remember the era when we made the Portnoy lab the best lab on Earth.

Jon, thanks for making lab a fun place and for providing so many jokes, even if some weren't worth any points, it was a morale booster. Go A's. To the remaining Portnoy lab members, I'm thankful for your scientific input and for making the lab such a fun place – Jason, Anastasia, Aaron, Bret, Chen, Paul, Regina, Susy, Michelle, Gabe, Rich, Qiongying, Kristy, Chelsea, Eric, Brittney, and Julia. Carry on the traditions, and always make sure there are enough ping-pong balls around for bxxr ball. To C-Rae, cheers, lysozyme-bros forever.

I would like to thank our collaborators at UC Berkeley, principally Dr. Tony Iavarone at the QB3 Mass Spectrometry Facility and Dr. Kent McDonald at the Electron Microscope Lab for their timely collaborations, helpful insights, and friendliness. Thank you, Dr. Linc Sonenshein for your generous gift of the SpoVG antibody. I was grateful for advice on EMSAs from members of the Collins lab, including George Katibah, Heather Upton, Alex Wu, and Brian Farley.

Russell, it was always a pleasure to work with you. Thank you for your support throughout my graduate career and for being so easy to communicate with. You may not know it, but there is a term floated around MCB called, "Being a Russell." It means being a superstar and just being awesome in general. I'm lucky to have firsthand experience of what Being a Russell is all about.

Laurent and Kathleen, thank you for your input over the years and for your scientific expertise. I've enjoyed all my meetings with you and am thankful for your input, curiosity, wisdom, and for critical reading of our manuscript.

Chapter 1

An introduction to *Listeria monocytogenes*

1.1 *Listeria monocytogenes,* a deadly foodborne pathogen

Listeria monocytogenes is a Gram-positive bacterial pathogen that is found ubiquitously in the environment and can cause deadly disease in humans upon ingestion. The organism lives as a saprophyte on decomposing plant matter, but can be found in soil, environmental water sources, and animal feces (1, 2). *L. monocytogenes* can infect a plethora of vertebrates via oral ingestion, including wild birds, deer, aquatic animals, and domesticated cattle, where it proliferates in the organism before being shed in feces back into the earth (3, 4). This cycle allows for the bacterium's persistence in the environment, and subsequently contributes to its prevalence in human food sources and food processing plants (5). Removal of the bacterium from food processing plants is complicated by its ability to grow at low temperatures, survive high concentrations of salt, and resist killing by disinfectants (5). Transmission to humans often occurs through food products that do not require cooking, such as soft cheese, and the pathogen is found in approximately 4% of raw milk (6). *L. monocytogenes* can also be found in a variety of other human food products including fruits, salads, sausages, and smoked fish (7, 8). Over 500 deaths are reported in the United States per year due to listeriosis, and the economic impact of the pathogen is estimated at over 2.5 billion dollars per year (9, 10).

Healthy individuals can normally clear infection by *L. monocytogenes*, while immunocompromised individuals may contract listeriosis. Listeriosis imposes a 20-30% mortality rate in humans, making it one of the most deadly bacterial diseases (8). The normal route of *L. monocytogenes* infection occurs after ingestion of high numbers of bacteria, many of which are eliminated upon entry to the acidic stomach (11). The bacteria then traverse the small intestine, where they invade the intestinal epithelium. M-cells and goblet cells are implicated as the initial entry sites of *L. monocytogenes*, after which the bacteria escape into the blood and the mesenteric lymph nodes (12-14). Upon entry into the blood, *L. monocytogenes* travels to the liver and spleen, where it can efficiently replicate and infect the gallbladder (15). If uncontrolled, the pathogen will infect other organs, reseed the intestine, and cause systemic infection. High numbers of bacteria in the blood can lead to eventual entry to the brain, causing meningitis and eventual death of the infected individual (8). *L. monocytogenes* is able to cross both the blood-brain barrier as well as the placental barrier, which leads to miscarriage of the fetus and makes pregnant women a high risk group for *L. monocytogenes* infection (8).

The immune response to *L. monocytogenes* infection

The early stages of *L. monocytogenes* infection result in robust expression of the cytokine IFN-β (16). The majority of IFN- β is produced upon detection of the pathogen associated molecular pattern (PAMP) cyclic diadenosine monophosphate (c-di-AMP) (17-19). This molecule is bound directly by the host adaptor protein STING, which then signals through the kinase TBK1 and the transcription factor IRF3 to produce IFN-β (20-22). Apart from c-di-AMP, a small amount of IFN- β is likely due to infrequent bacteriolysis in the cytosol, which can stimulate both IFN-β production and cell death (23). Bacteriolysis releases DNA into the host cytosol that is detected by a DNA sensor, cGAS, which then activates STING through the production of another cyclic dinucleotide, c-GMP-AMP (24). Bacteriolysis also activates formation of the Aim2 inflammasome, a large multi-protein complex that detects bacterial-derived ligands and activates pro-inflammatory proteases named caspases (23, 25-27). Caspase activation leads to processing of the pro-inflammatory cytokines IL-1β and IL-18 and activates a specialized form of inflammatory cell death termed pyroptosis (28-31). *L. monocytogenes*

mutants with weakened cell walls undergo increased bacteriolysis in the host cytosol and robustly activate pyroptosis, resulting in attenuation *in vivo* (23, 32).

Clearance of *L. monocytogenes* from infected mice occurs approximately 5 days postinfection, which is due to INF-γ activated macrophages and an acquired immune response characterized by an abundance of cytotoxic $CD8^+$ T-cells (33). Antigen-specific effector and long-lived $CD8^+$ T-cells play a major role in clearing infected cells and in protecting the organism from future challenge of *L. monocytogenes* (8, 33, 34). Genetic manipulability and the robust induction of $CD8^+$ T-cells makes *L. monocytogenes* a useful tool to induce host immune responses, and attenuated strains are being developed for use as anti-cancer therapies in humans (35).

1.2 Molecular determinants of infection and the pathogenicity island

The cellular infectious lifecycle of *L. monocytogenes* is well understood. The bacteria are able to infect a variety of cell types, including phagocytic cells such as macrophages and dendritic cells, and non-phagocytic cells such as hepatocytes and epithelial cells (8). Upon entry into the phagosome, expression of the pore-forming toxin Listeriolysin O (LLO) allows *L. monocytogenes* to escape to the cytosol (36-40). LLO belongs to the family of cholesterol dependent thiol-activated cytolysins and uses host cholesterol as a receptor for membrane docking (41). Upon membrane binding, LLO monomers oligomerize into large ring-shaped structures that then undergo a conformational change resulting in pore formation (42, 43). Pores measure approximately 30-50 nm in diameter, allowing the pathogen to escape into the cytosol by a mechanism that remains to be fully elucidated (44). LLO is sufficient for *L. monocytogenes* escape to the cytosol and expression of LLO in the non-pathogen *B. subtilis* allowed for escape to the cytosol of certain cell types (45). LLO is a primary virulence factor for *L. monocytogenes* pathogenesis and is completely required for virulence. *hly* mutants are over 10^5 fold attenuated upon *in vivo* infection of mice compared to Wt bacteria, and fail to induce protective immunity (46, 47).

Upon entry to the cytosol, *L. monocytogenes* expresses the protein ActA, which is necessary and sufficient for actin-based motility of the bacterium (48-50). ActA functions as a mimic of host WASP, which activates the Arp2/3 complex to polymerize actin (51, 52). Actin polymerization results in propulsion of the bacterium through the cytosol, forming "comet tails" of host actin (Figure 1.1)(53). Importantly, actin-based motility allows *L. monocytogenes* to spread from cell-to-cell without abandoning the sanctuary of the host cytosol. Propulsion of the bacterium into the plasma membrane forms pseudopods that extend into neighboring cells, resulting in the formation of a double-membrane (53). *L. monocytogenes* then escapes this vacuole using LLO, is released into the cytosol of the nearby cell, and the cell-to-cell spreading process is reinitiated (53).

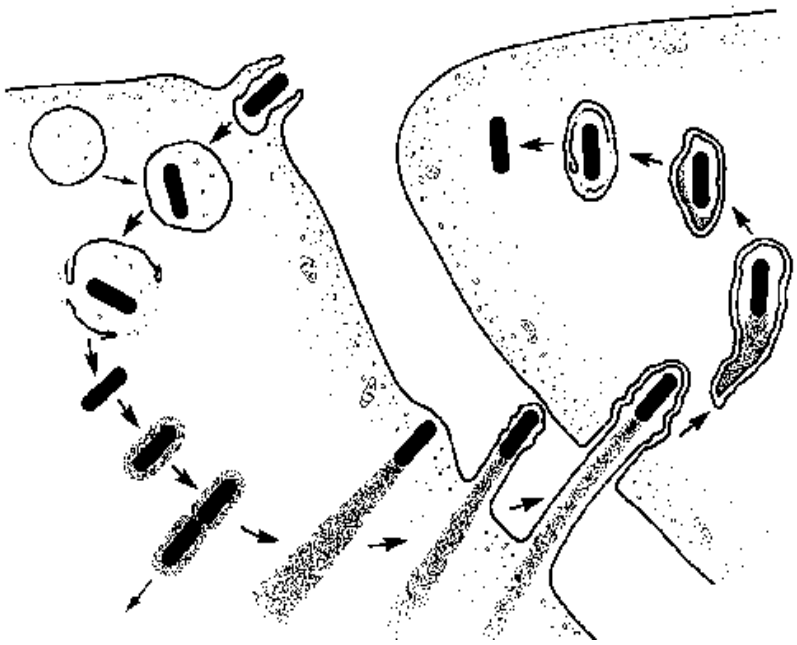

Figure 1.1: Cell-to-cell spread of *L. monocytogenes*. Figure adapted from (53).

actA and *hly* are two of the eight major virulence factors used by *L. monocytogenes* for intracellular infection and cell-to-cell spread. Among the other virulence factors are two phospholipases that help with autophagy avoidance and with escape from the vacuole, *plcA* and *plcB,* and a master virulence transcription factor, *prfA* (8, 54). These eight genes are encoded together on one chromosomal locus termed the pathogenicity island. Each gene is regulated transcriptionally by the PrfA protein, which itself is regulated by a small molecule cofactor, glutathione, and by the redox state of the bacteria (55). The pathogenicity island is specific to pathogenic species of *Listeria,* and is not found in the closely related *Listeria innocua* (56). The pathogenicity island of *L. monocytogenes* and numerous other pathogens are therefore thought to have been acquired via horizontal gene transfer (56, 57). Apart from the classical pathogenicity island, numerous other genes contribute to pathogenesis of *L. monocytogenes* that are not regulated by PrfA and may be conserved in non-pathogenic bacteria. Such is the case with proteins required for *L. monocytogenes* resistance to lysozyme, as discussed later.

Genetic manipulability, tissue culture models of infection, and *in vivo* models of infection

L. monocytogenes has served as a useful model organism with well-established assays for laboratory growth, tissue-culture models of infection, and *in vivo* models of infection. The organism robustly grows in aerobic or anaerobic conditions and can achieve an OD_{600} of approximately 4.0 in BHI, a rich media. Numerous genetic tools are available for manipulation of the *L. monocytogenes* genome, including site-specific integration vectors (58), plasmids used for constructing in-frame deletion mutants by homologous recombination (59), and a small non-polar transposon used for mutagenesis (60).

A variety of cell types are amenable to *L. monocytogenes* infection in tissue culture, including: fibroblasts (61), macrophage-like cell lines, primary bone-marrow derived macrophages (BMMs)(62), and others. Growth in primary BMMs over the course of 8 hours is used as a metric for escape, survival, and growth in macrophages, while infection of fibroblasts over the course of 3 days produces zones of dead cells where *L. monocytogenes* has proliferated,

which can be used as a metric for cell-to-cell spread (61, 62). *L. monocytogenes* has a well-established mouse model of infection, in which mice are typically infected by tail vein injection and spleens and livers are harvested at 48 hours postinfection. To examine the organism's ability to cross the placental barrier, a guinea pig model of infection has been established (14, 63-65). The many barriers to oral infection have limited the usefulness of oral models of infection (the natural method of infection) in mice; however recent advancements have made oral infection a reliable and reproducible model for understanding *L. monocytogenes* pathogenesis (66).

1.3 The cell wall and resistance to lysozyme

Alexander Fleming and the history of lysozyme

Lysozyme is a potent antibacterial enzyme found in high concentrations throughout the entire body of all vertebrates (67, 68). It was originally reported as an antibacterial molecule by Alexander Fleming in 1922 (Figure 1.2), where he immediately made a number of astute observations in his report, "On a remarkable bacteriolytic element found in tissues and secretions (69)." First, he observed that nasal mucus and many other human secretions were capable of robustly killing *Micrococcus lysodeikticus* (originally named by Fleming but later renamed *Micrococcus luteus*). Second, Fleming observed that lysozyme killed non-pathogens better than pathogens. Third, Fleming later reported that repeated subculture of bacteria with lysozyme increased their resistance to the enzyme (70). His search for an effective antibacterial molecule to kill pathogens led to the revolutionary discovery of penicillin in 1928, for which he would eventually receive the Nobel Prize along with Ernst Chain and Howard Florey, who learned to purify the molecule and produce it on a large scale (71).

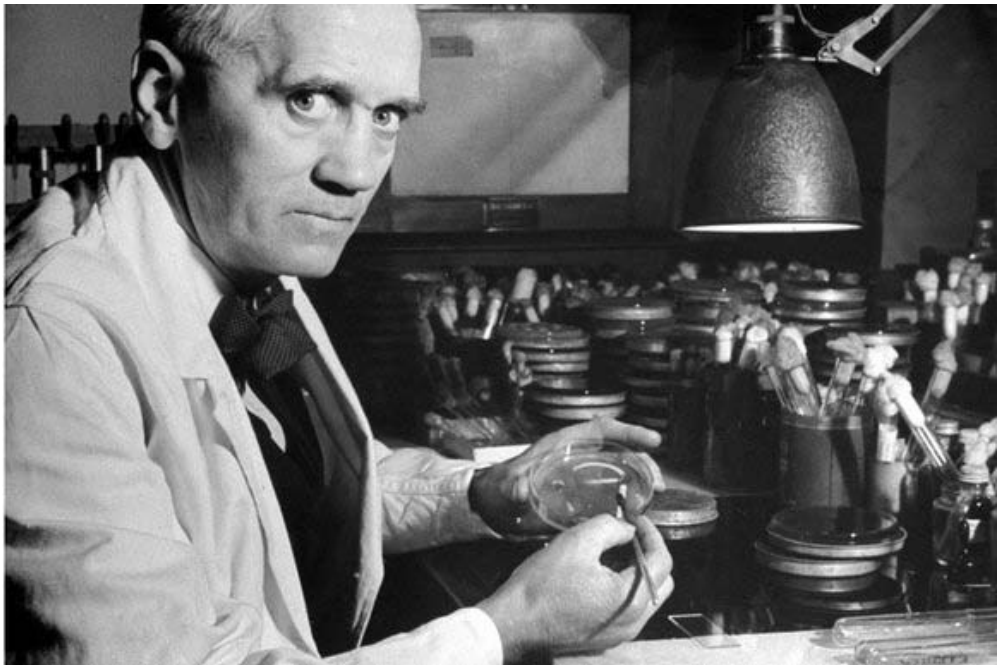

Figure 1.2 Sir Alexander Fleming, who discovered lysozyme in 1922 (69).

.

It remained a mystery for nearly 40 years how Fleming's lysozyme killed bacteria, despite significant efforts to identify the enzyme's substrate (72, 73). In 1959, Salton and Ghuysen discovered that lysozyme digestion of cell walls produced equimolar concentrations of

N-acetylglucosamine (NAG) and N-acetylmuramic acid (NAM), thereby making the pivotal discovery of the composition of the bacterial cell wall (74-78).

Fleming observed that lysozyme is found ubiquitously in the body, is found at extremely high concentrations in tears, and is stable in solution at room temperature for years (68-70). Indeed, more recent studies determined that lysozyme is found in tears at concentrations greater than 1 mg/ml and at concentrations of approximately 10 μg/ml in the blood (79-81). It is secreted by granulocytes at high concentrations and is found in the lysosomes of phagocytic cells such as macrophages (82, 83). Lysozyme can be purified to high concentrations from egg whites and it is highly stable in solution, making it a useful tool to study protein biochemistry (68, 69). For these reasons, lysozyme was the first enzyme whose structure was solved by X-ray crystallography in 1965, and was the second protein structure elucidated, after myoglobin in 1960 (84, 85).

Peptidoglycan and the molecular determinants for lysozyme resistance

Long alternating residues of NAG and NAM form the sugar backbone of the bacterial cell wall, and short amino acid chains that stem from NAM are cross-linked to form a lattice of sugars and peptides termed peptidoglycan (86). Over twenty layers of peptidoglycan in Gram-positive bacteria compose the cell wall, while in Gram-negative bacteria peptidoglycan can be as thin as one or perhaps only a few layers (87). Peptidoglycan is a highly dynamic structure that is constantly remodeled by proteins that incorporate new material to the bottom peptidoglycan layers, termed penicillin binding proteins (PBPs), and by peptidoglycan degrading enzymes found on the outer layers, termed autolysins (86, 88). Overabundance of autolysins results in cell lysis; therefore expression of these enzymes is likely to be tightly regulated.

Pathogenic bacteria such as *S. aureus* and *L. monocytogenes* are highly lysozyme-resistant and can tolerate concentrations of lysozyme greater than 1 mg/ml (89, 90). Despite immense interest in lysozyme biochemistry and despite the original observation by Fleming in 1922 that lysozyme was unable to kill pathogenic bacteria, it was not until the year 2000 that the first lysozyme resistance gene, *pgdA*, was characterized in bacteria (91). PgdA is a cell wall enzyme that deacetylates the amino group of NAG, while another enzyme, the O-acetyltransferase OatA, O-acetylates NAM (89, 91). These modifications convert peptidoglycan into a poor lysozyme substrate. To date, PgdA and OatA are the best characterized and most critical factors used by bacteria to maintain lysozyme resistance. Certain pathogenic bacteria such as *L. monocytogenes* encode both enzymes, but the *pgdA* enzyme is more critical for maintaining lysozyme resistance in *L. monocytogenes* (92). Other pathogens such as *Staphylococcus aureus* rely principally on *oatA* (89, 93, 94).

Alternative lysozyme resistance mechanisms exist in bacteria; however their functions appear less significant and are less well understood than the mechanisms of PgdA and OatA. Teichoic acid plays a complementary role to *oatA* in *Staphylococcus aureus* (95). In *Streptococcus suis*, mutation of a sugar transferase required for carbohydrate-based capsule formation resulted in increased lysozyme resistance (96). It remained unclear how capsule affected the ability of lysozyme to degrade the cell wall and whether this process involved *pgdA*. An opposite effect was observed in lactic acid bacteria, where formation of the carbohydrate-based β-glucan increased lysozyme resistance (97). Certain Gram-negative bacteria produce periplasmic lysozyme inhibitors, Ivy, PliC and PliG, that directly bind to lysozyme (98-101). Finally, the cell wall modifying enzyme PbpX is required for lysozyme resistance in *B. subtilis*, however the function of this protein remains unknown (102, 103).

Killing of bacteria by lysozyme

L. monocytogenes has served as a robust model organism to study lysozyme resistance because it encodes both *pgdA* and *oatA*, it is genetically manipulatable, and the *in vivo* murine model is well established (92). *L. monocytogenes* mutants that lack *pgdA* are attenuated approximately 10^3-fold below Wt in spleens and livers of mice upon i.v. infection, while mutants lacking *oatA* are attenuated approximately 10-10^2-fold (92, 104, 105). Accordingly, *pgdA oatA* double mutants were significantly more attenuated than either single mutant *in vivo* (92). Macrophages, serum, neutrophils, and intestinal lysozyme have all been attributed to killing lysozyme-sensitive bacteria *in vivo* (105-107). Infection of macrophages with lysozyme-sensitive bacteria induced secretion of host IFN-β and IL-1β, and infected macrophages underwent increased pyroptosis that was Aim2 dependent (92). These responses were due to small amounts of bacteriolysis that was dependent on host lysozyme (92).

The principal mechanism by which lysozyme kills bacteria is through its enzymatic activity, where it cleaves the backbone of peptidoglycan; however the protein also contains a highly charged region that can kill bacteria non-enzymatically (108). Other molecules produced by the immune system termed cationic antimicrobial peptides (CAMPs) function by a similar mechanism. These small peptides retain a high positive charge and bind to bacterial membranes to form pores, lysing the bacteria (94, 109). Analogous to lysozyme resistance, pathogenic bacteria are highly CAMP resistant while non-pathogens are CAMP sensitive. Resistance to CAMPs is mediated through enzymes that alter the charged state of the cell wall, either through D-alanylation of teichoic acid by proteins of the Dlt operon or through modification of phospholipids by the enzyme MprF (109, 110). *L. monocytogenes dlt* or *mprF* mutants are sensitive to CAMPs and attenuated 10-fold during *in vivo* infection (109-111). D-alanylation of teichoic acid plays a role in lysozyme resistance of *B. subtilis* and *S. aureus* (94, 112), which may function in repelling lysozyme by charge.

1.4 Small non-coding RNAs, an emerging class of gene regulators in bacteria

The advent of tiling array and RNA-seq technologies over the past decade has created a new paradigm for our understanding of gene regulation in bacteria. Hundreds of non-coding RNAs have been discovered in *L. monocytogenes* and other organisms, which can function in *cis* or in *trans*. *Cis* regulatory RNA elements are transcribed with their regulated transcript, such as riboswitches, which regulate expression of their downstream gene (113). *Trans* encoded RNAs are independently transcribed and regulate target RNAs through base-pairing interactions (114). *Trans* encoded sRNAs can regulate gene expression through four mechanisms. First, the majority of sRNAs regulate translation by pairing with a complementary RBS of a target gene (114). Secondly, sRNAs can pair with the coding region of a target mRNA, directing it to RNAse E mediated degradation (114). Third, sRNAs can activate gene expression by relieving the formation of an inhibitory hairpin in the 5' UTR of an mRNA that occludes the RBS (114, 115). Lastly, sRNAs can interact with proteins to either inhibit their function or to act together as a ribonucleoprotein complex (116, 117).

Investigations into small non-coding RNA (sRNA) based gene regulation has principally occurred in Gram-negative bacteria such as *Salmonella* and *E. coli*, which often differ from sRNA mediated gene regulation in Gram-positive bacteria because of the requirement for the RNA chaperone protein Hfq. Hfq is a small RNA binding protein that oligomerizes into a homohexamic ring structure and mediates sRNA:mRNA interactions (118). Hfq serves as a platform for RNA interactions and functions closely with RNAse E to either induce cleavage of

target RNAs or to protect RNA from cleavage (118). Mutants of *hfq* in Gram-negative bacteria display pleiotropic phenotypes, as the protein is required for an abundance of sRNA mediated regulation (119, 120). However, *hfq* mutants in Gram-positive bacteria, such as *Staphylococcus aureus* and *L. monocytogenes*, are viable and display less significant morphological or virulence phenotypes (119-121).

L. monocytogenes has served as a popular model organism for investigating sRNA mediated regulation in Gram-positive bacteria. Multiple studies have extensively identified *cis*, *trans*, and *anti-sense* RNAs, totaling over 200 non-coding regulatory RNAs (122-126). Identifying targets and phenotypes for these RNAs, however, remains a challenge. Target prediction programs that use base-pairing algorithms such as TargetRNA2, RNAPredator, and BLAST can help identify genes with high complementarity to a sRNA; however these programs can often generate dozens or perhaps hundreds of potential candidates (127-129). Target predictions are also complicated by the numerous mechanisms by which RNAs can regulate one another. For example, decoy RNAs can target sRNAs to sequester them from a target RBS (130, 131), and sRNAs can target the protein-coding region of an mRNA (114). For these reasons it remains challenging to discern which predictions may be decoys, which are noise, and which are *bona fide* sRNA targets.

1.5 SpoVG

SpoVG is conserved across the firmicute clade and has been studied since 1981, when it was the first gene cloned from *B. subtilis* (132). *spoVG* in *Bacillus subtilis* is a Sigma H dependent gene expressed during sporulation, where mutants are defective in late stage sporulation (132, 133). *spoVG* mutants display pleiotropic phenotypes in a variety of firmicutes, including: asymmetric division defects in *B. subtilis* (134), capsule formation defects in *Staphylococcus aureus* (135), decreased secretion of extracellular enzymes in *S. aureus* (136), increased sensitivity to methicillin in *S. aureus* (137), and suppressing ppGpp related defects in *L. monocytogenes* (138). The mechanism of SpoVG regulation has remained unknown and SpoVG contains no detectable homology to any protein of known function, however one study described it as a site-specific DNA binding protein (139). Translation of SpoVG in *S. aureus* is regulated by an sRNA, SprX (140), and SpoVG protein abundance is increased in mutants of another sRNA, RsaA (141).

Biochemical studies have characterized the crystal structure of SpoVG from *B. subtilis* and from *Staphylococcus epidermidis* at 3.0 A^o and 1.8 A^o resolution, respectively (142, 143). SpoVG is a small protein of approximately 100 amino acids, and dimerizes in the asymmetric unit of the crystal structure. The protein contains four β-strands that overlay a C-terminal α-helix. Two paralogs of *spoVG* exist in *L. monocytogenes* and are transcribed together in a two-gene operon (125). The proteins are 84% identical, differing mostly at the C-terminal α-helix. Lastly, a phosphopeptide was identified from the second paralog of *spoVG*, *lmo0197* (144), indicating that post-translational modifications may regulate the protein activity.

1.6 Metabolism of 6-carbon sugars in *L. monocytogenes*

L. monocytogenes is routinely cultured in brain-heart infusion (BHI) media for standard laboratory assays. This rich media contains mammalian cell lysate and is supplemented with glucose, which *L. monocytogenes* and many other bacteria prefer as a sugar source (145). Defined minimal media have been developed for *L. monocytogenes* using glucose as the lone carbon source, and growth is supported by substituting glucose with other 6-carbon sugars such

as fructose, mannose, and NAG (145, 146). Growth is also supported using disaccharides of 6-carbon sugars, including trehalose, cellobiose, and chitobiose (145). Glycerol is the only non-6-carbon sugar source known to support growth of *L. monocytogenes*. Attempts to grow the bacteria in other carbon sources were unsuccessful, including case amino acids, 5-carbon sugars such as arabinose and ribose, pyruvate, and succinate (145).

These data imply that *L. monocytogenes* is highly dependent on 6-carbon sugars for growth. Importation of carbohydrates in bacteria occurs through the phophoenolpyruvate (PEP)-phosphotransferase systems (PTSs), and indeed the *L. monocytogenes* genome encodes more PTS system components than any other known bacterium (147). PTS systems function in the recognition, import, and phosphorylation of specific sugars into the cell using a phosphoryl relay, and a given PTS system is specific for a given sugar or sugar class (147). First, the phospho group is transferred from PEP to the protein EI, then to HPr. These two proteins contain no specificity for a given sugar and are required for all PTS systems. HPr then transfers the phosphor group to the sugar-specific PTS component IIA, then to IIB, and finally to the incoming sugar. The sugar is transported across the membrane by an integral membrane protein, IIC (147, 148). The PTS classes are highly redundant in *L. monocytogenes*, and multiple PTS systems are often dedicated to importing a single sugar (148).

Among the PTS families are importers for N',N'-diacetylchitobiose and cellobiose, the disaccharide breakdown products of chitin and cellulose, respectively. Chitin and cellulose are the two most abundant polysaccharides on Earth (129, 149). Cellulose consists of β-1,4 linked glucose molecules and forms the cell walls of plants, while chitin consists of β-1,4 linked NAG and forms the cell walls of fungi and crustaceans. Importantly, NAG contains nitrogen, making chitin a preferable energy source in low-nitrogen environments (150).

Chapter 2

Listeria monocytogenes is resistant to lysozyme through the regulation, not the acquisition, of cell wall-modifying enzymes

Sections of this chapter were published in:

Burke, T.P., Loukitcheva, A., Zemansky, J., Wheeler, R., Boneca, I.G., & Portnoy, D.A. (2014). Listeria monocytogenes Is Resistant to Lysozyme through the Regulation, Not the Acquisition, of Cell Wall-Modifying Enzymes. *Journal of bacteriology, 196* (21), 3756-3767.

2.1 Summary of results

Listeria monocytogenes is a Gram-positive facultative intracellular pathogen that is highly resistant to lysozyme, a ubiquitous enzyme of the innate immune system that degrades cell wall peptidoglycan. Two cell wall modifying enzymes, *pgdA* and *oatA*, confer lysozyme resistance to *L. monocytogenes*, however these enzymes are also conserved in lysozyme-sensitive, non-pathogens such as *Bacillus subtilis*. We sought to identify additional factors responsible for lysozyme resistance in *L. monocytogenes*. A forward genetic screen identified 174 transposon insertion mutants that were killed by lysozyme and insertions mapped to 13 individual genes. Four of these thirteen mutants were killed exclusively by lysozyme and not other cell wall targeting molecules. These genes were: the peptidoglycan deacetylase *pgdA*, the putative carboxypeptidase *pbpX*, the response regulator *degU*, and a highly abundant non-coding RNA, *rli31*. Both *degU* and *rli31* mutants had reduced expression of *pbpX* and *pgdA*, yet DegU and Rli31 did not regulate one another. Since *pbpX* and *pgdA* are also present in lysozyme-sensitive bacteria, this suggested that the acquisition of novel enzymes was not responsible for lysozyme resistance, but rather, the regulation of conserved enzymes by DegU and Rli31 conferred high lysozyme resistance to *L. monocytogenes*. Each lysozyme-sensitive mutant identified in this study was attenuated for virulence in mice. Greater than 95% of lysozyme-sensitive bacteria were killed within 30 minutes of intravenous infection, suggesting that they were killed in the blood. This phenotype was recapitulated using purified blood, where the most lysozyme-sensitive mutant lost over 1,000-fold CFU within 30 minutes. Collectively, these data indicate that lysozyme resistance is a highly regulated, essential determinant of *L. monocytogenes* pathogenesis and is required to avoid the enzymatic activity of lysozyme present in the blood.

Introduction

Lysozyme is a ubiquitous bactericidal enzyme found in the blood, bodily secretions, and phagocytic cells of all animals (67, 81, 83). Lysozyme degrades the bacterial cell wall by hydrolyzing the β1-4 linkage between the N-acetylglucosamine (NAG) and N-acetylmuramic acid (NAM) residues that comprise the peptidoglycan backbone, often resulting in bacteriolysis (86). Not surprisingly, many pathogens have evolved mechanisms of lysozyme resistance (151, 152). The best characterized mechanisms of lysozyme resistance involve the acetylation state of the peptidoglycan, catalyzed by the deacetylase PgdA and/or the acetyltransferase OatA. PgdA deacetylates the amino group of NAG while OatA O-acetylates NAM, converting the sugar backbone into a poor lysozyme substrate (89, 91). *pgdA* mutants of *Streptococcus pneumoniae* and *oatA* mutants of *Staphylococcus aureus* are lysozyme-sensitive, and in each case lysozyme-sensitive mutants are attenuated in animal models of infection (89, 91, 92, 105).

L. monocytogenes is a facultative intracellular pathogen of animals and humans that causes severe disease in pregnant women and immunocompromised individuals (8). Both PgdA and OatA contribute to lysozyme resistance in *L. monocytogenes* and *pgdA* mutants are attenuated during oral and intravenous (i.v.) infection of mice (92, 104, 105). Indeed, *pgdA oatA* double mutants are extremely lysozyme-sensitive and more than 1000-fold less virulent in mice (92). Attenuation of lysozyme-sensitive mutants *in vivo* has been attributed to intestinal lysozyme and survival in macrophages (105). *In vitro*, *pgdA oatA* double mutants show increased killing upon phagocytosis by macrophages and undergo bacteriolysis in the macrophage cytosol leading to induction of macrophage cell death by pyroptosis (92).

Gram-positive pathogens such as *L. monocytogenes*, *B. anthracis*, *S. aureus*, and *S. pneumoniae* are extremely lysozyme-resistant, while many related, but non-pathogenic species, are lysozyme-sensitive (112). One possible explanation for the evolution of lysozyme resistance is the acquisition of enzymes such as PgdA and OatA (93). However, this is probably not the case since *pgdA* and *oatA* are conserved in many non-pathogenic members of the *Bacilli* and *Staphylococci* (112). Why, then, are *L. monocytogenes* and other pathogens so lysozyme-resistant? In this study we sought to answer this question by performing a forward genetic screen for lysozyme-sensitive mutants in *L. monocytogenes*. Rather than identify novel cell wall modifying enzymes, the screen identified a transcription factor (DegU) and an abundant non-coding RNA (Rli31) necessary for lysozyme resistance in *L. monocytogenes*.

2.2 Results:

2.2.1 A screen to identify lysozyme-sensitive mutants

To identify genes required for lysozyme resistance in *L. monocytogenes*, a library of approximately 40,000 distinct transposon mutants was generated using a *Himar1* transposon delivery vector in wild-type (WT) *L. monocytogenes* 10403S (60). Bacteria were plated on BHI-agar at a concentration of approximately 200 CFU/plate and replica-plated onto BHI-agar plates containing 1 mg/ml lysozyme. This concentration of lysozyme was chosen because it was sufficient to completely restrict growth of Δ*pgdA* (data not shown), had no effect on WT bacteria, and is a relevant concentration during infection (80, 81). BHI plates were visually compared to BHI-lysozyme plates for the loss of individual colonies (Figure 2.1A). Screening was repeated using a previously described Tn*917* library (153), totaling over 50,000 screened colonies. 174 mutants were identified and the insertion sites were defined by a nested PCR based sequencing method (see Materials and Methods). For each gene identified, transposon insertions were transduced into a WT background and re-screened using a lysozyme-disk-diffusion assay (data not shown). Transposon insertions mapped to 13 individual genes, with most genes being identified by multiple independent transposon insertions (Table 2.1).

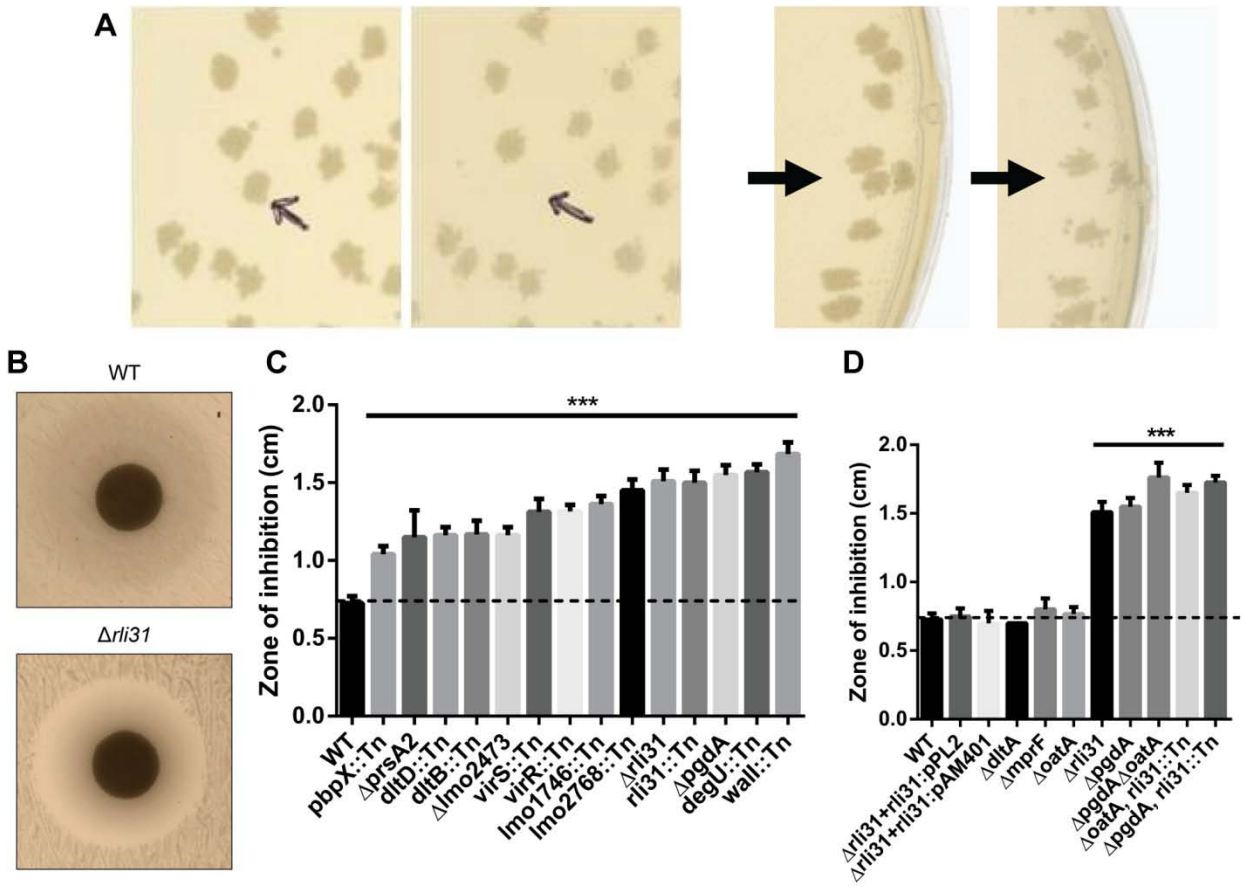

Figure 2.1 A screen to identify lysozyme-sensitive mutants in *L. monocytogenes*
(A) *L. monocytogenes* transposon mutants were replica plated from BHI (left panels) onto BHI-lysozyme plates (right panels) containing 1mg/ml chicken egg white lysozyme (Sigma). Arrows indicate colonies defective on BHI lysozyme plates. (B,C,D) Strains were grown in 2ml BHI overnight shaking at 37^{o} and 30 μL was spread onto BHI agar. Filter disks containing 1mg of lysozyme were placed onto the agar, incubated overnight at 37^{o}, and zones of clearance were measured. Means and standard deviations from at least 3 separate experiments are presented, where *** indicates $P < 0.001$. The dotted line indicates zone of inhibition by lysozyme in WT bacteria.

Lysozyme sensitive mutants identified in *L. monocytogenes*						
#	Gene	Gene Name	Description	# of unique insertions	Killing by CAMPs	Killing by antibiotics
1	*lmo0415*	*pgdA*	Peptidoglycan deacetylase	2	-	-
2	*lmo0540*	*pbpX*	Putative carboxypeptidase	4	-	-
3	Intergenic	*rli31*	Non-coding RNA	1	-	-
4	*lmo2515*	*degU*	Orphan response regulator	4	-	-
5	*lmo0290*	*yycI*	Regulator of WalRK 2-component system	2	++	++
6	*lmo0971*	*dltD*	Operon that adds D-ala to techoic acid	4	+	+
7	*lmo0973*	*dltB*	Operon that adds D-ala to techoic acid	10	+	+
8	*lmo1741*	*virS*	2-component system kinase	3	++	++
9	*lmo1745*	*virR*	Response regulator	6	++	+
10	*lmo1746*	-	ABC family transporter, *vir* operon	9	++	+
11	*lmo2219*	*prsA2*	Extracellular chaperone	1	+	++
12	*lmo2473*	-	Unknown	3	+	++
13	*lmo2768*	-	Unknown	2	++	-

Table 2.1 – Lysozyme sensitive mutants identified in *L. monocytogenes*
For killing by CAMPs and antibiotics: - indicates no killing, + indicates moderate killing, and + + indicates significant killing for the indicated strains, as observed for the data presented in Figure 2.1. Two-component system is abbreviated as TCS.

To compare sensitivity of these strains to one another and to WT, mutants were tested for their susceptibility to lysozyme by disk diffusion (Figure 2.1B,C), confirming that all of the identified mutants were significantly more susceptible to lysozyme than WT *L. monocytogenes*. The screen was validated by identification of *pgdA* and *prsA2* mutants, both of which have been shown to be required for lysozyme resistance in *L. monocytogenes* (92, 154). Insertions in *oatA* were not identified in the screen, however this was not surprising as the *oatA* phenotype is only significant when paired with Δ*pgdA* (Figure 2.1D and (92)) and *oatA* mutants grew on lysozyme plates (data not shown). All mutants grew normally in broth other than the *prsA2* mutant, which had delayed growth kinetics (Figure 2.2).

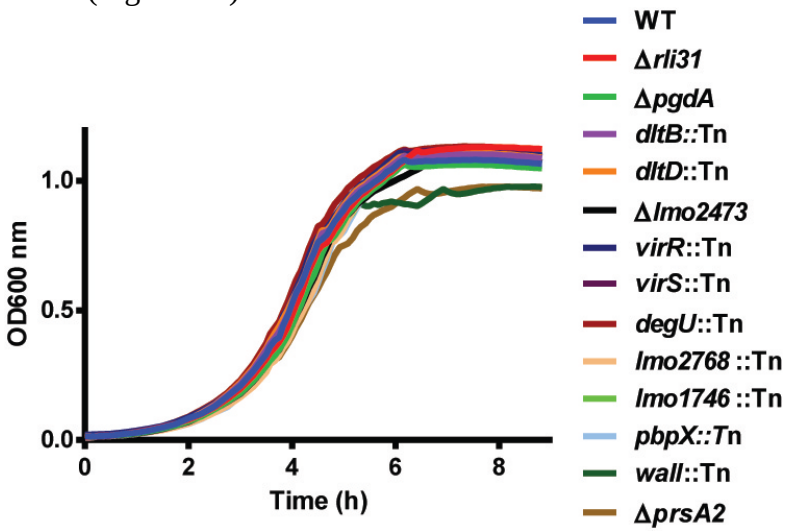

Figure 2.2 Growth in liquid media of lysozyme-sensitive mutants
Stationary phase cultures of the indicated strains were diluted to an OD_{600} of 0.05 in sterile filtered BHI. Cultures were shaken in a 96 well plate over time and turbidity was monitored every 10 minutes. Data are representative of at least 3 separate experiments.

The screen for lysozyme-sensitive mutants identified seven genes that have been previously shown to regulate cell wall and membrane architecture. Of these, the enzyme PrsA2 is a posttranslocation chaperone required for activity of numerous secreted proteins (154, 155). WalI is a negative regulator of the essential two-component system WalRK, which is required for expression of autolysins and other cell wall related enzymes (156-160). Lastly, multiple genes were identified in the *vir* operon, which regulates the *dlt* operon, and is the only two-component system required for *L. monocytogenes* virulence (111). The *dlt* operon is required for D-alanylation of teichoic acid (110) and mutants deficient in *dltD* result in increased autolysis (161).

Apart from *pgdA*, the contribution of the remaining six genes to lysozyme resistance or to the cell wall architecture was unknown. *lmo2473* encodes an uncharacterized protein that has been hypothesized to function in the synthesis of peptidoglycan precursors (23), and *lmo2768* encodes an uncharacterized membrane protein with an ABC transporter domain. *lmo0540* (hereafter referred to as *pbpX*) is the homolog of *pbpX* in *B. subtilis*, which is required for lysozyme resistance in *B. subtilis* (102). *pbpX* encodes a β-lactamase domain, however it has been reported in *Mycobacterium smegmatis* that PbpX does not contribute to β-lactam antibiotic resistance. Rather, it was proposed to function as a D,D-carboxypeptidase important for peptidoglycan cross linking, however this has never been confirmed biochemically (103). DegU is an orphan response regulator that regulates flagellar and chemotaxis genes in *L. monocytogenes* and is severely attenuated during infection of mice (162-166). Interestingly, one report suggested that, of 15 response regulators in *L. monocytogenes*, *degU* was the only mutant attenuated in mice (167). The phenotype of the *degU* mutant, however, has remained unexplained since flagellar and chemotaxis genes are not required for virulence (163, 164, 167). Lastly, *rli31* encodes an uncharacterized non-coding RNA, and *rli31* mutants are attenuated fivefold in spleens and livers of infected mice for unknown reasons (122, 123).

Because the *rli31* mutant was identified from only one unique transposon insertion, we sought to confirm that the *rli31* transposon (position 578,052 on *L. monocytogenes* genome CP002002.1) disrupted function of the sRNA and not neighboring genes. An *rli31* deletion mutant was constructed (see Materials and Methods) and shown to be sensitive to lysozyme (Figure 2.1C). *rli31* was then integrated with its native promoter on a unique locus of the chromosome using the plasmid pPL2 (58), which conferred complete lysozyme resistance to Δ*rli31* (Figure 2.1D). Lysozyme resistance of Δ*rli31* was also complemented by the non-integrative, high copy number plasmid pAM401 encoding the *rli31* gene and native promoter (Figure 2.1D). Δ*rli31* mutants had identical susceptibilities to lysozyme as *rli31::*Tn as shown by disk diffusion (Figure 2.1D) and these strains behaved identically in all assays.

Nine lysozyme-sensitive mutants are killed by cationic peptides and display increased sensitivity to β-lactam antibiotics

Seven genes identified in the screen are known to broadly affect cell wall homeostasis and their phenotypes were likely not specific to lysozyme resistance. To determine if the phenotypes of the remaining mutants were specific to lysozyme, the lysozyme-sensitive mutants were treated with CRAMP, a cationic antimicrobial peptide (CAMP, Figure 2.3A) and with cefuroxime and penicillin G, two β-lactam antibiotics (Figure 2.3B, C). Mutants of *dltA* and *mprF* served as positive controls for susceptibility to CAMPs and were both killed in this assay. DltA is required for D-alanylation of teichoic acid (110) and *mprF* is required for the transfer of L-lysine onto phospholipids (109), both of which confer a positive charge to the cell surface

leading to CAMP resistance. The *pgdA* mutant served as a control that is only killed by lysozyme and was not killed in either assay (Figure 2.3). As predicted, the 7 genes known to be involved with cell wall homeostasis were killed by both CRAMP and/or had increased susceptibility to β-lactam antibiotics. It was consistently observed that *lmo2473* and *prsA2* mutants were killed by CRAMP; however these mutants were the least susceptible and exhibited only a small amount of additional killing compared to WT bacteria. These two mutants were the most susceptible to penicillin, suggesting that their role in lysozyme susceptibility is primarily due to cell wall and not membrane integrity.

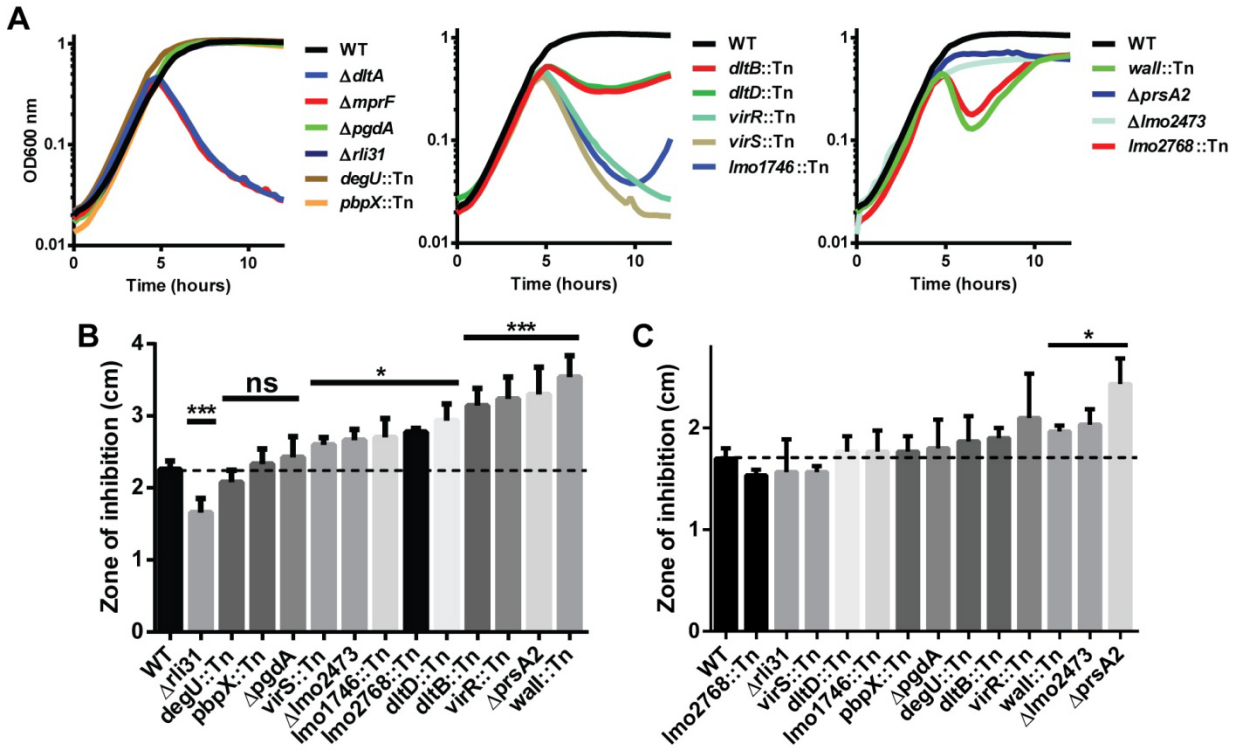

Figure 2.3 Treatment of lysozyme-sensitive strains with CRAMP and cell wall acting antibiotics

(A) A final concentration of 10μg/ml of purified mouse CRAMP (Anaspec) was added to the indicated strains of mid-exponential phase *L. monocytogenes* at 37^{o} in BHI and turbidity was monitored at 10 min intervals. Data are representative of at least 3 separate experiments and divided into 3 panels for clarity. (B,C) 30 μL of overnight *L. monocytogenes* were plated onto BHI and disks containing 700 ng cefuroxime (B) or 500 ng of penicillin G (C) were added. Plates were incubated overnight at 37^{o} and zones of inhibition were measured. Data are shown as the means of at least 3 separate experiments and error bars represent standard deviations of the mean, where * indicates $P < 0.05$ and *** indicates $P < 0.001$ as determined by unpaired two-tailed T-test.

Four mutants (*pgdA*, *rli31*, *degU*, and *pbpX*) were equally resistant to both antibiotics and CAMP treatment as WT bacteria. To further determine if these mutants were killed by antimicrobial peptides, the *pgdA*, *degU*, *pbpX*, and *rli31* mutants were also treated with high

concentrations of a cationic peptide derived from human (RAWVAWRNR) and chicken (NAWVAWRNR) lysozyme (Figure 2.4). Identical phenotypes were observed between each mutant and WT bacteria, while *dltA* and *mprF* mutants were killed by both peptides (Figure 2.4). Together, these data led to the conclusion that four *L. monocytogenes* genes are specifically involved with lysozyme resistance. Two of these genes were cell wall acting enzymes (*pgdA* and *pbpX*) with relatively well known or predicted functions; however the *rli31* and *degU* mutant phenotypes were completely uncharacterized with regard to lysozyme sensitivity. We chose to focus on characterizing the lysozyme susceptibility phenotype of the *rli31* mutant.

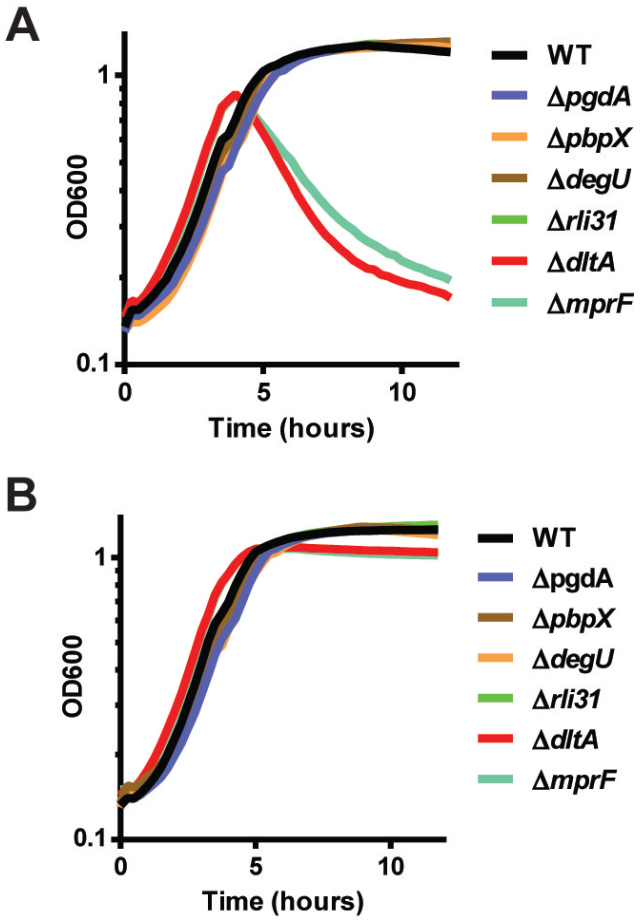

Figure 2.4 Treatment of lysozyme-sensitive strains with cationic peptides derived from chicken and human lysozyme

A final concentration of 1 mg/ml of the cationic peptide derived from (A) human and (B) chicken lysozyme (ELIM Biopharm) was added to the indicated strains of mid-exponential phase *L. monocytogenes* at 37^{o} in BHI and turbidity was monitored at 10 min intervals. Data are representative of at least 3 separate experiments.

Rli31 is a constitutively expressed, abundant RNA

To better characterize the *rli31* mutant phenotype, the relative expression of Rli31 was analyzed at various stages of growth in broth by Northern analysis using a probe specific for Rli31. Rli31 was constitutively expressed during all growth phases, from early-exponential (OD_{600}= 0.3) to mid-exponential (1.3 and 2.3) and stationary phase (3.9) (Figure 2.5A). Rli31

migrated at its predicted size of 144 nucleotides (123) and was not processed into smaller fragments. In addition, Rli31 was observed to be strikingly abundant. Upon staining total RNA from *L. monocytogenes* lysates with a non-specific nucleotide dye, Rli31 was observable in WT *L. monocytogenes* lysates alongside other abundant RNAs such as the ribosomal 5S and the 6s sRNA (Figure 2.5B). This band was confirmed as Rli31 by Northern analysis using a probe specific for Rli31 (Figure 2.5C). The appearance of Rli31 as the only RNA between 100 and 170 nucleotides was surprising, as over 40 non-coding RNAs are predicted to exist in *L. monocytogenes* corresponding to this length (123).

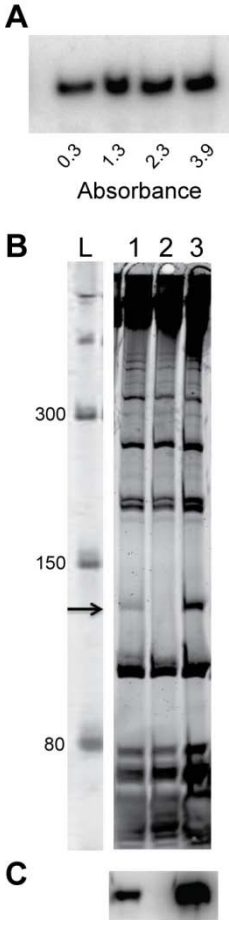

Figure 2.5 Rli31 is highly abundant and expressed at all growth phases
(A) 20 µg of total RNA collected at the indicated phases of growth in BHI was separated on 6% polyacrylamide. Nucleotides were transferred to a nylon membrane, probed using ^{32}P labeled TB13 primer, and imaged with Typhoon. (B) 20 µg of total RNA collected at mid-exponential phase in BHI at 37^{o} from 1.WT, 2.Δ*rli31*, 3.Δ*rli31*+pAM401:*rli31* was separated on 6% polyacrylamide and stained with SYBR Gold (Invitrogen). The arrow indicates Rli31 and L indicates the ladder. (C) RNA from (B) was transferred to a nylon membrane, probed using ^{32}P labeled TB13 primer, and imaged with Typhoon

2.2.2 Characterization of the *rli31* mutant phenotype

To determine how the *rli31* mutant was killed by lysozyme, cell walls from WT *L. monocytogenes* and the *rli31* mutant were purified and the muropeptide compositions of these strains were analyzed by reverse-phase HPLC (Figure 2.6A). O-acetylation and covalently attached modifications were also analyzed by omitting hydrofluoric acid treatment during the cell wall purification (Figure 2.6B). Muropeptide composition was confirmed by mass spectrometry and the abundance of eluted molecules was measured as a percent of total absorbance at 206nm (Table 2.2). In these analyses, the cell walls of the *rli31* mutant contained a similar abundance of O-acetylated muropeptides as WT bacteria, while multiple species of N-deacetylated glycans were less abundant (GlcNMTriP$_{DAPNH2}$, for example: 8.49% to 5.72%, Table 2.2). The analysis also identified a significant increase in muramyl-tripeptides in the *rli31* mutant (3.85% to 5.27%) and an increase in 3-4 (D-ala – DAP) linkages (3.62% to 5.65%), indicating a difference in peptide cross linking. The difference in acetylation suggested that *pgdA* was misregulated in the *rli31* mutant. The alterations in cross-linking suggested that *pbpX* may also contribute to the *rli31* mutant phenotype.

Cell wall analysis of the *rli31* mutant		
% of total peaks, purified peptidoglycan		
WT	Δ*rli31*	Peak
8.11	8.02	GlcNAcMTriP$_{DAPNH_2}$
8.49	5.72	GlcNMTriP$_{DAPNH_2}$
9.74	9.91	GlcNAcMTriP$_{DAPNH_2}$-GlcNAcMTetraP$_{DAPNH_2}$
13.85	10.53	GlcNMTriP$_{DAPNH_2}$-GlcNAcMTetraP$_{DAPNH_2}$
7.47	5.09	GlcNMTriP$_{DAPNH_2}$-GlcNMTetraP$_{DAPNH_2}$
% of total peaks, extracted cell walls		
WT	Δ*rli31*	Peak
3.85	5.27	GlcNAcMTriP$_{DAPNH_2}$
7	5.52	GlcNMTriP$_{DAPNH_2}$
2.66	2.82	GlcNM(OAc)TriP$_{DAPNH_2}$
3.62	5.65	GlcNAcMTriP$_{DAPNH_2}$-GlcNAcMTetraP$_{DAPNH_2}$
8.07	9.23	GlcNMTriP$_{DAPNH_2}$-GlcNAcMTetraP$_{DAPNH_2}$
6.97	4.76	GlcNMTriP$_{DAPNH_2}$-GlcNMTetraP$_{DAPNH_2}$
2.52	3.63	GlcNAcM(OAc)TriP$_{DAPNH_2}$-GlcNAcMTetraP$_{DAPNH_2}$
4.62	4.1	GlcNAcM(OAc)TriP$_{DAPNH_2}$-GlcNMTetraP$_{DAPNH_2}$

Table 2.2 – Cell wall analysis of the *rli31* mutant
HPLC analysis of the muropeptide composition of WT and Δ*rli31 L. monocytogenes*. Deacetylated muropeptides are indicated in red and O-acetylated muropeptides are indicated in

blue. Abbreviations for muropeptides are as follows: Glc*N*Ac, *N*-acetylglucosamine; Glc*N*, glucosamine; M, *N*-acetylmuramic acid; TriPDAPNH2, L-alanyl-γ-D-glutamyl-amidated *meso*diaminopimelic acid; TetraPDAPNH2, L-alanyl-γ-D-glutamyl-amidated *meso*diaminopimelyl-D-alanine; and Oac, *O*-acetylated.

A genetic approach was then undertaken in which suppressor mutations were generated in the Δ*rli31* background that restored lysozyme resistance to this mutant. Individual *rli31* colonies were subcultured in broth with increasing concentrations of lysozyme (50, 100, 200, 500, 1,000 μg/ml) until these uniquely derived mutants were resistant to 1mg/ml lysozyme (Figure 2.6C). Three of these strains were then deep sequenced and single nucleotide polymorphism (SNP) analysis revealed that all 3 strains had a single thymidine insertion 16 nucleotides upstream of the *pgdA* transcriptional start site, position 436,736 on the chromosome (Table 2.3). qPCR analysis of *pgdA* transcript levels in these strains revealed a 3.1(+/- 0.39)-fold upregulation of *pgdA*. These data strongly suggested that the *rli31* phenotype could be complemented by overexpression of *pgdA*.

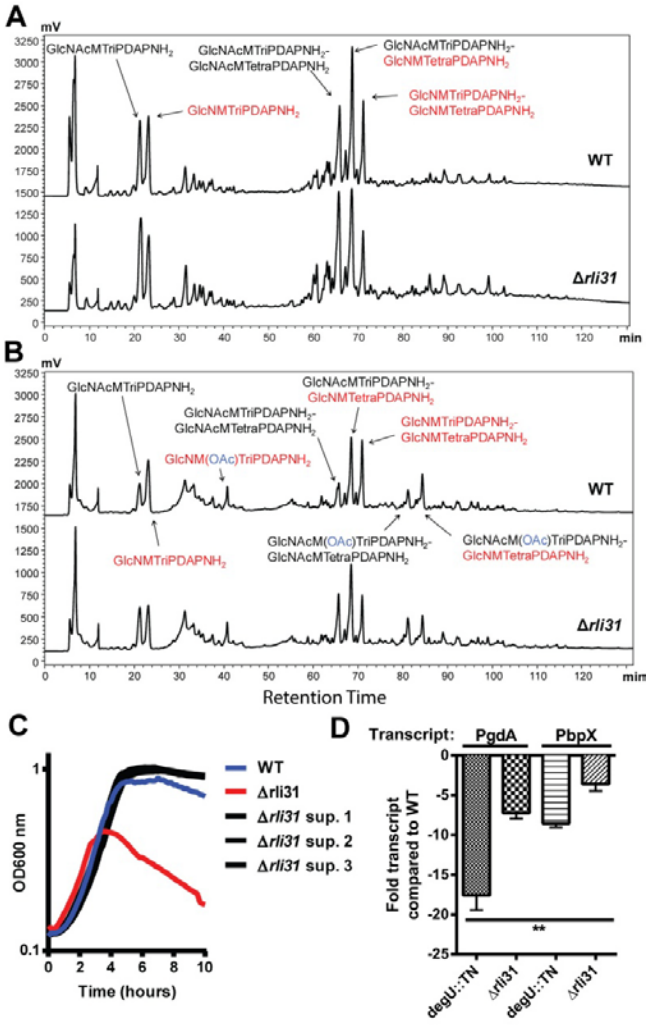

Figure 2.6 Characterization of the *rli31* mutant phenotype
(A,B) HPLC analysis of the muropeptide composition of WT and Δ*rli31 L. monocytogenes.* Deacetylated muropeptides are indicated in red and O-acetylated muropeptides are indicated in

blue. Abbreviations for muropeptides are as follows: Glc*N*Ac, *N*-acetylglucosamine; Glc*N*, glucosamine; M, *N*-acetylmuramic acid; TriPDAPNH2, L-alanyl-γ-D-glutamyl-amidated *meso*diaminopimelic acid; TetraPDAPNH2, L-alanyl-γ-D-glutamyl-amidated *meso*diaminopimelyl-D-alanine; Oac, *O*-acetylated. (A) Samples were treated with hydrofluoric acid. (B) Samples were not treated with hydrofluoric acid to retain covalent modifications. (C) Multiple *rli31* and *pgdA* mutants were independently passaged with increasing concentrations of lysozyme (50, 100, 200, 500, 1,000 μg/ml) in BHI broth shaking at 37^{o}. The resulting strains were grown to mid-exponential phase and treated with 1mg/ml lysozyme along with the parent strain Δ*rli31*. Turbidity was monitored at 10 minute intervals. (D) PgdA and PbpX transcripts of indicated strains were measured by qPCR, normalized to BglA, and compared to transcript levels in WT *L. monocytogenes*. Error bars represent standard deviations of the means. Statistics were performed using a two-tailed T-test assuming a null hypothesis of one, where ** indicates $P < 0.01$.

Together, the biochemical and genetic analyses suggested that the *rli31* mutant phenotype was due to misregulation of *pgdA* and possibly *pbpX*. To determine if Rli31 regulated *pgdA* or *pbpX*, RNA was purified from WT bacteria and the *rli31* mutant and real-time PCR (qPCR) was performed using DNA oligonucleotides specific for these 2 genes. These data showed that *pgdA* was significantly downregulated (8-fold below WT) and *pbpX* was slightly downregulated in the *rli31* mutant (3-fold below WT, Figure 2.6D). These qPCR data matched the biochemical and genetic analyses and provided an explanation for the lysozyme sensitivity of the *rli31* mutant.

Variants identified in *rli31* mutant suppressor strains				
Strain	**Location**	**Reference**	**Alteration**	**Description**
Δ*rli31* suppressor 1	436736	-	T	16nt upstream of *pgdA* transcriptional start site
Δ*rli31* suppressor 2	436736	-	T	16nt upstream of *pgdA* transcriptional start site
Δ*rli31* suppressor 3	436736	-	T	16nt upstream of *pgdA* transcriptional start site
	2418019	A	-	Intergenic region, 5' of *lmo2387*

Table 2.3 Variants identified in Δ*rli31* suppressor strains that were lysozyme-resistant

Rli31 functions independently of DegU

It remained unclear why the *degU* mutant was lysozyme-sensitive and if this phenotype involved Rli31. RNA was purified from WT and the *degU* mutant and qPCR was performed using primers specific for transcripts of *pgdA*, *pbpX*, and *rli31*. Significant downregulation of *pgdA* (18-fold below WT) and of *pbpX* (8-fold below WT) were consistently observed in the *degU* mutant (Figure 2.6D). However no difference in abundance of Rli31 was observed between WT and the *degU* mutant. Additionally, there was no change in the amount of *degU* transcript in the *rli31* mutant. These data suggested that lysozyme sensitivity of the *degU* mutant was due to regulation of *pgdA* and *pbpX* and was independent of *rli31*.

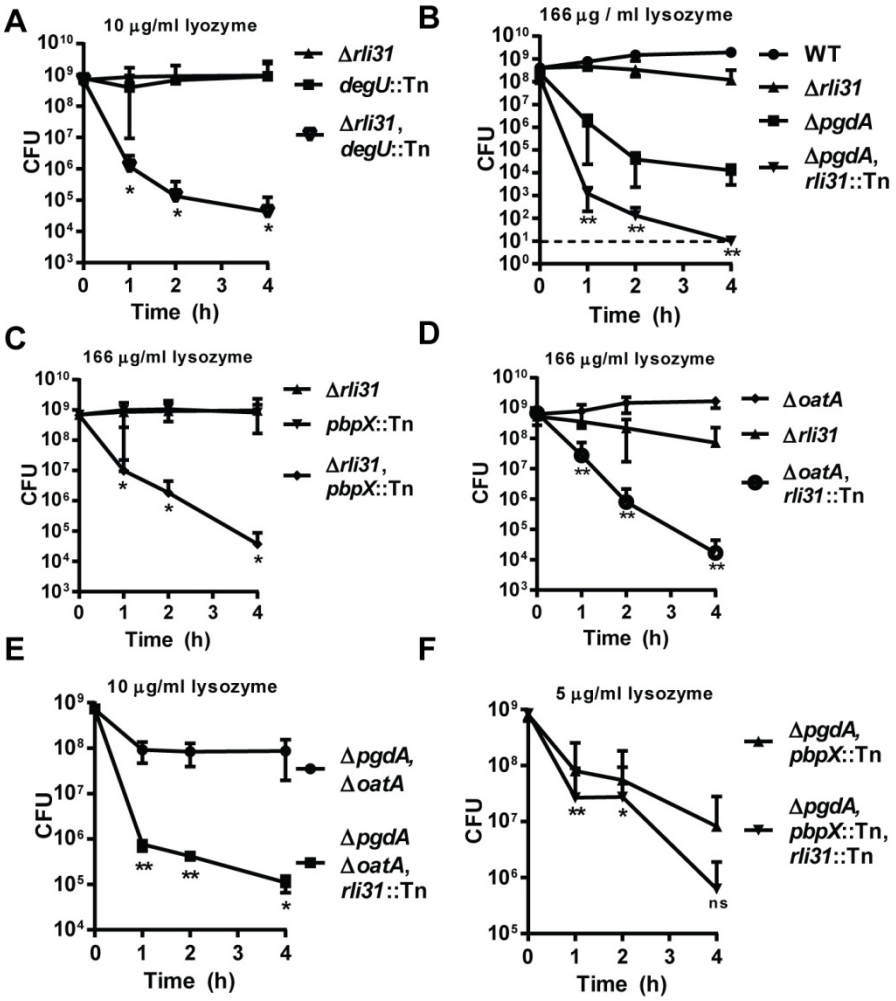

Figure 2.7 The *rli31* mutant phenotype is principally due to regulation of *pgdA* and *pbpX*
The indicated strains were grown to an OD_{600} of 0.5 and the indicated concentrations of lysozyme were added. Bacteria were plated for CFU at the given intervals. Data are the average of at least 3 independent experiments and error bars specify standard deviation of the mean. Two-tailed T-tests indicate statistical difference between (A) *degU*::Tn vs. Δ*rli31 degU*::Tn, (B) Δ*pgdA* vs. Δ*pgdA rli31::*Tn, (C) Δ*pbpX* vs. Δ*pbpX rli31::*Tn, (D) Δ*oatA* vs. Δ*oatA rli31::*Tn, (E) Δ*pgdA*Δ*oatA* vs. Δ*pgdA*Δ*oatA rli31::*Tn, and (F) Δ*pgdA pbpX*::Tn vs. Δ*pgdA pbpX*::Tn *rli31*::Tn, where ** indicates $P < 0.01$, * indicates $P<0.05$, and ns indicates no significant difference.

These data suggested that the lysozyme-sensitive phenotypes of the *rli31* and *degU* mutants were both due to regulation of *pbpX* and *pgdA*. To determine if Rli31 and DegU functioned epistatically, the *degU* mutation was transduced into Δ*rli31* and the resulting double mutant was treated with 10 μg/ml lysozyme (Figure 2.7A). The *rli31 degU* double mutant was killed significantly more than either single mutant upon treatment with lysozyme. Because DegU regulates chemotaxis and motility genes, any regulation of DegU by Rli31 would result in a motility phenotype. Upon inoculation into semisolid agar, neither the *rli31* mutant nor the *rli31* overexpression construct displayed a motility defect, while the *degU* mutant was not

motile, as expected (Figure 2.8). These data suggested that Rli31 and DegU both regulated *pgdA* and *pbpX*, but by independent mechanisms.

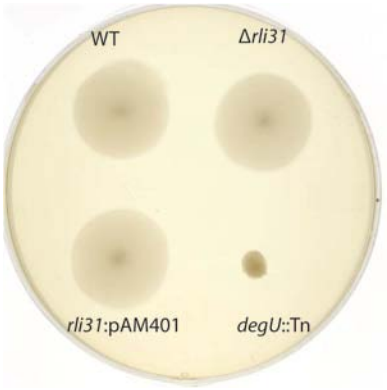

Figure 2.8 DegU and Rli31 do not regulate one another
The indicated strains of *L. monocytogenes* were grown overnight in BHI at 30^{o} and 1 μl of culture was inoculated into 0.35% BHI agar and incubated at 30^{o} for 2 days.

The *rli31* mutant phenotype is due to regulation of *pgdA* and *pbpX*

To determine if the lysozyme sensitivity of the *rli31* mutant was exclusively due to regulating *pgdA* and *pbpX*, the *rli31* transposon was transduced into the Δ*pgdA* mutant and the resulting double mutant strain was treated with a concentration of lysozyme that did not fully kill either single mutant (167 μg/ml). In this assay, the double mutant was significantly more attenuated than either Δ*rli31* or Δ*pgdA* alone (Figure 2.7B). A similar phenotype was also observed with the *pbpX rli31* double mutant (Figure 2.7C), the *oatA rli31* double mutant (Figure 2.7D) and the *oatA pgdA rli31* triple mutant (Figure 2.7E). The *pgdA pbpX rli31* triple mutant was then compared to the *pgdA pbpX* double mutant (Figure 2.7F). The differences between these strains were small compared to the other experiments, where only a 2 to 10-fold difference was observed between these strains at 1h and 2h, and no statistical difference existed at 4h. These data suggested that the majority of the *rli31* mutant phenotype was attributed to regulation of *pgdA* and *pbpX*. However, because the *rli31* phenotype was somewhat additive when paired with the *pgdA pbpX* double mutant at 1h and 2h, this suggested that the target of Rli31 must have a small, additional function distinct from *pgdA* and *pbpX* regulation that are required for lysozyme resistance in *L. monocytogenes*.

The *rli31* phenotype was additive with the *pgdA* and *oatA* phenotypes *in vitro*, yet it remained unclear how the *rli31* phenotype affected the *pgdA* and *oatA* phenotypes during infection. Upon intravenous (i.v.) infection of CD-1 mice, the *oatA rli31* double mutant was significantly more attenuated than *oatA* alone (Figure 2.9A). When infected with strains harboring *pgdA* mutations, however, CFU were barely recoverable from infected mice. The dynamic range was small and no statistical difference was observed between *pgdA* and *pgdA rli31* using a total of 10 mice. Despite this, the difference between the *pgdA oatA* double mutant and the *pgdA oatA rli31* triple mutant was significant (Figure 2.9B). These data provided *in vivo* evidence that Rli31 functioned independently of PgdA and OatA.

In summary, the data suggested that the *rli31* mutant phenotype was due to downregulation of *pgdA* and *pbpX*, yet Rli31 contained no detectable complementarity to these genes and was not completely epistatic with the *pgdA pbpX* double mutant. We therefore

conclude that downregulation of *pgdA* and *pbpX* is most likely an indirect consequence of *rli31* regulating another, yet to be identified target gene(s).

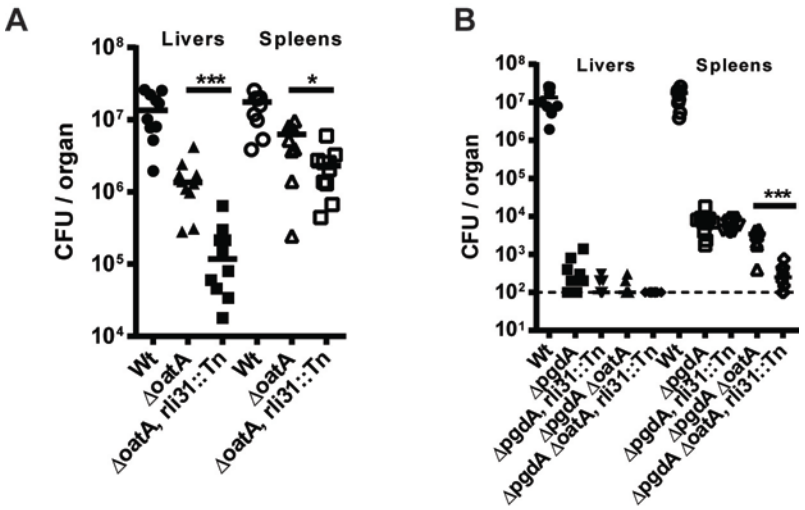

Figure 2.9 The *rli31* phenotype is additive with *pgdA* and *oatA in vivo*
Data shown represent CFU in organs of CD-1 mice that were infected i.v. for 48h. Data shown are the combination of two separate experiments totaling 10 mice. * indicates $P < 0.05$ and *** indicates $P < 0.0001$, as determined by two-tailed Mann Whitney T-test between WT and the indicated group.

2.2.3 Understanding how lysozyme-sensitive bacteria are killed during infection

To evaluate the contribution of the four genes that were required for resistance to the enzymatic activity of lysozyme, the phenotypes of these mutants were analyzed *in vivo*. 6-8 week old CD-1 female mice were infected i.v. and CFUs were evaluated in spleens and livers after 48h. *pgdA* and *degU* mutants were attenuated 3-5 logs, while *rli31* and *pbpX* mutants were attenuated fivefold (Figure 2.10A).

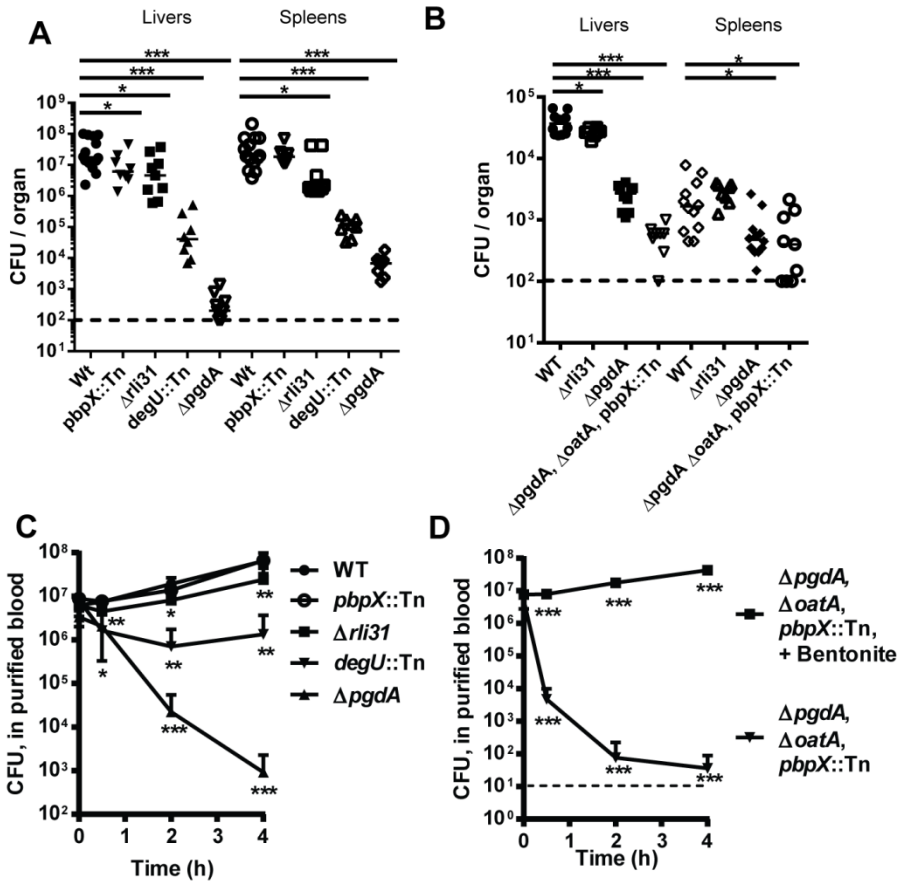

Figure 2.10 Serum kills lysozyme-sensitive *L. monocytogenes*
(A) Data shown represent CFU in organs of CD-1 mice that were infected i.v. for 48h. Data shown are the combination of two separate experiments totaling at least 8 mice per group. A two-tailed Mann Whitney T-test was used for statistical analysis for each group compared to WT, where * indicates $P < 0.05$, ** indicates $P < 0.01$, and *** indicates $P < 0.0001$. (B) Data shown represent CFU in organs of CD-1 mice that were infected i.v. for 30 minutes with the indicated strains of bacteria. Data shown are the combination of at least two separate experiments totaling at least 8 mice per group. A two-tailed *P* value is reported for each group in comparison to WT, where * indicates $P<0.05$, ** indicates $P < 0.01$, and *** indicates $P < 0.0001$. (C,D) Strains were grown to mid-exponential phase in BHI, washed with PBS, and diluted 1:100 into defibrinated sheep or horse blood (Hemostat). Bacteria were plated for CFU at the indicated times. Data represent means and standard deviations of the mean from at least 3 separate experiments. (D) For bentonite treated blood, blood was treated with 5mg of bentonite (Sigma) for 30 minutes at 4^{o} immediately prior to inoculation. A two-tailed *P* value is reported for the *pgdA oatA rli31* (no bentonite) strain in comparison to WT. A two-tailed *P* value is also reported for the *pgdA oatA rli31* (bentonite) values in comparison to the *pgdA oatA rli31* (no-bentonite) values, where *** indicates $P < 0.0001$.

We sought to explain the severe loss of virulence of lysozyme-sensitive *L. monocytogenes* observed *in vivo.* Lysozyme concentration varies from organ to organ (168, 169); therefore the defect observed *in vivo* may be due to killing in a specific organ. However,

the *rli31* mutant phenotype was similar between various organs, ranging from 5 to 20-fold (Figure 2.11A). We next reasoned that the major bactericidal factor could be macrophages, neutrophils, or serum, all having been previously implicated in killing lysozyme-sensitive bacteria (105, 106, 170). Upon infection of bone-marrow derived macrophages, only a small defect was observed using the *pgdA oatA rli31* triple mutant, the most lysozyme-sensitive strain (Figure 2.11B). Infection of macrophages with other lysozyme-sensitive strains showed even smaller differences between the mutants and WT bacteria (data not shown).

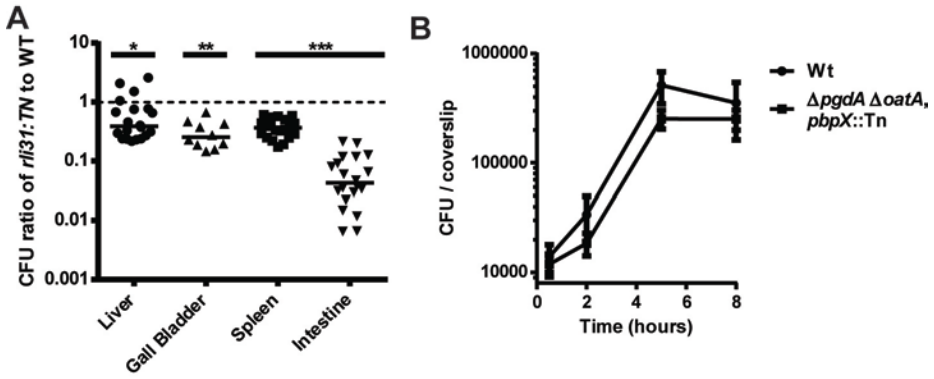

Figure 2.11 Examining the *in vivo* defect of lysozyme-sensitive bacteria
(A) C57BL/6J mice were infected with 10^5 bacteria at a 1:1 ratio of WT and *rli31::*Tn mutants. Organs were harvested from at least 10 mice from 2-4 separate experiments and plated on LB / LB + erythromycin. Ratios were determined and horizontal bars represent median values. Statistics were performed using one-sample Wilconox tests assuming a null hypothesis of one. A *P* value is reported for each group, where * indicates $P < 0.05$, ** indicates $P < 0.01$, and *** indicates $P < 0.0001$. (B) Bone marrow-derived macrophages (3×10^6) were plated onto coverslips and infected with the indicated strains. Bacteria were washed at 30 minutes post infection, gentomycin was added at 1h post infection, and bacteria were plated for CFU at the given intervals.

Next, to test if serum could kill lysozyme-sensitive mutants, infections were performed i.v. and mice were sacrificed at 30 minutes postinfection, a timepoint when *L. monocytogenes* has encountered the blood but neutrophils have not yet migrated to areas of infection (171). For these infections we chose 3 mutants that varied in lysozyme susceptibility: the *rli31* mutant, the *pgdA* mutant, and the *pgdA oatA rli31* triple mutant. Surprisingly, the *pgdA oatA rli31* triple mutant lost 97% viability after 30 minutes, the *pgdA* mutant lost 92.5%, and the *rli31* mutant lost a small but significant number of CFU (Figure 2.10B). These data suggested that serum was a major factor responsible for killing lysozyme-sensitive *L. monocytogenes* during infection.

To directly test if serum killed lysozyme-sensitive bacteria, the four strains specifically killed by lysozyme were inoculated into purified blood and plated for CFU over time. The *pgdA* mutant lost over 10^4 CFU and the *degU* mutant lost over 40-fold CFU after 4 hours (Figure 2.10C). The *rli31* mutant was killed fivefold below WT and the *pbpX* mutant was similar to WT. Most strikingly, the *pgdA oatA rli31* triple mutant lost 10^3 CFU within 30 minutes and CFU were barely recoverable after 2 hours (Figure 2.10D). The loss in CFU observed in blood between various lysozyme-sensitive strains correlated precisely to lysozyme susceptibility and to the defect observed *in vivo.* To directly test if lysozyme was the responsible bactericidal factor, the blood was treated with bentonite, which removes lysozyme activity from serum but leave

complement intact (172, 173). Upon bentonite treatment, the *pgdA oatA rli31* triple mutant behaved identically to WT bacteria at all timepoints (Figure 2.10D). Bentonite treatment also fully rescued killing of the *pgdA* mutant in blood (data not shown). To assure that the bentonite treatment did not remove a bactericidal factor other than lysozyme, bentonite treated blood was supplemented with 10 or 25 μg/ml of chicken egg white lysozyme, which are physiological concentrations found in the blood (81, 174). Lysozyme addition completely restored the bactericidal activity of blood (Figure 2.12).

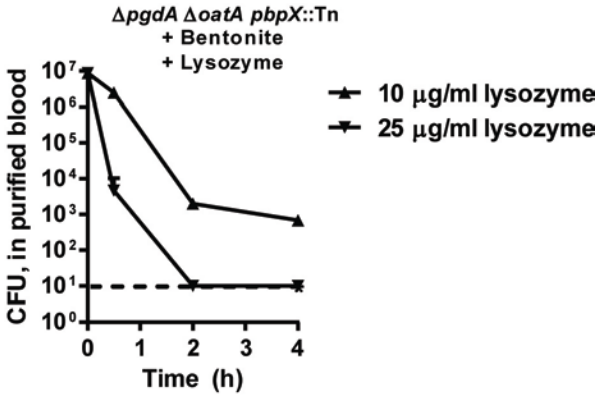

Figure 2.12 Addition of lysozyme to bentonite treated blood
The *pgdA oatA rli31* mutant was grown to an OD_{600} of 0.5, washed with PBS, and diluted 1:100 into bentonite treated blood that had been supplemented with the indicated concentrations of lysozyme from chicken egg white. CFU were then monitored at the given intervals.

2.3 Discussion

The results of this study, based on an exhaustive genetic screen, show that *L. monocytogenes* uses three enzymes (PgdA, PbpX and OatA) and two regulators to resist the bactericidal activity of lysozyme. The two regulators, DegU and Rli31, and one of the enzymes, PbpX, were previously not associated with *L. monocytogenes* lysozyme resistance. *degU* and *rli31* mutants were extremely susceptible to lysozyme and were attenuated during *in vivo* infection. Both *degU* and *rli31* mutants displayed reduced abundance of *pbpX* and *pgdA* mRNA, and *rli31* suppressor mutants upregulated expression of *pgdA*. These data suggested that DegU and Rli31 are the major regulators of lysozyme resistance in *L. monocytogenes* that act by increasing expression of *pgdA* and *pbpX*. Finally, we demonstrated that all of these factors contributed to *L. monocytogenes* pathogenesis in mice and were required for surviving exposure to lysozyme in the blood.

Rli31 is a 144 nucleotide non-coding RNA that contains a Rho-independent transcriptional terminator and is predicted to be transcribed by the essential housekeeping transcription factor SigA (123). A previous study showed that *rli31* abundance was relatively low during growth in broth but upregulated during infection, and that *rli31* mutants were attenuated fivefold in spleens and livers of infected mice (123). In agreement, we also observed that *rli31* mutants were fivefold attenuated in spleens and livers of infected mice, but in contrast to the previous study, we found that Rli31 was among the most abundant RNAs in *L. monocytogenes*. *pgdA* and *pbpX* were downregulated in the *rli31* mutant, and upregulation of *pgdA* restored lysozyme resistance to the *rli31* mutant. Lastly, the *pgdA pbpX* double mutant was

killed to similar extents as the *pgdA pbpX rli31* triple mutant upon lysozyme treatment, suggesting that the *rli31* mutant phenotype was due to regulation of the two major lysozyme resistance enzymes, *pgdA* and *pbpX*. Small non-coding RNAs (sRNAs) have diverse functions in bacteria, including the regulation of translation, targeting mRNA for degradation, and modulating protein activity (114). It was therefore possible that Rli31 interacted directly with the *pgdA* and *pbpX* transcripts, leading to mRNA degradation or to translational repression. However, both genes contain relatively small 5' UTRs (44 and 26 nucleotides, respectively, (125)), and neither gene contains any homology to Rli31 by BLAST searches, by target prediction programs (TargetRNA (127), RNApredator (128)), or by any other method of measuring homology. In the future we aim to identify the target(s) of Rli31 to explain how Rli31 regulates *pgdA* and *pbpX*.

The results of this and three other studies show that *L. monocytogenes degU* mutants are considerably attenuated in mice (163, 164, 167). Remarkably, DegU was the only response regulator required for *L. monocytogenes* pathogenesis (167). DegU is responsible for expression of chemotaxis and flagellar genes, but chemotaxis genes are not required for *L. monocytogenes* virulence (163, 164, 167, 175). The data presented here suggest that the attenuation of the *degU* mutant *in vivo* is due to lysozyme sensitivity caused by downregulation of *pbpX* and *pgdA*. In *B. subtilis*, DegU is cotranscribed with its cognate kinase, *degS*, but *L. monocytogenes* lacks *degS* and it remains unclear how DegU is regulated post-translationally. Future studies will be required to determine if DegU regulates *pgdA* and *pbpX* directly or indirectly and determine whether this regulation is affected by phosphorylation of DegU.

B. subtilis also encodes *pbpX*, *oatA*, and multiple peptidoglycan deacetylases (102, 112, 176), yet *B.subtilis* is not a pathogen and is significantly more sensitive to lysozyme that *L. monocytogenes*. The minimal inhibitory concentration of lysozyme is 6 μg/ml for WT *B. subtilis* (112), and 2,000 μg/ml for *L. monocytogenes* (data not shown). Therefore, there is over a 300-fold difference between these two species in lysozyme sensitivity despite both encoding highly related enzymes. Why, then, is *L. monocytogenes* so lysozyme-resistant? Our data suggests that *L. monocytogenes* has not acquired novel enzymes to mediate lysozyme resistance, but rather utilizes two regulators of gene expression, DegU and Rli31, to regulate expression of common cell wall modifying enzymes. Therefore, it is the regulation of lysozyme resistance by DegU and Rli31 that accounts for the difference in lysozyme resistance between *L. monocytogenes* and *B. subtilis*. Microarray analysis of the *degU* regulon in *B. subtilis* did not identify *pbpX* or a deacetylase (177), suggesting that *L. monocytogenes* has evolved lysozyme resistance by modifying the DegU regulon to include *pgdA* and *pbpX*. The conservation of these enzymes across bacterial species suggests that these enzymes are also required in non-pathogens for growth and/or for surviving exposure to low concentrations of antibacterial molecules found in the environment. However, overexpression of these enzymes can convert them into factors essential for pathogenesis. A similar mechanism was described during the emergence of *Yersinia pestis* from *Yersinia pseudotuberculosis* (178).

Pathogenic staphylococci are lysozyme resistant due to expression of *oatA* while non-pathogenic species are often lysozyme-sensitive (89, 93). It was previously suggested that these non-pathogens lack *oatA* (93), but simple BLAST searches indicate that genes with high homology to *S. aureus oatA* exist in many non-pathogenic, lysozyme-sensitive *Staphylococci*, including *S. carnosus* (76% identity), *S. xylosus* (77% identity), and *S. equorum* (62% identity). Based on the results of our study, we hypothesize that *oatA* is likely expressed at very low levels in these organisms and is probably upregulated in pathogenic *Staphylococci* by uncharacterized

regulators. Indeed, inducible expression of *S. aureus oatA* in lysozyme-sensitive *S. carnosus* led to increased lysozyme resistance (93). Considering that lysozyme is ubiquitous in the environment, from animal secretions, to plants, to other bacteria, it is perhaps not surprising that even non-pathogenic bacteria are slightly lysozyme resistant (68).

Lysozyme resistance clearly represents a common mechanism of bacterial pathogenesis, as lysozyme-sensitive mutants are severely attenuated in multiple models of infection (92, 104, 179, 180). However, it has been difficult to assign a direct role for lysozyme *in vivo* since mice encode two lysozyme genes, *LysM* and *LysP*. *LysM LysP* double mutant mice do not exist to our knowledge and *LysM*$^{-/-}$ mice still have nearly WT levels of lysozyme in their blood (92, 181). However, bone marrow-derived macrophages from *LysM*$^{-/-}$ mice lack lysozyme and are therefore appropriate models to examine the roles of lysozyme during interaction with macrophages (92). Lysozyme-sensitive *L. monocytogenes* are more susceptible to killing in bone marrow-derived macrophages from B6 mice leading to hyper-induction of multiple inflammatory pathways, but show no differences in *LysM*$^{-/-}$ macrophages (92). Therefore, *pgdA* mutants are clearly more susceptible to killing by lysozyme in macrophages, resulting in increased inflammation. However, these phenotypes do not result in a significant loss of CFU during macrophage infection ((92) and Figure 2.11B). The most striking bactericidal activity observed *in vivo* occurred during the first 30 minutes after i.v. infection, where lysozyme-sensitive bacteria lost over 90% CFU, a phenotype that can be faithfully recapitulated *in vitro* in blood (Figure 2.10). These data suggest that serum is a major host factor responsible for killing lysozyme-sensitive bacteria *in vivo*, at least upon i.v. infection. During oral infection, *L. monocytogenes* disseminates to the liver in blood via the portal vein (14), and a large number of bacteria in the blood is essential for causing meningitis (8, 182). Therefore, exposure to blood is likely to occur during human listeriosis, where *L. monocytogenes* causes meningitis, abortion in pregnant women, and sepsis (8). The results of this and other studies suggest that the role of lysozyme *in vivo* is multifactorial (92, 104, 105, 107, 170), but that serum lysozyme is the major protective factor against lysozyme-sensitive *L. monocytogenes* during i.v. infection. The robust killing of lysozyme-sensitive bacteria *in vivo* illustrates why pathogens have evolved multiple and novel regulatory strategies to rewire the expression of essential cell wall processes to become lysozyme-resistant.

Strains		
Description	**Strain number**	**Reference**
ΔprsA2	DP-L5751	Zemansky *et al.,* (2009)
Δlmo2473	DP-L5958	Sauer *et al*., (2010)
ΔpgdA	DP-L5188	Rae *et al*., (2011)
ΔoatA	DP-L5189	Rae *et al*., (2011)
ΔpgdAΔoatA	DP-L5220	Rae *et al*., (2011)
mprf::Himar1	DP-L5577	Zemansky *et al.,* (2009)
ΔdltA	DP-L6102	This study
Δrli31	DP-L6147	This study
ΔpgdA, rli31::TN917	DP-L6148	This study
ΔoatA, rli31::TN917	DP-L6149	This study
ΔpgdAΔoatA, rli31::TN917	DP-L6150	This study
rli31::TN917	DP-L6151	This study
pgdA::Himar1	DP-L6152	This study
virS::Himar1	DP-L6153	This study
lmo1746::Himar1	DP-L6154	This study
lmo2768::Himar1	DP-L6155	This study
lmo2473::Himar1	DP-L6156	This study
dltD::Himar1	DP-L6157	This study
dltB::Himar1	DP-L6158	This study
pbpX::Himar1	DP-L6159	This study
degU::Himar1	DP-L6160	This study
yycI::Himar1	DP-L6161	This study
prsA2::Himar1	DP-L6162	This study
virR::Himar1	DP-L6163	This study
ΔpgdA, pbpX ::Tn	DP-L6180	This study
ΔpgdA, pbpX ::Himar1, *rli31* ::Tn917	DP-L6181	This study
Δrli31, degU::Himar1	DP-L6182	This study

Table 2.4 Bacterial strains used in Chapter 2

Primers		
Name:	**Description**	**Nucleotides**
TB1	Lmo0540 qPCR F	GGGTATATGTATGCAAATCGTG
TB2	Lmo0540 qPCR R	GGTATATACTTCGAAATTGGATC
TB3	PgdA qPCR F	CAG ATG GAC AGA CTA ATG AAA
TB4	PgdA qPCR R	GGCCATTCTATGCTTTTGGTA
TB5	Rli31 qPCR F	TATCCCATAGAGATTGTCA
TB6	Rli31 qPCR R	TAA TTA TAG CAC AGA ATC TGG G
TB7	*rli31* deletion A	AAAGTCGACATCAGGAGAAATATGGATAGCG
TB8	*rli31* deletion B	ATAATTATAGCACAGAATCTGGGTGGGATAAGTATATCTTACATTACT
TB9	*rli31* deletion C	AGTAATGTAAGATATACTTATCCCACCCAGATTCTGTGCTATAATTAT
TB10	*rli31* deletion D	TTTCTGCAGAAAGTCCGAACCATAGAATCAC
TB11	*rli31* complement F	ATTACGGCCG GCCAATTCCTCCTATATATAAGAT
TB12	*rli31* complement R	ATTAGTCGAC CCTCATTTTCAGAGCATCTCTA
TB13	Rli31 northern probe	AT ATT TCT ATG GGG GAA GTA ATT TAT
TN1	TN sequencing	GCTTCCAAGGAGCTAAAGAGGTCCCTAGCGCC
TN2	TN sequencing	CGGGGAATTTGTATCGATAAGGAATAGATTTAAAAATTTCGCTGTTATTTTG
TN SEQ	TN sequencing	ACAATAAGGATAAATTTGAATACTAGTCTCGAGTGGGG
ARB1	TN sequencing	GGCCACGCGTCGACTAGTACNNNNNNNNNNCTTCT
ARB2	TN sequencing	GGCCACGCGTCGACTAGTAC

Table 2.5 Oligonucleotides used in Chapter 2

Chapter 3

SpoVG and the abundant non-coding RNA Rli31 are opposing, intimately related regulators of gene expression in *Listeria monocytogenes*

3.1 Summary of results:

Bacterial pathogens must resist high concentrations of antibacterial molecules of the innate immune system to successfully establish infection. Not surprisingly, bacterial resistance genes are expressed through complex regulatory processes. Such is the case with *Listeria monocytogenes* resistance to lysozyme, a potent antibacterial molecule found ubiquitously in all animals. Lysozyme resistance is dependent on the highly abundant small non-coding RNA Rli31, yet the target(s) of Rli31 remain unknown. In this study the *spoVG* mRNA and the *spoVG* proteins are described as molecules that oppose the function of Rli31 in relation to lysozyme sensitivity and, independently, in relation to regulating a chitobiose import gene. Deletion of the *spoVG* operon increased lysozyme resistance of 14 previously described lysozyme-sensitive mutants, and the data suggested that an uncharacterized mechanism of lysozyme resistance existed in *L. monocytogenes*. Curiously, the 5' UTR of the *spoVG* operon contained 14/14 nucleotides of perfect complementarity to Rli31, yet the protein was not regulated by the sRNA. In Gram-negative bacteria, chitobiose import genes are regulated by an abundant sRNA and an RNA decoy, which appeared analogous to Rli31 and SpoVG. These findings suggested that, despite over a billion years of divergent evolution and despite non-homologous chitobiose import proteins, RNA mimicry based gene regulation involving an sRNA may be conserved in *L. monocytogenes*. Together, this study characterized Rli31 and SpoVG as intimately related, opposing regulators of gene expression that may regulate one another.

Introduction

Listeria monocytogenes is an intracellular Gram-positive foodborne pathogen and is the causative agent of listeriosis, a serious disease in pregnant women and immunocompromised individuals (8). Pathogenesis of *L. monocytogenes* requires high resistance to antibacterial molecules of the immune system, such as cationic antimicrobial peptides (CAMPs) and lysozyme, which it encounters throughout the course of infection (92, 109). Lysozyme is a major antibacterial molecule in humans and throughout the animal kingdom, and is found in the body at concentrations greater than 1 mg/ml (67, 68, 79, 81). Lysozyme degrades the bacterial cell wall, cleaving the β 1-4 linkage between the N-acetylglucosamine and N-acetylmuramic acid residues that compose peptidoglycan (78, 86).

The peptidoglycan deacetylase PgdA and the O-acetyltransferase OatA are two major enzymes responsible for conferring lysozyme resistance to many pathogens, including *L. monocytogenes*, *Staphyloccocus aureus*, *Helicobacter pylori*, *Streptococcus pneumonia*, and *Bacillus anthracis* (89, 90, 105, 183, 184). By modifying the acetylation state of the cell wall, these enzymes alter peptidoglycan into a poor lysozyme substrate (89, 91). A third enzyme, PbpX, is required for lysozyme resistance of *L. monocytogenes*; however the function of this enzyme remains unclear (90, 103). Loss of lysozyme resistance in *L. monocytogenes* and other pathogens leads to killing in blood, lysis in host cells, and upregulation of proinflammatory cytokines, resulting in a severe attenuation during *in vivo* infection (90, 92, 105, 106).

The lysozyme resistance genes *pgdA*, *oatA*, and *pbpX* are also encoded in non-pathogens, such as *B. subtilis*, but are upregulated in pathogens to confer high lysozyme resistance (90). In *L. monocytogenes*, upregulation of *pgdA* and *pbpX* requires the transcription factor DegU and the abundant small non-coding RNA (sRNA) Rli31 (90). Bacterial sRNAs are an emerging class of gene regulators that function through four principal mechanisms. First, the majority of sRNAs regulate translation by pairing with a complementary ribosomal binding site (RBS) of a target gene (114). Secondly, sRNAs can pair with the coding region of a target mRNA, directing it to

RNAse mediated degradation (114). Third, sRNAs can activate gene expression by relieving the formation of a hairpin in the 5' UTR of an mRNA, which occludes the RBS (114, 115). Lastly, sRNAs can interact with proteins to either inhibit their function or to act together as a ribonucleoprotein complex (116, 117, 185). Predicting sRNA targets *in silico* remains challenging, as a given sRNA may contain significant complementarity to dozens of potential target genes (129).

Numerous sRNAs regulate carbohydrate metabolism in bacteria (186). In *E. coli* and *Salmonella*, an abundant, constitutively expressed sRNA, ChiX (MicM), blocks translation of the chitoporin ChiP (YbfM) to regulate import of chitobiose (130, 131). Chitobiose is a disaccharide composed of two N-acetylglucosamine sugars and is the breakdown product of chitin. Chitin is the second most abundant polysaccharide on Earth besides cellulose, and composes the cell walls of fungi and crustaceans (130, 150). Chitin differs from cellulose because it contains nitrogen, making it a preferable energy source in environments lacking nitrogen (150). Upon detection of chitobiose in these Gram-negative bacteria, a second chitobiose import operon is transcribed, which contains a decoy target for the ChiX sRNA. ChiX is sequestered to this decoy, allowing for translation of ChiP mRNA (130, 131).

L. monocytogenes encodes over 140 sRNAs and nearly 100 antisense RNAs, yet very few *bona fide* targets of these sRNAs have been characterized to date (123, 124, 126). Rli31 was originally identified in a screen for lysozyme-sensitive mutants along with 12 other genes including *pgdA* and *pbpX* (90). The majority of these 13 mutants were also killed by cell wall acting antibiotics and by CAMPs, suggesting that they were not required exclusively for lysozyme resistance; however, *rli31* mutants were uniquely sensitive to lysozyme. This phenotype was principally due to reduced abundance of *pgdA* and *pbpX* transcript and was complemented by *pgdA* overexpression. Rli31 contained no detectable complementarity to PgdA or PbpX transcript, suggesting that this regulation was indirect (90).

spoVG in *Bacillus subtilis* is a Sigma H dependent gene expressed during sporulation, where mutants are defective in late stage sporulation (132, 133). *spoVG* mutants display pleiotropic phenotypes in a variety of firmicutes, including: asymmetric division defects in *B. subtilis* (134), capsule formation defects in *Staphylococcus aureus* (135), decreased secretion of extracellular enzymes in *S. aureus* (136), increased sensitivity to methicillin in *S. aureus* (137), and suppressing ppGpp related defects in *L. monocytogenes* (138). While the mechanism of SpoVG regulation has remained unknown, one study described it as a site-specific DNA binding protein (139). Curiously, translation of SpoVG in *S. aureus* is regulated by a sRNA, SprX (140), and SpoVG protein abundance is increased in mutants of another sRNA, RsaA (141).

In this study, multiple approaches were undertaken to better characterize Rli31. The findings suggested that Rli31 and the protein SpoVG coordinately but oppositely regulated gene expression. An untranslated region of the SpoVG mRNA contained significant complementarity to the apical loop of Rli31, suggesting that the SpoVG mRNA may regulate Rli31 activity by serving as a decoy RNA. These findings illustrate a complex and intimate relationship between Rli31 and SpoVG.

3.2 Results

Secondary structure of Rli31

Secondary structure prediction of Rli31 yielded a 5' hairpin and a 3' transcriptional terminator (187) (Figure 3.1A). To experimentally validate this prediction, Rli31 was cloned into the site-specific integration vector pPL2 with its endogenous promoter and mutations were

constructed in the two hairpins and in the 5' apical loop. These mutants were then introduced into Δ*rli31* and assayed for lysozyme resistance. Wt Rli31 fully complemented lysozyme resistance of Δ*rli31*, while mutations in either the 5' hairpin (mutants A and B) or the 3' hairpin (mutants C and D) resulted in loss of lysozyme resistance (Figure 3.1B). Mutations in the 5' apical loop (mutant E) also resulted in loss of lysozyme resistance (Figure 3.1B). Complementary mutations that rebuilt the 5' hairpin (mutant A+B) or the 3' transcriptional terminator (mutant C+D) restored lysozyme resistance to Wt levels (Figure 3.1C). These results suggested that Rli31 was highly double-stranded, consisting of two long hairpins and a C-rich apical loop.

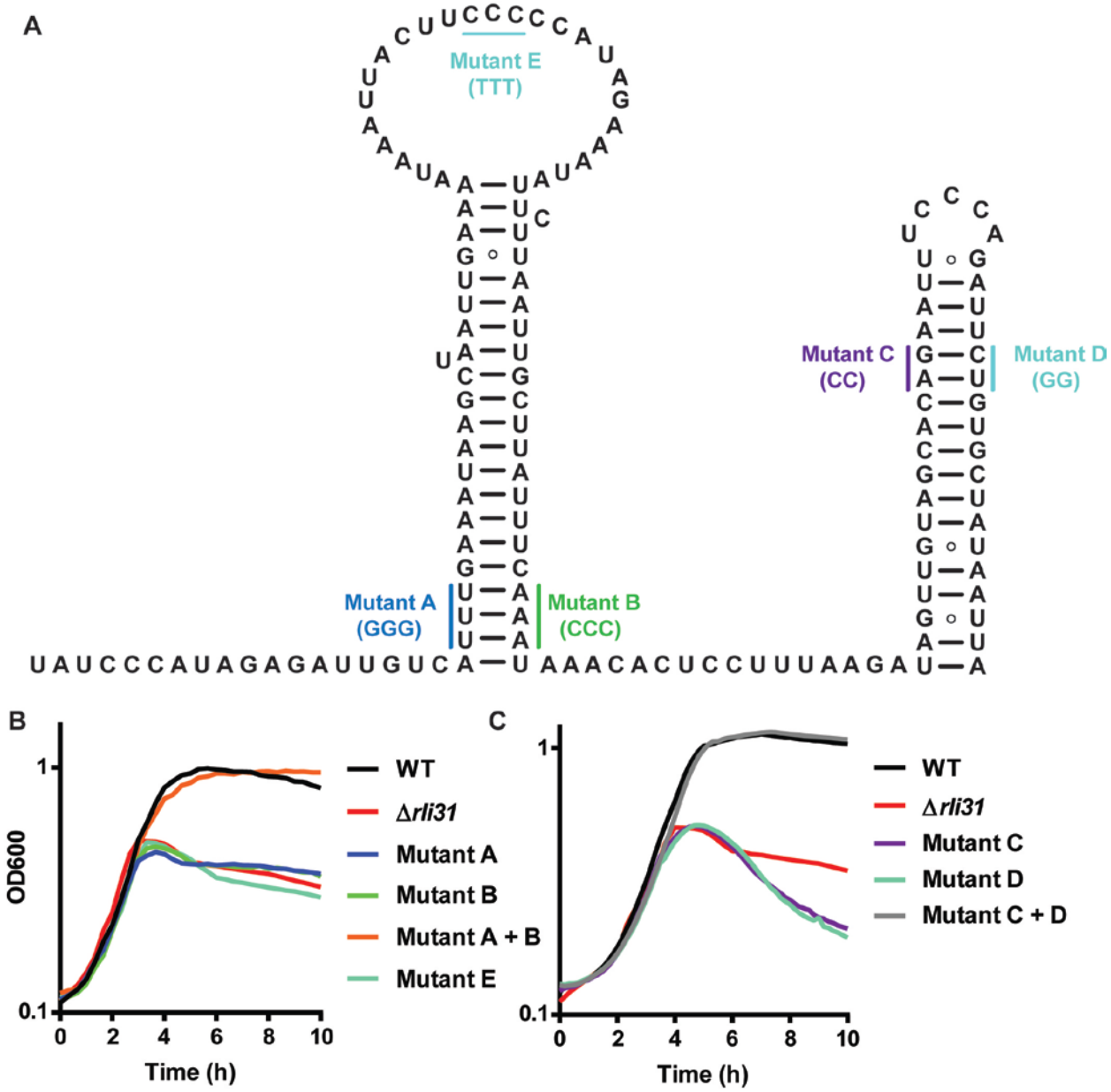

Figure 3.1 Secondary structure of Rli31

A) The secondary structure of Rli31 B,C) The indicated mutations were introduced into *rli31*:pPL2 and integrated into Δ*rli31* bacteria. The indicated strains were grown to mid-

exponential phase and cultures were treated with 1 mg/ml lysozyme. Turbidity was monitored at 10 minute intervals. Data are representative of at least three separate experiments.

Predicted mRNA targets of Rli31

Rli31 contained a C-rich apical loop, typical of sRNAs that interact with G-rich RBSs (188, 189). This region had high complementarity to numerous predicted targets using TargetRNA2, RNApredator, and BLAST (127, 128). The most significant of these targets are listed in Table 3.1, along with the amount of complementarity between Rli31 and the target. Between the various predictions, a commonality existed in relation to carbohydrate metabolism. *lmo0901* (chitobiose/cellobiose PTS component), the *lmo0301* operon (chitobiose PTS component), and *lmo1883* (chitinase A) were all related to metabolism of the disaccharide chitobiose. *lmo2110* (mannose 6-P isomerase) and *lmo1254* (alphaphosphotrehalase) were also related to carbohydrate metabolism. The uncharacterized gene *lmo0196* (*spoVG*) contained the highest complementarity to Rli31 among all the predicted targets, with 14/14 nucleotides of perfect complementarity in the 5' UTR of the mRNA, approximately 70 nucleotides upstream of the RBS; however the function of this protein was unknown.

Although many of the predicted targets were related to carbohydrate metabolism, the screen for lysozyme-sensitive mutants did not identify any mutants related to metabolism. *lmo1743* was a predicted target, and mutants of the *vir* two-component system are lysozyme-sensitive, however these mutants are also killed by cationic peptides and by cell wall antibiotics while Δ*rli31* was not. Therefore *lmo1743* was unlikely to be the lysozyme resistance gene regulated by Rli31. Secondly, the complementarity between Rli31 and many of the predicted targets was either not highly significant (below 12 nucleotides of complementarity) or not at the RBS. We concluded that none of these predictions were obvious Rli31 targets and a forward genetic approach utilizing lysozyme sensitivity suppressor mutations was undertaken to identify the target(s) of Rli31.

Program	Gene	Gene description	Location of complementarity
TargetRNA2			
	lmo0901	Chitobiose PTS component IIC	At RBS, 12/12
	lmo0335	Small uncharacterized protein	35 nt upstream of TSS, 8/8
	lmo1688	Enoyl (acyl carrier protein) reductase	At RBS, 12/13
	lmo1883	Chitinase	At RBS, 8/11
	lmo1277	Tyrosine recombinase XerC	Within ORF, near start codon, 8/9
	lmo1336	5-formyltetrahydrofolate cyclo-ligase	At RBS, 9/9
	lmo0121	Similar to bacteriophage tail protein	At RBS, 7/7
	lmo1743	Within Vir operon	At RBS, 8/8
	lmo1698	Ribosomal protein, alanine N-acetyltransferase	Within ORF, near start codon, 7/7
	lmo1950	Segregation and condensation protein B	At RBS, 7/7
RNApredator			
	Intergenic	Between *lmo0301* and *lmo0302* operons	*lmo0301* operon - chitobiose PTS, 13/13
	lmo0196	*spoVG* operon	5' UTR, 70nt from RBS, 14/14
	lmo1856	Purine nucleoside phosphorylase	Within ORF, 17/18
	lmo0901	Chitobiose PTS component	At RBS, 12/12
	lmo0282	Uncharacterized hydrolase	Within ORF, 10/10
	lmo2377	Multidrug efflux pump	Within ORF, 17/19
	lmo0893	Anti anti sigma factor	At RBS, 13/14
	lmo2109	Uncharacterized hydrolase	Within ORF, 19/23
	lmo2110	Mannose 6P isomerase	Within ORF, 19/24. Distinct from *lmo2109*
	lmo0335	Unknown	35 nt upstream of TSS
	lmo1385	Unknown	Within ORF, 10/10
BLAST			
	lmo0196	*spoVG* operon	5' UTR, 14/14, 70nt from RBS
	Intergenic	Between *lmo0149* and *lmo0150,* unknown proteins	Intergenic region, 16/18
	lmo0901	Chitobiose PTS component IIC	At RBS, 12/12
	lmo1254	Alphaphosphotrehalase	Within ORF, 16/17
	lmo1176	Ethanolamine lyase	Within ORF, 14/15

Table 3.1 Predicted targets of Rli31
Predicted targets of the 5' apical loop of Rli31 using TargetRNA2, RNApredator, and BLAST (128, 190). Transcriptional start sites are abbreviated as TSS and determined from (125).

Identification of suppressor mutations that increase lysozyme resistance
As originally observed by Alexander Fleming upon his discovery of lysozyme in 1922, lysozyme-sensitive bacteria can be repeatedly subcultured with lysozyme until the resulting strain is stably lysozyme-resistant (69, 70). To generate suppressor mutations in *L monocytogenes*, the Δ*rli31* strain was repeatedly passaged with increasing concentrations of lysozyme until the resulting strain was equally resistant to lysozyme as Wt bacteria (Figure 3.2A). This procedure was repeated using Δ*pgdA*, the double mutant *rli31 pgdA*, and the triple mutant *pgdA oatA rli31*. Whole-genome sequencing and variant analysis identified single nucleotide polymorphisms (SNPs) of fourteen individually derived strains. Of the six *rli31* suppressor strains, five contained an identical SNP in the promoter of *pgdA*, twelve nucleotides upstream of the transcriptional start site. qPCR analysis of these strains revealed a three-fold increase in *pgdA* transcript levels (90).

Lysozyme-resistant suppressor strain	Genomic Location	Reference allele	Alteration	Description of mutation
Δ*rli31* #1	436736	-	T	16 nt upstream of *pgdA* TSS
Δ*rli31* #2	436736	-	T	16 nt upstream of *pgdA* TSS
Δ*rli31* #3	436736	-	T	16 nt upstream of *pgdA* TSS
Δ*rli31* #4	193393-195495		Deletion	Region 5' of *lmo0196* (*spoVG*)
Δ*rli31* #5	436736	-	T	16nt upstream of *pgdA* TSS
	2418019	A	-	Intergenic region, 5' of *lmo2387*
Δ*rli31* #6	436736	-	T	16nt upstream of *pgdA* TSS
	2244954	T	-	Frameshift mutation in *lmo2196* (*oppA*)
	2456579	C	G	R164G in *lmo2433* (esterase)
Δ*pgdA* #1	307762	G	T	*lmo0287* (walR) - G92Y
Δ*pgdA* #2	194393	T	-	14 nt 5' of *lmo0196* TSS
	312197	A	G	*lmo0290* (*walI*) - T220A
	1788717	A	C	Silent mutation, *lmo1759*
Δ*pgdA* #3	194393	T	-	14 nt 5' of *lmo0196* TSS
	309675	G	A	*lmo0288* (*walK*) - M430I
	2151278-2151294		Insertion	*lmo2113*
Δ*pgdA* #4	194393	T	-	14 nt 5' of *lmo0196* TSS
	307741	C	T	*lmo0287* (*walR*) - S85F
Δ*pgdA* #5	194393	T	-	14 nt 5' of *lmo0196* TSS
	307792	C	T	*lmo0287* (*walR*) - T102M
Δ*pgdA rli31::* Tn #1	194393	T	-	14 nt 5' of *lmo0196* TSS
	1292872	A	ATTC	Intergenic, between *lmo1305* and *lmo1306*
	732886-732902	-	Insertion	*lmo0720*
	1627292-1627308	-	Insertion	*lmo1625*
	1969473-1969505	-	Insertion	*lmo1938*
Δ*pgdA ΔoatA rli31::* Tn #1	194393	T	-	14 nt 5' of *lmo0196* TSS
	307741	C	T	*lmo0287* (*walR*) - S85F
	559048	C	A	*lmo0540,* in 5' UTR
	622535	C	A	*lmo0600,* N82K
	1093551	-	A	*lmo1079,* frameshift
	2515523	T	-	Intergenic, between *lmo2485* and *lmo2486*
	732886-732902		Insertion	*lmo0720*
	1627292-1627308		Insertion	*lmo1625*
Δ*pgdA ΔoatA rli31::* Tn #2	194393	T	-	14 nt 5' of *lmo0196* TSS
	307741	C	T	*lmo0287* (*walR*) - S85F
	559048	C	A	*lmo0540,* in 5' UTR
	622535	C	A	*lmo0600,* N82K
	1093551	-	A	*lmo1079,* frameshift
	2442569	-	A	*lmo2416,* frameshift
	732886-732902	-	Insertion	*lmo0720*
	1627292-1627308	-	Insertion	*lmo1625*

Table 3.2: Variants identified by whole-genome sequencing of lysozyme-resistant strains
The indicated mutations were mapped to the 10403S genome (GenBank accession number CP002002.1) and SNP/InDel/structural variations were detected (CLC Genomics Workbench, CLC bio). Variations marked as insertions and deletions were structural or InDel mutations and the nature of the mutations was not annotated. Transcriptional start site is abbreviated as TSS and determined from (125).

Seven of the fourteen strains contained single amino acid substitutions in the *walRK* two-component system operon, which is considered essential in many bacteria including *L. monocytogenes* and upregulates expression of autolysins and other cell wall components (156, 159, 167, 191). Five mutations mapped to the response regulator *walR*, one mapped to the

histidine kinase *walK*, and one mapped to *walI*, a negative regulator of *walRK* that is required for lysozyme resistance in *L. monocytogenes* (90). Increased lysozyme resistance was likely conferred through a partial inactivation of WalR, leading to a thicker peptidoglycan layer. Transmission electron microscopy (TEM) of mutants encoding WalR SNPs confirmed this hypothesis (Figure 3.2C,D,), while *walI* mutants had thinner cell walls (Figure 3.2E). Resolution of the cytosol during electron microscopy varied between strains, likely as a result of the penetration of the microscopy reagents. These data implicated the WalRK two-component system as a major contributor to lysozyme sensitivity in *L. monocytogenes*. However, it was unlikely that WalRK was related directly to Rli31, as *walI* mutations led to gross morphological changes such as susceptibility to CAMPs and antibiotics, while mutation of *rli31* did not (90).

Nine of the fourteen strains contained an identical mutation in the promoter of the *spoVG* operon, which contained two paralogs (84% identity) of the gene *spoVG* (*lmo0196* and *lmo0197*). Because this was the most prevalent mutation identified from the whole-genome sequencing and because the *spoVG* 5' UTR contained significant homology to the Rli31 apical loop, we chose to focus on understanding the relationship between SpoVG and Rli31. The remaining variants identified by whole-genome sequencing were not further characterized.

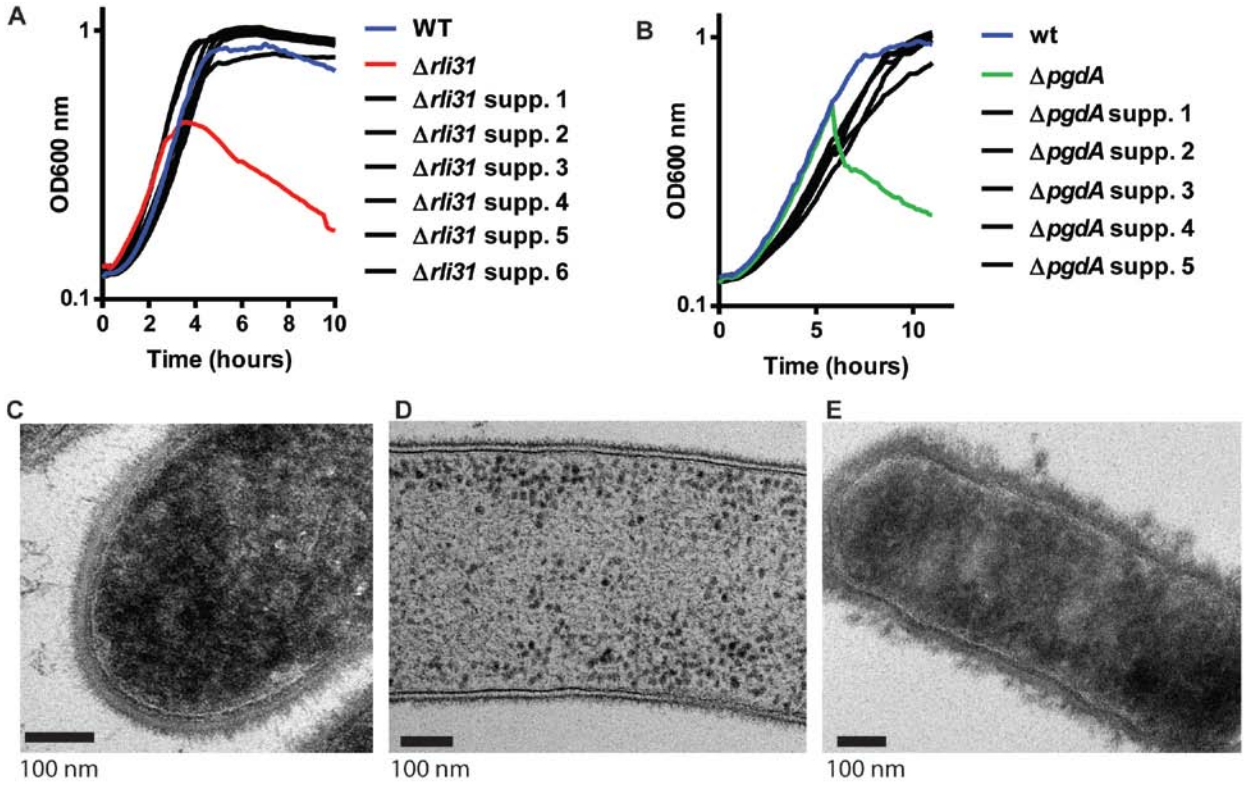

Figure 3.2 Characterization of variants that increase lysozyme resistance
A, B) After repeated subculture of Δ*rli31* and Δ*pgdA* with lysozyme, the resulting strains were grown to mid-exponential phase and treated with 1 mg/ml lysozyme along with the parent strain. Turbidity was monitored at 10 minute intervals and data are representative of at least 3 separate experiments. C) Transmission electron microscopy of WT (C), *walI*::Tn (D), and a *walR* point mutation that increased lysozyme resistance (E).

3.2.2 Deletion of the *spoVG* operon increases lysozyme resistance

The mutation in the promoter of the *spoVG* operon led to a 27-fold downregulation of *spoVG* transcript compared to Wt bacteria, as determined by qPCR (Figure 3.3A). In-frame deletion of both *spoVG* genes and the 5' UTR (hereafter referred to as the *spoVG* mutant) increased lysozyme resistance of Δ*rli31* back to Wt levels (Figure 3.3B). In-frame deletion of the *spoVG* open reading frames (hereafter referred to as the $spoVG_{ORF}$), which left the UTR and promoter intact, also restored lysozyme resistance to *rli31* mutants and behaved identically to the *spoVG* mutant in regards to lysozyme resistance (Figure 3.3B). Introducing stop codons into each *spoVG* paralog in the Δ*rli31* background did not alter lysozyme sensitivity of the *rli31* mutant, suggesting that the function of the paralogs was redundant and perhaps explained why suppressor mutations were identified in the promoter of the operon, rather than an ORF (data not shown). A mutant lacking the *spoVG* operon in the Wt background was significantly more lysozyme-resistant than Wt bacteria, while the *spoVG rli31* double mutant was similar to Wt (Figure 3.3C). Deletion of the *spoVG* operon alone did not affect virulence in mice; however, deletion of the *spoVG* operon increased lysozyme resistance and virulence of Δ*pgdA* during *in vivo* infection by 100-fold and restored *in vivo* attenuation of the *rli31* mutant back to Wt levels (Figure 3.3D,E).

In summary, deletion of *spoVG* in an otherwise Wt background increased lysozyme resistance to be greater than Wt. However, deletion of *rli31* in the *spoVG* mutant background reduced lysozyme resistance to Wt levels. The *rli31* phenotype was similar: deletion of *rli31* significantly reduced lysozyme resistance; however, deletion of *spoVG* in the *rli31* mutant background increased lysozyme resistance to Wt levels. Therefore, the Δ*rli31* phenotype was dependent on *spoVG*, and the Δ*spoVG* phenotype was dependent on *rli31*. These observations indicated that Rli31 and the SpoVG proteins regulated the same target gene in an opposite manner, and perhaps suggested that Rli31 and SpoVG negatively regulate one another.

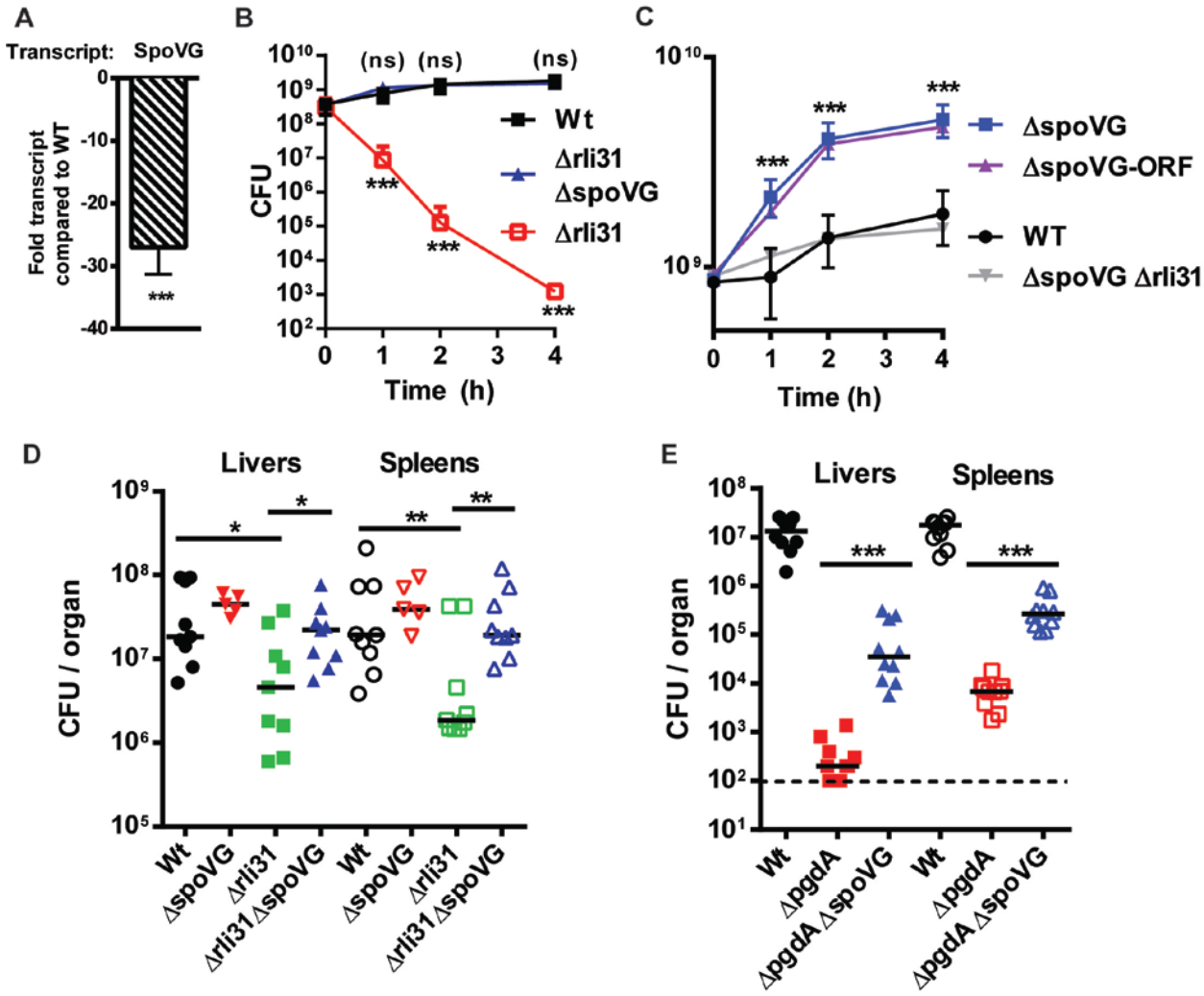

Figure 3.3 Deletion of *spoVG* increases lysozyme resistance and virulence of Δ*rli31* and Δ*pgdA*

A) qPCR analysis comparing Wt bacteria to suppressor strains with mutations in the *spoVG* promoter. Primers were specific for the *spoVG* mRNA (*lmo0196*). B,C) The indicated strains were grown to mid-exponential phase and treated with 1 mg/ml lysozyme, then CFUs were measured at the indicated times. A two-tailed *P* value is reported for each strain in comparison to Wt, where *** indicates $P < 0.0001$. D,E) Data shown represent CFU in organs of CD-1 mice that were infected i.v. for 48h. The data are a combination of two separate experiments totaling at least 8 mice per group, with the exception of Δ*spoVG*, in which the data represent one experiment totaling 5 mice. The dotted line indicates the limit of detection. A two-tailed Mann Whitney T-test was used for statistical analysis for each group, where * indicates $P < 0.05$, ** indicates $P < 0.01$, and *** indicates $P < 0.0001$.

3.2.3 Characterization of the *spoVG* mutant cell wall and lysozyme resistance phenotype

Attempts were made to identify the lysozyme resistance enzyme(s) regulated by Rli31 and SpoVG. To determine if SpoVG regulated one of the fourteen previously characterized lysozyme resistance genes, transposon mutants that conferred lysozyme sensitivity were transduced into Δ*spoVG* and assayed for lysozyme resistance by disk diffusion. Deletion of the

spoVG operon increased lysozyme resistance of all fourteen previously identified lysozyme-sensitive mutants (Figure 3.4A)(90). To determine if the *spoVG* mutant phenotype was specific for lysozyme resistance or if it was a general cell wall defect, the *walI* mutant was transduced into Δ*spoVG* and these mutants were assayed for CAMP resistance using CRAMP. Deletion of *spoVG* did not alter sensitivity of the *walI* mutant towards CRAMP (Figure 3.4B). Similar results were obtained using the CAMP sensitive *mprF* mutant (data not shown). Finally, to determine if the regulation by SpoVG was redundant with the major lysozyme resistance genes, the *pbpX*::Tn mutation was transduced into Δ*pgdA*Δ*spoVG* and this strain was assayed for lysozyme resistance. In this experiment deletion of *spoVG* significantly increased lysozyme resistance of the *pgdA pbpX* double mutant (data not shown). In summary, these data indicated that the *spoVG* mutant phenotype was not due to regulation of a previously characterized lysozyme resistance gene. The same conclusion was previously drawn regarding the *rli31* mutant phenotype, indicating that both SpoVG and Rli31 regulated an uncharacterized lysozyme resistance gene.

Attempts were then made to characterize the *spoVG* mutant cell wall. TEM was performed with Wt and *spoVG* mutants, which revealed that *spoVG* mutants retained normal cell wall thickness but displayed altered cell wall morphology (Figure 3.4C,D). The *spoVG* mutant cell wall appeared significantly smoother than Wt bacteria, which displayed a spikier surface. *spoVG* mutants in *S. aureus* are defective for capsule formation (137), suggesting that this material may be extracellular polysaccharide (EPS). Indeed, *spoVG* mutants were significantly more white than Wt bacteria when grown on agar plates containing congo red, a dye that interacts with β-1,4 sugar linkages that is commonly used to measure biofilm abundance (Figure 3.4E) (192, 193). This finding was recapitulated using bacteria grown in liquid culture (Figure 3.4F) and was quantified by fluorescence (Figure 3.4G). *rli31* mutants were more red than Wt bacteria in this assay when grown on congo red plates (Figure 3.4E). Attempts were made to further characterize this material. Bacteria can produce multiple species of EPS, such as cellulose (194), poly N-acetylglucosamine (PNAG) (195), or strain-specific EPS (192). Wt bacteria were treated with cellulase and β-glucanase in conjunction with lysozyme, but these enzymes did not alter lysozyme sensitivity of Wt bacteria (data not shown). Together, these data suggested that Rli31 and SpoVG regulated an unidentified lysozyme resistance gene, which was likely required for production of a β-1,4 linked sugar modification on the outermost area of the cell wall.

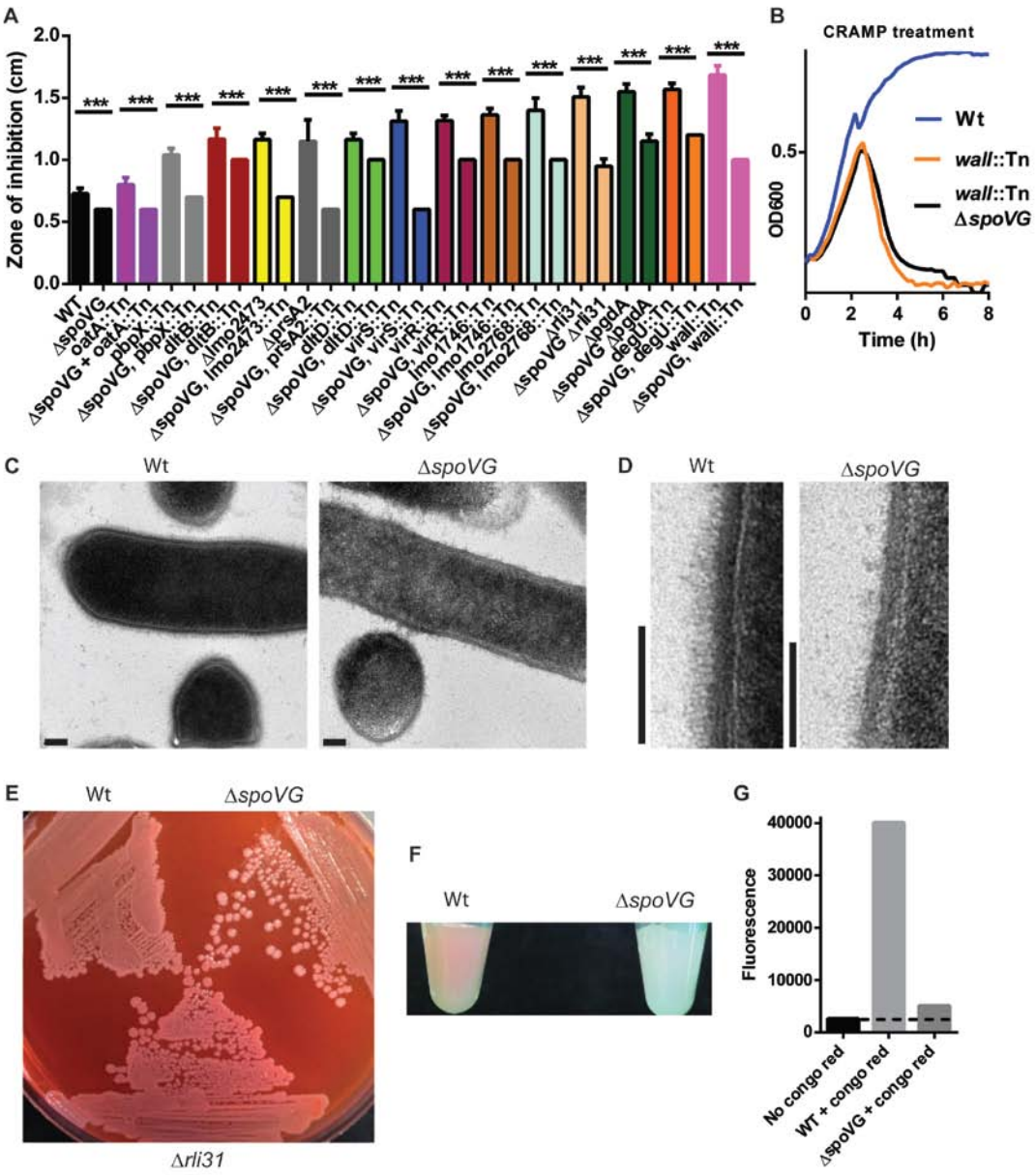

Figure 3.4 Characterization of the *spoVG* mutant cell wall and lysozyme resistance phenotype

A) The indicated strains were spread onto BHI agar and filter disks containing 1 mg of lysozyme were placed onto the agar, incubated overnight at 37^{o}, and zones of clearance were measured. Means and standard deviations from at least 3 separate experiments are presented, where *** indicates $P < 0.001$. B) The indicated strains were grown in BHI media and treated with 50 μg/ml CRAMP at mid-exponential phase. Turbidity was monitored at 10 minute intervals. C) Transmission electron microscopy of the indicated strains. All scale bars represent 100 nm. D) Images shown are representative areas of the cell wall, taken from the images presented in (C). E) The indicated strains were grown on BHI agarose plates containing 40 μg/ml congo red. F) The indicated strains were grown to exponential phase in BHI media containing 80 μg/ml congo red, pelleted by centrifugation, washed, and resuspended in water.

G) Fluorescence intensity was measured from samples shown in (F), excitation/emission spectra were 496/608 nm. The dotted line indicates the emission spectra of bacteria grown with no congo red.

Rli31 does not regulate mRNA or protein abundance of SpoVG

The 5' apical loop of Rli31 contained fourteen nucleotides of perfect complementarity to the 5' UTR of SpoVG that included the C-rich motif CCCCC (Figure 3.5A). We hypothesized that Rli31 regulated SpoVG by either an mRNA degradation mechanism or by inhibiting translation. However, mRNA abundance of SpoVG was unaltered between Wt and Δ*rli31 L. monocytogenes* (Figure 3.5B). SpoVG protein abundance was analyzed by Western blot using a SpoVG-specific antibody (134); however no difference existed between Wt and Δ*rli31* (Figure 3.5C). In these assays, a non-specific band that reacted with an antibody to Listeriolysin-O (LLO) was used as a loading control. Because SpoVG I (Lmo0196) and SpoVG II (Lmo0197) were the same molecular weight, these proteins may have overlapped during Western blot analysis. To determine if Rli31 regulated either paralog, a six-histidine epitope tag was chromosomally added to SpoVG I, which shifted its molecular weight apart from SpoVG II. The *rli31*::Tn mutant was transduced into this strain and Western blot analysis determined that neither SpoVG I nor II was altered by mutation of *rli31* (Figure 3.5D). This assay also determined that SpoVG I was significantly more abundant than SpoVG II. Lastly, as lysozyme resistance genes are upregulated in response to lysozyme in *B. subtilis* and *Enterococcus faecalis* (112, 196), we hypothesized that Rli31 regulated SpoVG in response to lysozyme. A time course of lysozyme treatment revealed that SpoVG abundance was unaltered between Wt and Δ*rli31* bacteria from zero to thirty minutes post-treatment (Figure 3.5E). These data suggested that Rli31 did not alter mRNA nor protein abundance of SpoVG.

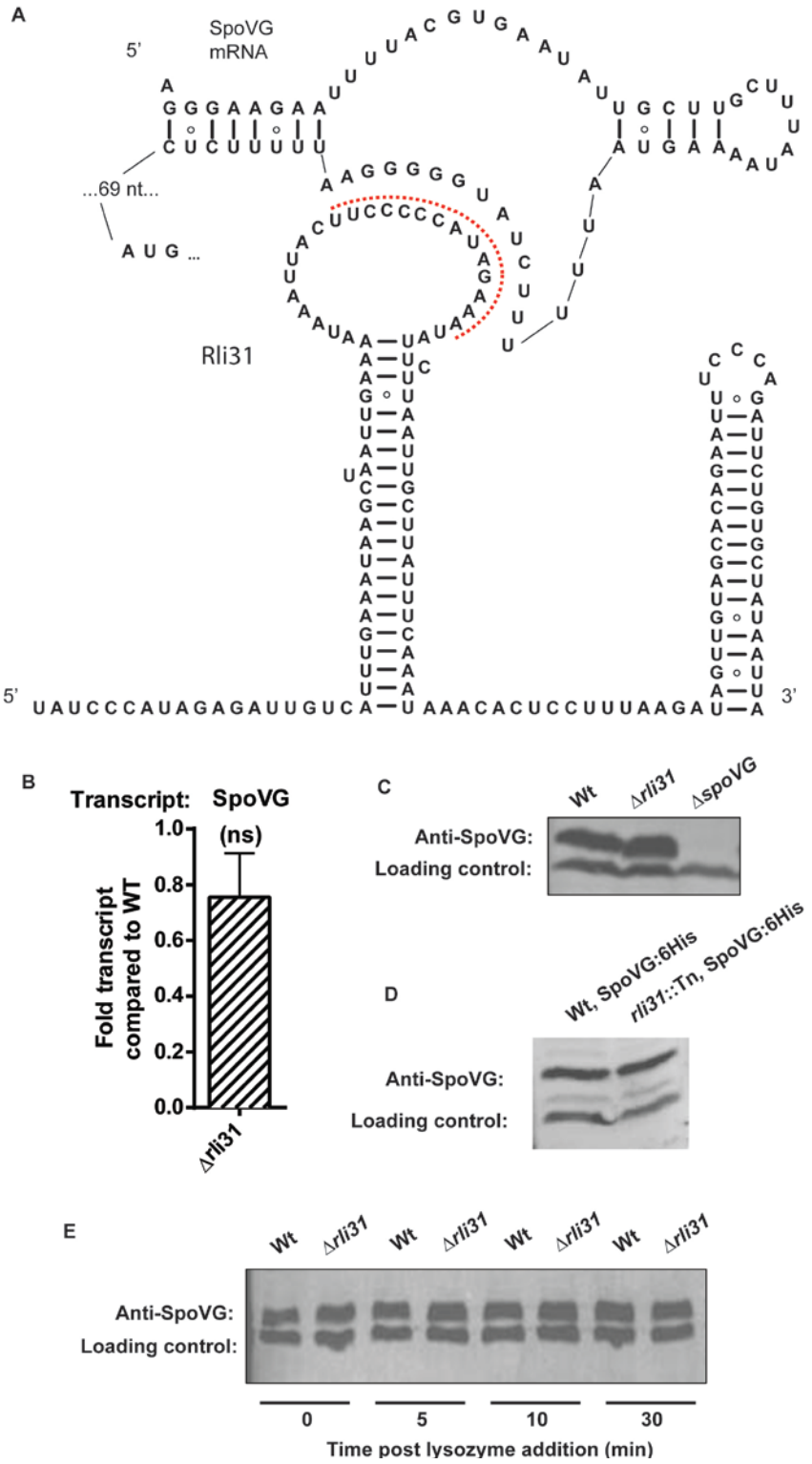

Figure 3.5 Deletion of *rli31* does not affect mRNA nor protein abundance of *spoVG*
A) The secondary structure of Rli31 and the SpoVG mRNA. The red dotted line indicates complementarity between the RNAs. B) qPCR analysis of SpoVG mRNA in *rli31* mutants, as compared to Wt. C,D,E) *L. monocytogenes* lysates were collected from the indicated strains, separated by gel-electrophoresis, and imaged by Western blot using an antibody specific for

SpoVG. A non-specific band that reacted with the LLO antibody was used as a loading control. For E), lysozyme was added at a concentration of 200 μg/ml.

3.2.4 Rli31 and SpoVG regulate the chitobiose import gene Lmo0901

In *Escherichia coli* and *Salmonella*, an abundant, constitutively expressed sRNA blocks translation of the poorly expressed chitobiose import protein ChiP (130, 131, 197). The sRNA is sequestered by a decoy RNA, which allows for translation of ChiP (130, 131). The Rli31/SpoVG regulatory system appeared analogous to the decoy mechanism in Gram-negative bacteria because the SpoVG 5' UTR contained significant complementarity to Rli31 but SpoVG was not regulated by Rli31. Secondly, Rli31 contained significant complementarity to the RBS of the chitobiose PTS component Lmo0901 (Table 1).

To test if Rli31 regulated translation of Lmo0901, the promoter, 5' UTR, and first 10 amino acids of *lmo0901* were fused to GFP, cloned into pPL2, and integrated into *L. monocytogenes*. Western blot analysis determined that *lmo0901* expression was upregulated in Δ*rli31* bacteria when compared to Wt (Figure 3.6A). qPCR analysis of Wt and Δ*rli31* bacteria determined that Lmo0901 transcript was unaltered between these strains (data not shown) suggesting that Rli31 inhibited Lmo0901 translation by pairing with the Lmo0901 RBS. To test if the RBS was involved with this regulation, a single nucleotide mutation was introduced to the *lmo0901* RBS, altering it from GGGGG to GGAGG. Abundance of Lmo0901 was reduced to Wt levels in the *rli31* mutant in this assay (Figure 3.6B). The *spoVG* mutant was also included in these experiments, and curiously, Lmo0901 abundance was significantly reduced in this mutant (Figure 3.6A). This phenotype was likely not due to regulation of Rli31, as Lmo0901 protein was also reduced upon mutation of the RBS (Figure 3.6B). These data suggested that SpoVG regulated protein abundance of Lmo0901 independently of Rli31.

To determine if regulation of *lmo0901* was responsible for the lysozyme phenotypes of the *rli31* and *spoVG* mutants, an in-frame mutant of *lmo0901* was generated in the Wt, *rli31*, and *spoVG* backgrounds. Deletion of *lmo0901* did not affect lysozyme resistance of Wt or *spoVG* mutant bacteria and did not significantly increase lysozyme resistance of the *rli31* mutant (Figure 3.6D,E). This finding suggested that the regulation of Lmo0901 by Rli31 and SpoVG was independent of their regulation of lysozyme resistance gene(s).

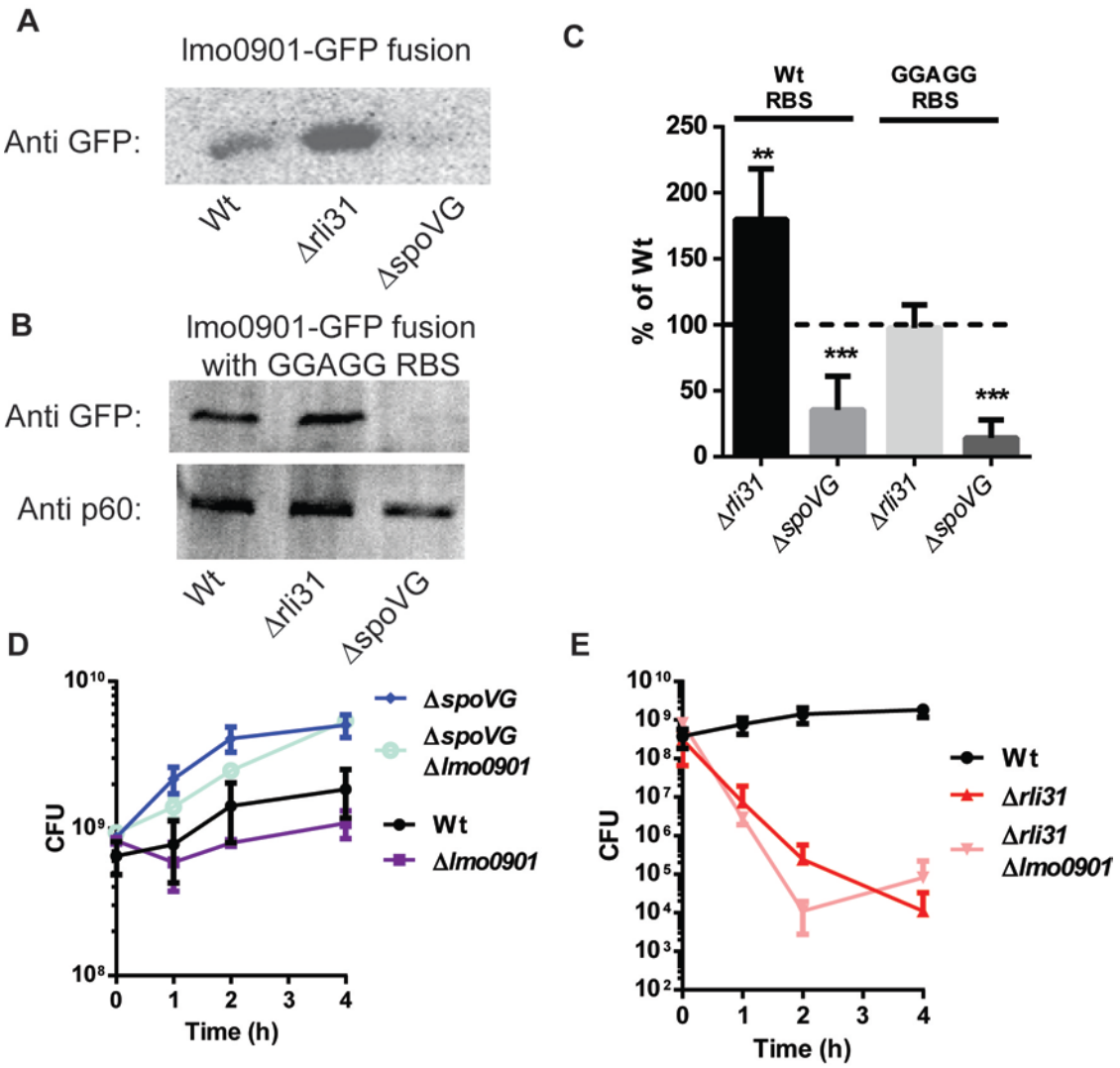

Figure 3.6 Regulation of Lmo0901 transcript by Rli31 and SpoVG

A,B) 30 ml of the indicated strains were grown to mid-exponential phase in LB media, collected by centrifugation, and lysed by bead-beating and boiling in buffer containing SDS. Protein abundance was normalized to OD_{600} and soluble proteins were separated by denaturing gel electrophoresis. Western blot analysis using anti-GFP was performed for a minimum of six separate experiments in (A) and at least two separate experiments in (B) Abundance of Lmo0901-GFP in *rli31* and *spoVG* mutants was quantified and is illustrated as a comparison to Wt in (C). p60 abundance was measured as a loading control. Means and standard deviations are presented, where *** indicates $P < 0.005$. D) The indicated strains were grown to mid-exponential phase in BHI and treated with 1 mg/ml lysozyme, then CFUs were measured at the indicated times. Data represent the means and standard deviations of at least 3 separate experiments, where no significant difference was observed between the *lmo0901* mutants and their respective background strains at any time point.

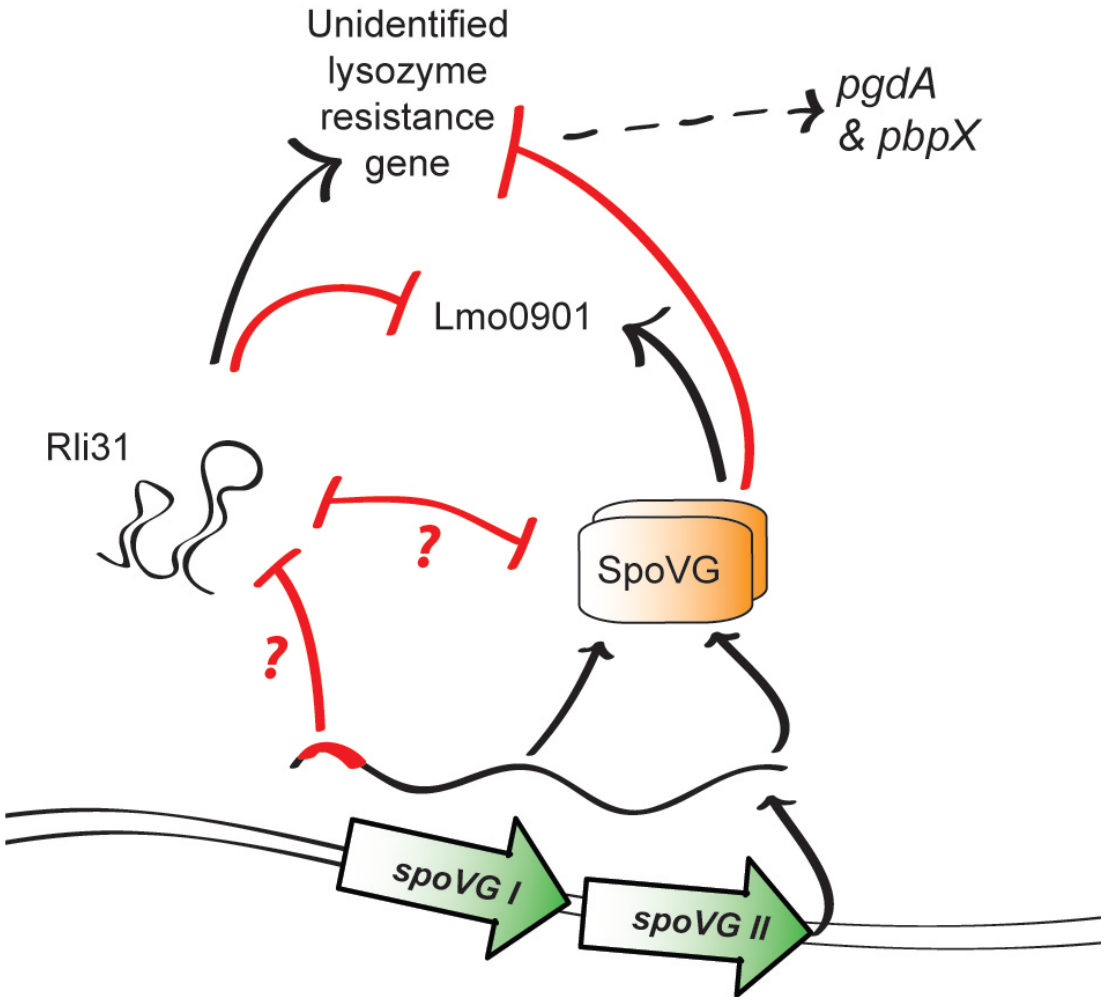

Figure 3.7 Model of Rli31 and SpoVG regulation
A model is proposed whereby SpoVG and Rli31 independently regulate Lmo0901 and, separately, an unidentified lysozyme resistance gene. Rli31 negatively inhibits expression of Lmo0901 through a base-pairing mechanism at the RBS, while SpoVG regulates this gene by an unknown mechanism. Rli31 and SpoVG maintain opposite phenotypes in relation to lysozyme resistance, but deletion of both genes results in a Wt phenotype, suggesting that their phenotypes are dependent on one another and that these molecules may negatively regulate one another. mRNA abundance of *pgdA* and *pbpX* is reduced in *rli31* mutants, suggesting indirect regulation, as represented by dotted lines. The SpoVG mRNA contained 14/14 nucleotides of perfect homology to the Rli31 apical loop, but SpoVG translation was not regulated by Rli31, which may suggest that this mRNA functions as a decoy target for Rli31.

3.3 Discussion

This study sought to characterize the abundant non-coding RNA Rli31, and subsequently understand the relationship between Rli31 and SpoVG. Both Rli31 and SpoVG regulated expression of the chitobiose import gene *lmo0901*, and separately, regulated expression of an unknown lysozyme resistance gene(s). The lysozyme resistance phenotypes of these mutants suggest that Rli31 and SpoVG may negatively regulate one another. The secondary structure of

Rli31 was determined, and the apical loop contained 14/14 nucleotides of perfect complementarity to the 5' UTR of the *spoVG* mRNA, but Rli31 did not regulate protein nor mRNA abundance of *spoVG*. Together, these findings suggested a model whereby Rli31 and SpoVG function as opposing regulators of gene expression in *L. monocytogenes*, and may also regulate one another by two separate mechanisms (Figure 3.7).

A complex mechanism involving a sRNA and an RNA decoy in *E. coli* and *Salmonella* for regulating chitobiose import genes appears analogous to Rli31 and SpoVG (130, 131). Both sRNAs are abundant and constitutively expressed; the target gene is poorly expressed and is a chitobiose import protein, and an RNA decoy exists on the mRNA of an operon that is involved with sugar metabolism (130, 131). From these data we conclude that the RNA mimicry mechanism has been conserved for chitobiose import across billions of years of evolution, despite no conservation of the required proteins at the amino acid level (198). This conclusion is surprising given the complexity of the regulatory mechanism. Considering that two sRNAs regulate expression of SpoVG in the Gram-positive pathogen *S. aureus*, we hypothesize that intimate regulatory mechanisms between sRNAs and SpoVG exist in *S. aureus* and across the firmicute clade (140, 141).

The original purpose of this study was to identify the lysozyme resistance gene(s) regulated by Rli31. Instead, another regulator of gene expression was identified that was also not epistatic with any of the 14 previously described lysozyme-sensitive mutants. These data suggested that a previously uncharacterized mechanism of lysozyme resistance existed in *L. monocytogenes* and was regulated by Rli31 and SpoVG. We sought to characterize this phenotype and observed morphological differences between the *spoVG* mutant cell wall and Wt. The Δ*spoVG* cell surface appeared to lack a outer cell wall modification, and because the *spoVG* mutant bound significantly less congo red than Wt, we hypothesize that this material is a β-1,4 linked sugar, likely either peptidoglycan or EPS. In *Streptococcus suis*, strains producing less capsule due to mutation of a glycosyltransferase had increased resistance to lysozyme (96). We hypothesize that the unknown gene is either a glycosyltransferase responsible for EPS production or a carboxypeptidase responsible for cell wall cross-linking. The production of capsule in other organism such as *Staphylococcus aureus* has been well appreciated, yet the discovery of EPS production in *L. monocytogenes* remains relatively recent (192, 193). Future studies aim to identify this gene and to better understand the role that EPS production plays in terms of *L. monocytogenes* pathogenesis.

It remains unclear how *pgdA* and *pbpX* are downregulated in the *rli31* mutant, which is responsible for its lysozyme sensitivity phenotype (90). Because no homology exists between Rli31 and the PgdA/PbpX mRNAs, it is unlikely that Rli31 regulates these genes directly. Rather, *pgdA* and *pbpX* are likely regulated in response to signals relating to cell wall homeostasis, and thus the downregulation of *pgdA* and *pbpX* in Δ*rli31* may be an indirect consequence relating to the abundance of certain sugars used as peptidoglycan precursors or to the expression of the unknown cell wall modifying enzyme.

These findings suggest that Rli31 regulates at least two genes in *L. monocytogenes* and we speculate that it regulates many more. Among the other predicted targets of Rli31, many are involved with carbohydrate metabolism. The intergenic region between the *lmo0301* and *lmo0302* operons is predicted to be the best Rli31 target by RNApredator. Curiously, the *lmo0301* operon is another chitobiose PTS operon, and expression of the *lmo0302* operon is controlled by another sRNA, LhrA, which also controls expression of the chitinase ChiA (199). The multitude of putative targets relating to sugar metabolism may suggest that Rli31 is either

controlled by multiple decoy RNAs, or alternatively, that Rli31 controls expression of many of these genes. The idea that RNA sponges are prevalent in bacteria has been proposed previously (129, 130, 149, 200); however, limited examples exist. Future endeavors in the field of sRNA mediated gene regulation in bacteria will help understand what distinguishes between a *bona fide* target of an sRNA vs. a decoy.

Table 3.3 - *L. monocytogenes* strains used in this chapter
Wt 10403S
Δ*rli31*
Δ*rli31* + pPL2:*rli31*
Δ*rli31* + pPL2:*rli31* Mutant A
Δ*rli31* + pPL2:*rli31* Mutant B
Δ*rli31* + pPL2:*rli31* Mutant A+B
Δ*rli31* + pPL2:*rli31* Mutant C
Δ*rli31* + pPL2:*rli31* Mutant D
Δ*rli31* + pPL2:*rli31* Mutant C+D
Δ*rli31* + pPL2:*rli31* Mutant E
Δ*rli31* suppressor #1
Δ*rli31* suppressor #2
Δ*rli31* suppressor #3
Δ*rli31* suppressor #4
Δ*rli31* suppressor #5
Δ*rli31* suppressor #6
Δ*pgdA*
Δ*pgdA* suppressor #1
Δ*pgdA* suppressor #2
Δ*pgdA* suppressor #3
Δ*pgdA* suppressor #4
Δ*pgdA* suppressor #5
Δ*pgdA, rli31*::Tn
Δ*pgdA, rli31*::Tn suppressor #1
Δ*pgdA* Δ*oatA,* rli31::Tn
Δ*pgdA* Δ*oatA,* rli31::Tn suppressor #1
Δ*pgdA* Δ*oatA,* rli31::Tn suppressor #2
Δ*spoVG*
Δ*spoVG-ORF*
Δ*rli31* + stop codon in *spoVG I*
Δ*rli31* + stop codon in *spoVG II*
Δ*rli31* Δ*spoVG*
Δ*spoVG* Δ*pgdA*
rli31::TN917
pgdA::Himar1
virS::Himar1
lmo1746::Himar1
lmo2768::Himar1
lmo2473::Himar1

dltD::Himar1
dltB::Himar1
pbpX::Himar1
degU::Himar1
yycI::Himar1
prsA2::Himar1
virR::Himar1
*oatA::*Tn
ΔspoVG + rli31::TN917
ΔspoVG + pgdA::Himar1
ΔspoVG + virS::Himar1
ΔspoVG + lmo1746::Himar1
ΔspoVG + lmo2768::Himar1
ΔspoVG + lmo2473::Himar1
ΔspoVG + dltD::Himar1
ΔspoVG + dltB::Himar1
ΔspoVG + pbpX::Himar1
ΔspoVG + degU::Himar1
ΔspoVG + yycI::Himar1
ΔspoVG + prsA2::Himar1
ΔspoVG + virR::Himar1
ΔspoVG + *oatA*::Tn
10403S, chromosomal *spoVG I*:6His
Chromosomal *spoVG I*:6His + *rli31*::Tn
WT + pPL2:*lmo0901*-GFP fusion
Δ*rli31* + pPL2:*lmo0901*-GFP fusion
Δ*spoVG* + pPL2:*lmo0901*-GFP fusion
WT + pPL2:*lmo0901*-GFP fusion, with GGAGG RBS
Δ*rli31* + pPL2:*lmo0901*-GFP fusion, with GGAGG RBS
Δ*spoVG* + pPL2:*lmo0901*-GFP fusion, with GGAGG RBS
Δ*lmo0901*
Δ*rli31* Δlmo0901
Δ*spoVG* Δlmo0901

Table 3.4 Oligonucleotides used in Chapter 3	
TB14 Rli31 Mutant A Forward	cccatagagattgtcaggggaaataagctaattgaaaataaa
TB15, Rli31 mutant A Reverse	tttattttcaattagcttatttcccctgacaatctctatggg
TB16, Rli31 mutant B Forward	cttaattgcttatttcccctaaacactcctttaagatag
TB17, Rli31 mutant B Reverse	ctatcttaaaggagtgtttaggggaaataagcaattaag
TB18, Mutant D Forward	gatagttgtagcacCCaatttcccagattGGg
TB19, Mutant D Reverse	cCCaatctgggaaattGGgtgctacaactatc
TB20 Mutant C Forward	cagaatttcccagattgggtgctataattatgtagaaatag
TB21 Mutant C Reverse	ctatttctacataattatagcacccaatctgggaaattctg
TB22 Mutant E Forward	gaaaataaattacttttccatagaaatattcttaattgcttatttc
TB23 Mutant E Reverse	gaaataagcaattaagaatatttctatggaaaaagtaatttattttc
TB140: rli31 promoter Forward with EagI	attaCGGCCG gccaattcctcctatatataagat
TB141: rli31 Reverse with SalI	attaGTCGAC cctcattttcagagcatctcta
TB211: lmo0196/7 deletion A - Forward -BamHI	tca ggatcc gaataactgcaggaaccattatattctcct
TB212: lmo0196/7 deletion B - Reverse	tgaaaattttaaattattcagcagaaacggtattcacgtaaaattcttccctatgaaca
TB213: lmo0196/7 deletion C -Forward	tgttcatagggaagaattttacgtgaataccgtttctgctgaataatttaaaatttttca
TB214: lmo0196/7 deletion D - Reverse – SalI	gta gtcgac ctacaatgcctaggtcatcacgagataac
TB248: lmo0196/7 Forw from UTR with BamHI, for stop codons	tca ggatcc agggaagaattttacgtgaatattgctt
TB249: lmo0196/7 Rev from TT, with SalI, for pKSV7	gta gtcgac catagccaaaatagaagaccaaggc
TB274: SpoVG Rev from stop, to add his tag	gttttcttctacaatactttcgtctgc
TB275: SpoVG For from stop, with his tag	catcatcatcatcatcat taaaaaaatcctcggttagggagaacg
TB281: SpoVG I Stop, Forward	c gta gct atg cct agt TAA cgt acg ccg gat ggt gag ttt ag
TB282: SpoVG I Stop Reverse	ctaaactcaccatccggcgtacgTTAactaggcatagctacg
TB283: SpoVG II Stop Forward	c gta gct atg cca agt TAA cgt ggt gtt gac ggt gaa ttc cg
TB284: SpoVG II Stop Reverse	cggaattcaccgtcaacaccacgTTAacttggcatagctacg
TB508: lmo0901 delete A, KpnI, forward	GTACA GGTACC TGATGAATATATTACCCAAGCGCC
TB313: lmo0901 deletion B, Forw, with tail for SOE	AACGTTTTCTTTTTAGAAAAATATCATGTT AGAGAATCAGAGGCGGCTATCAAATAAGTT
TB314: lmo0901 deletion C, Reverse, for SOE	AACATGATATTTTTCTAAAAAGAAAACG
TB509: lmo0901 delete D,SalI, reverse	AATTC GTCGAC AATTTGTAAACCGGTTGATCTGC

TB584: A forward for lmo0901 SOE, with EagI	atcg cggccg CTCGGAAATTACAAGCATTCAAAAGGC
TB585: B, reverse, for lmo0901 SOE	agttcttctcctttgctagcTTCCCCAAGTAACTCCATAA ACTTATTCAC
TB586: SOE forward, for lmo0901 GFP SOE	TTTATGGAGTTACTTGGGGAAgctagcaaaggagaa gaacttttcact
TB304: GFP Reverse , for lmo0901 SOE	ctat ctgcag tcaccgacaaacaacagataaaacg
TB604: lmo0901 qPCR , try2 Forward	GATGCATTCATGTTGGCATTTCC
TB605: lmo0901 qPCR try2 Reverse	ACAGTCATAATACTCATCGTGGC
TB607: lmo0901 RBS from GGGGG to GGAGG, Forward	GGAAGTAAAGTGAATAAGTTTATGG
TB608: lmo0901 RBS mutation, Reverse	TCCAAACATGATATTTTTCT
TB216: lmo0196 Forward, for qPCR	gtgagattacgacgtgttgagaca
TB217: lmo0196 Reverse, for qPCR	ggatgagcgatatctctaaactcac

Chapter 4

SpoVG is a methylated RNA-binding protein required for swarming motility of *Listeria monocytogenes*

4.1 Summary:

Listeria monocytogenes is a Gram-positive bacterial pathogen that encodes over 100 small non-coding RNAs (sRNAs) and Hfq, an RNA chaperone protein that mediates mRNA:sRNA interactions. Mutants of *hfq* in proteobacteria often display severe, pleiotropic phenotypes, while *hfq* mutants in firmicutes are viable and display few phenotypes for unknown reasons. In this study mutants of the uncharacterized gene regulator *spoVG* were observed to be non-motile in semisolid agar, and suppressor mutations that increased swarming motility mapped to RNAse J1, Rho, and NusG. We hypothesized that SpoVG interacted directly with nucleic acid, and indeed purified SpoVG bound with high affinity and specificity to multiple sRNAs *in vitro*. SpoVG did not bind to the 6S RNA or the SRP RNA, which have known protein partners. Analysis of the SpoVG crystal structure revealed two positively charged grooves that may be responsible for nucleotide binding, suggesting a model by which SpoVG binds RNA. From these findings and from numerous other studies describing *spoVG* mutant phenotypes across the firmicute clade, we propose that SpoVG represents a new class of RNA-binding proteins in Gram-positive bacteria, whose function may be analogous to, or an alternative to, Hfq in Gram-negative bacteria.

Introduction

L. monocytogenes is a Gram-positive bacterial foodborne pathogen that causes listeriosis, one of the most fatal bacterial diseases contracted by humans (8). The organism is ubiquitous in the environment and lives on decaying plant matter, environmental water sources, and in soil (1, 2). Due to its genetic manipulability, fast growth rate, and well-understood intracellular lifecycle, *L. monocytogenes* has served as a useful model bacterial organism (53). Several studies have contributed to identifying over 200 non-coding RNAs in the bacteria, yet only a handful have been studied individually and even fewer have known targets (120, 122-125, 199, 201-204).

Bacterial sRNAs are an emerging class of gene regulators that function through four principal mechanisms. First, the majority of sRNAs regulate translation by pairing with a complementary ribosomal binding site (RBS) of a target gene (114). Secondly, sRNAs can pair with the coding region of a target mRNA, directing it to RNAse mediated degradation (114). Alternatively, sRNAs can activate gene expression by relieving the formation of RBS-occluding hairpins in the 5' UTR of an mRNA (114, 115). Lastly, sRNAs can interact with proteins to either inhibit their function or to act together as a ribonucleoprotein complex (116, 117, 185). Predicting sRNA targets *in silico* remains challenging, as a given sRNA may contain significant complementarity to dozens or perhaps hundreds of potential target genes (129).

In proteobacteria such as *Escherichia coli* and *Salmonella*, the proteinaceous RNA chaperone Hfq often mediates sRNA:mRNA interactions by serving as a platform for RNA binding. Hfq has a multitude of regulatory roles involving sRNAs, including: protecting RNA from RNAse E mediated degradation (118, 205), leading to RNA degradation by RNAse E (118), and interacting with Rho to inhibit transcriptional termination (206). Not surprisingly, *hfq* mutants in proteobacteria display severe pleiotropic phenotypes, such as attenuated virulence, loss of motility, and an inability to form biofilms (119). Hfq in the firmicute clade, however, is less necessary for sRNA:mRNA interactions . Few interactions have been reported between sRNAs and Hfq in Gram-positive organisms, and *hfq* mutants display few remarkable phenotypes (119-121). Mutants of *hfq* in *S. aureus* displayed no growth defect, no defect in stress tolerance, no defect in secreted proteins, and high-throughput phenotypic analysis did not detect any *hfq* mutant phenotype among ~2,000 tested phenotypes (121). Mutants of *hfq* in *L.*

monocytogenes are viable and are sensitive towards certain stresses, such as high concentrations of ethanol and salt, and are 10-fold attenuated *in vivo* (207). Co-immunoprecipitation experiments with Hfq in *L. monocytogenes* identified 3 interacting RNAs (120). In contrast, co-immunoprecipitation experiments with Hfq in the Gram-negative *Salmonella* identified over 700 mRNA and over 60 sRNA interactors (208).

Rli31 is one of the most abundant *L. monocytogenes* sRNAs and is required for resistance to lysozyme, a cell wall degrading enzyme of the host innate immune system. Rli31 has a complex relationship with the protein SpoVG, as both molecules regulated lysozyme resistance genes and independently regulate a chitobiose import gene. The SpoVG mRNA contains 14/14 nucleotides of perfect complementarity in its 5' UTR to the apical loop of Rli31, yet Rli31 does not regulate SpoVG translation. This complementarity may serve as a decoy that regulates Rli31 expression; however the role of SpoVG UTR remains unclear.

spoVG in *Bacillus subtilis* is a Sigma H dependent gene expressed during sporulation, where mutants are defective in late stage sporulation (132, 133). *spoVG* mutants display pleiotropic phenotypes in a variety of firmicutes, including: asymmetric division defects in *B. subtilis* (134), capsule formation defects in *Staphylococcus aureus* (135), decreased secretion of extracellular enzymes in *S. aureus* (136), increased sensitivity to methicillin in *S. aureus* (137), and increased resistance to lysozyme in *L. monocytogenes* (Figure 3.3). The mechanism of SpoVG regulation has remained unknown and SpoVG contains no detectable homology to any protein of known function; however one study described it as a site-specific DNA binding protein (139). Translation of SpoVG in *S. aureus* is regulated by an sRNA, SprX (140), and SpoVG protein abundance is increased in mutants of another sRNA, RsaA (141). The *spoVG* operon in many bacteria resides within a cluster of genes relating to purine metabolism, including *prs* and *purR*, and deletion of *spoVG* rescues phenotypes related to ppGpp deficiencies in *L. monocytogenes* (138).

This study sought to better characterize SpoVG and determined that it is an RNA binding protein that is required for swarming motility in *L. monocytogenes*. These findings and others indicate that SpoVG and Hfq have many features in common, and we conclude that SpoVG may serve a similar function in the firmicutes as Hfq serves in proteobacteria.

4.2 Results:

4.2.1 SpoVG is required for swarming motility of *L. monocytogenes*

spoVG mutants in *L. monocytogenes* were more resistant to lysozyme than Wt bacteria, and *spoVG* mutants in *S. aureus* were defective for secretion of extracellular enzymes (136). These data suggested that an extracellular enzyme required for lysozyme resistance may be differentially secreted in the *L. monocytogenes spoVG* mutant. To assess secreted proteins, supernatants from exponentially growing bacteria were precipitated, separated by electrophoresis, and visualized by coomassie staining (Figure 4.1A). One band appeared in Wt precipitates that was lost in Δ*spoVG*, and mass spectrometry identified this protein as flagellin (FlaA). In-frame deletion of *flaA* in *L. monocytogenes* did not alter lysozyme resistance (data not shown); however these data suggested that *spoVG* may be required for proper expression of motility genes.

To determine if *spoVG* mutants displayed reduced swarming motility, 30^{o} C stationary phase cultures were stab inoculated into semisolid agar plates and grown for three days at 30^{o} C. Compared to Wt bacteria, *spoVG* mutants appeared rough, densely populating the original zone of inoculation, and displayed a significant reduction in swarming motility (Figure 4.1B). This

phenotype was consistent between *spoVG* mutants lacking both copies of *spoVG* and the 5' UTR of this operon (herafter referred to as the *spoVG* mutant) and mutants lacking only the open reading frames of the *spoVG* paralogs (the $spoVG_{ORF}$ mutant). Observation using light microscopy of *spoVG* mutants in liquid culture determined that the bacteria appeared motile and did not chain, suggesting that this phenotype was specific to swarming motility in semi-solid media.

qPCR analysis of *spoVG* mutants determined that transcripts of genes within the major flagellar operon (*fliN*, *fliP* and *gmaR*) were similar to Wt bacteria. Transcript levels of the regulators of flagellar expression (*degU* and *mogR*) were also similar to Wt; however transcript levels of *flaA* were reduced 10-fold below Wt (Figure 4.1D). These data suggested that the *spoVG* proteins were required for swarming motility through regulation of *flaA*, and that a small amount of *flaA* expression was likely sufficient to appear motile in broth, but was not sufficient for motility in semisolid media.

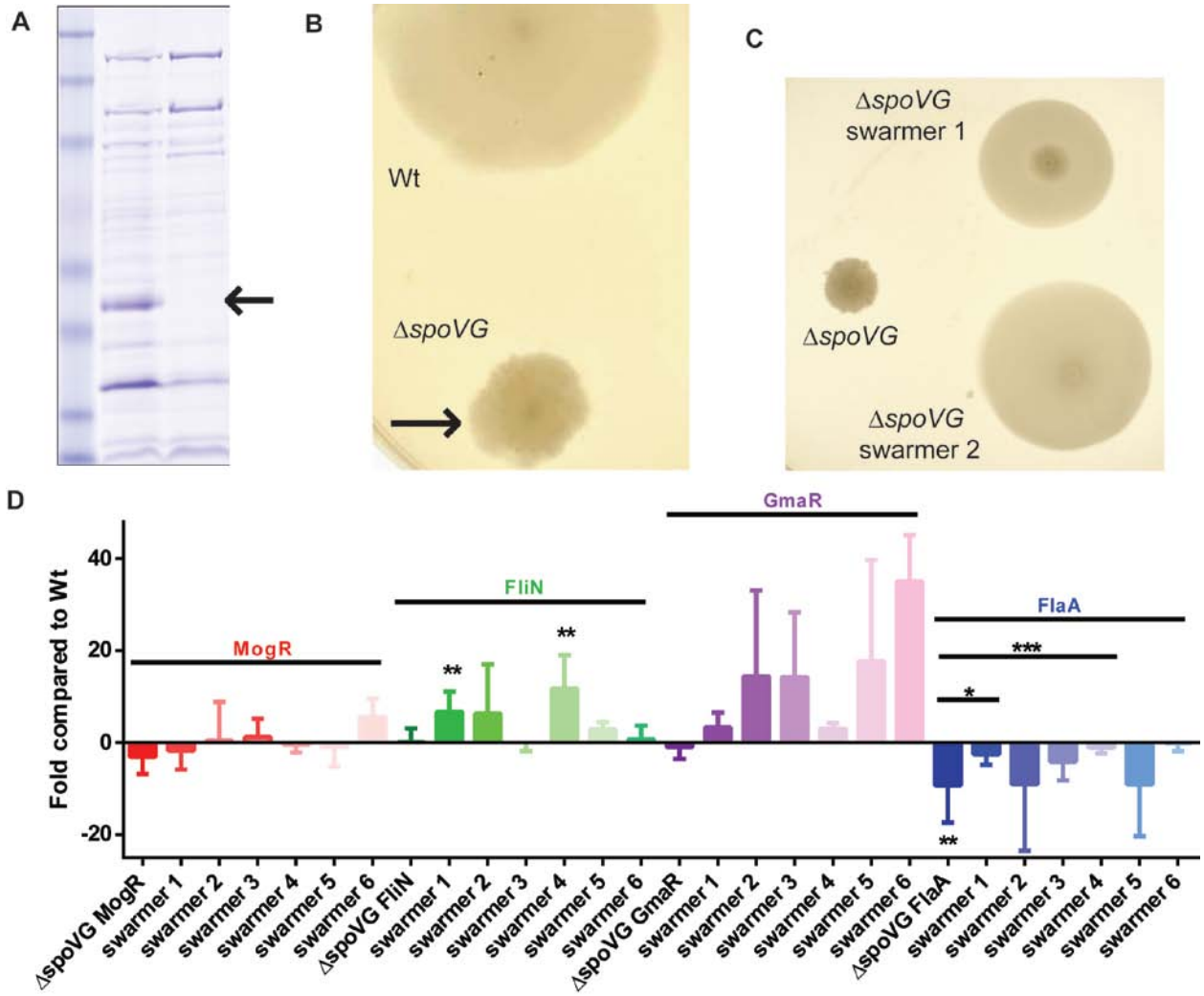

Figure 4.1 *spoVG* mutant bacteria are non-motile in semisolid agar

A) Precipitated supernatants of Wt and *spoVG* mutant bacteria were purified, separated by denaturing gel-electrophoresis, and visualized by coomassie staining. B) 30° C stationary phase cultures of Wt and Δ*spoVG* bacteria were stab-inoculated into 0.35% agar BHI plates and

incubated for 3-5 days at 30°C. The arrow indicates motile revertants starting to swarm away from the original colony. C) Motility revertants that were isolated from Δ*spoVG* parental colonies were isolated, grown to stationary phase, and grown as in (B). D) qPCR analysis of *spoVG* mutant bacteria and motility revertants. Primers were specific to MogR, FliN, GmaR, and FlaA. Data are presented as fold compared to Wt bacteria and were normalized to BglA transcript and 5S RNA. Data are representative of at least two separate experiments, where * indicates $P<0.05$, ** indicates $P<0.01$, and *** indicates $P < 0.001$.

4.2.2 Suppressor mutations restore swarming motility to *spoVG* mutants

Prolonged incubation of *spoVG* mutants in semisolid 0.35% agar led to spontaneous mutants that migrated away from the original colony (Figure 4.1B). Isolation of these bacteria and re-inoculation into semisolid agar determined that these mutants formed a larger swarming radius than the parental *spoVG* strain, and the smooth morphology of these swarming mutants appeared similar to Wt bacteria (Figure 4.1C). Six swarming mutants were chosen for whole-genome sequencing.

Whole-genome sequencing and variant detection identified mutations in each suppressor strain. Four of the six strains contained point mutations that led to single amino acid substitutions in RNAse J1 (Table 4.1). One strain contained a point mutation in the transcription termination factor Rho, while another strain contained a mutation in the transcription elongation/termination factor NusG. Lastly, two strains contained intergenic single nucleotide insertions between the *mogR* and *fliN* operons. qPCR analysis of these strains determined that the intergenic mutation between *mogR* and and the *fliN* operon did not alter expression of *mogR*, but led to a 9.2-fold upregulation over Wt of the *fliN* operon (Figure 1D). Suppressor mutants also had increased expression of *gmaR* and *flaA* as compared to *spoVG* mutant bacteria (Figure 1D).

	Rho	Intergenic, between *mogR* and *fliP*	NusG	RNAse J1	Other mutations
Δ*spoVG* Swarmer 1	R90S	130nt 5' of *fliP* start codon			
Δ*spoVG* Swarmer 2			V132F	H364Y	
Δ*spoVG* Swarmer 3				E19V	*lmo2588* deletion
Δ*spoVG* Swarmer 4		130nt 5' of *fliP* start codon			*lmo0562* inversion, *lmo1885* inversion
Δ*spoVG* Swarmer 5				N198T	*lmo2586* V120M
Δ*spoVG* Swarmer 6				G391C	

Table 4.1 Mutations identified in Δ*spoVG* swarming mutants
High-throughput DNA sequencing data was assembled and aligned to the 10403S genome (GenBank accession number CP002002.1) and SNP/InDel/structural variations were detected

(CLC Genomics Workbench, CLC bio). Variations marked as inversions or deletions were structural or InDel mutations and the nature of the mutations was not annotated.

Swarming suppressor mutations do not alter lysozyme resistance phenotypes of the *spoVG* mutant

To determine if the identified mutations affected other *spoVG* phenotypes, the *pgdA*::Tn mutation was transduced into the *spoVG* suppressor strains and assayed for lysozyme resistance. Despite the swarming suppressor mutations, mutation of *spoVG* still increased lysozyme sensitivity of the *pgdA* mutant (Figure 4.2). This finding suggested that the *spoVG* swarming and lysozyme resistance phenotypes could be dissected, and indicated that RNAse J1/Rho/NusG were not exclusive downstream interactors of SpoVG.

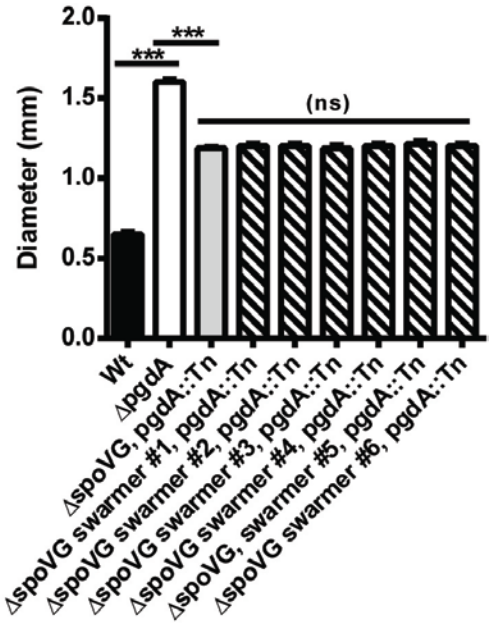

Figure 4.2 Swarming mutations did not alter lysozyme resistance phenotype of Δ*spoVG*. The *pgdA*::Tn mutation was phage-transduced into Δ*spoVG* and into the described Δ*spoVG* swarming suppressor strains. Bacteria were grown to stationary phase, spread onto BHI-agar plates, a filter-disk containing 1 mg of lysozyme was added to the plate, and zones of clearance were measured. Means and standard deviations from at least 3 separate experiments are presented, where *** indicates $P < 0.001$ and (ns) signifies no significant difference between the swarming strains and Δ*spoVG, pgdA*::Tn.

SpoVG weakly interacts with single-stranded DNA and does not interact with double-stranded DNA

It remained unclear how SpoVG regulated gene expression, yet multiple lines of evidence suggested that it was involved with nucleotide regulation. SpoVG was described as a site-specific DNA binding protein (139), and the following indirect data suggested that SpoVG may be involved with RNA regulation. First, SpoVG is regulated by multiple sRNAs in *S. aureus* and co-regulates genes with Rli31 in *L. monocytogenes*. Second, mutation of *spoVG* resulted in loss of *lmo0901* expression, which was not due to transcriptional changes. Lastly, the swarming suppressor mutations described in this study suggested a relationship between SpoVG and RNA

regulatory proteins. Based on these data, we hypothesized that SpoVG was either a DNA or an RNA binding protein.

To assess DNA binding, SpoVG (Lmo0196) was purified to high concentrations and homogeneity from *Escherichia coli* BL21 (λDE3) containing a pLysS vector (Figure 4.3A). Electrophoretic Mobility Shift Assays (EMSAs) were performed using the Cap41 promoter from *S. aureus* and the *pgdA* promoter from *L. monocytogenes* as DNA probes (139). Binding affinities for Cap41 were greater than 3 uM for single stranded DNA and no binding was observed for double stranded DNA (Figure 4.3B). SpoVG bound to various *pgdA* promoter probes with equal affinity to Cap41 and also bound to a probe corresponding to the *pgdA* ORF (Figure 4.3C). These results suggested that DNA binding was not specific, and indeed SpoVG bound to various scrambled DNA probes with equal affinity as the Cap41 and *pgdA* probes (Figure 4.3C).

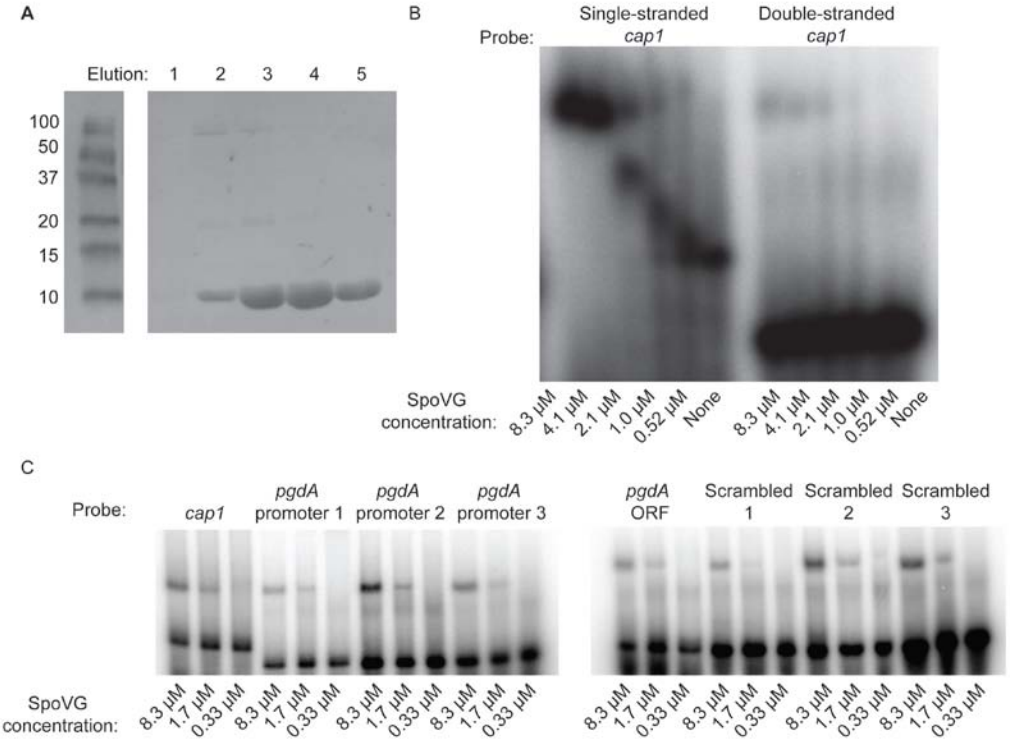

Figure 4.3 SpoVG binds non-specifically to single-stranded DNA and does not bind to double-stranded DNA

A) SpoVG-6His was purified from *E. coli* using Ni-affinity resin and eluted with five increasing concentrations of imidazole. Fractions 3-5 were pooled and concentrated for use in EMSAs. B,C) The indicated concentrations of SpoVG were incubated with 250 ng of the indicated ^{32}P labeled oligonucleotides for 30 minutes, as described in Materials and Methods, and separated by non-denaturing gel electrophoresis. For double stranded DNA, complementary *cap1* oligonucleotides were heated to 95^{o} C and slowly cooled for 1h to allow for annealing. Oligonucleotide sequences are described in Table 4.3.

4.2.3 SpoVG interacts with multiple RNAs *in vitro*, including Rli31

To assess RNA binding, EMSAs were performed using a variety of *L. monocytogenes* RNAs that had well established 5' and 3' ends and were between 100-300 nucleotides in length, which was a sufficient size to observe gel-shifts (123, 125). These probes were: 6S, Rli31, Rli32, SRP RNA, RliI, and Rli109. Two of these molecules, 6S RNA and SRP RNA, are well-described RNAs with known protein binding partners. The 6S RNA interacts with RNA polymerase (116) and SRP RNA forms a highly conserved ribonucleoprotein complex termed the signal recognition particle (SRP) (185). Rli32, RliI, and Rli109 are uncharacterized sRNAs in *L. monocytogenes* that are abundantly expressed and of similar size to Rli31 (125). All EMSAs were performed with non-specific DNA, RNA, and protein competitors as described in Materials and Methods.

The described RNAs were *in vitro* transcribed, EMSAs were performed, and gel-shifts were observed with binding constants of approximately 260 nM for Rli31 (Figure 4.4A). No gel-shifts were observed with 6S or SRP, the RNAs with known protein binding partners. SpoVG displayed extremely weak binding to RliI, bound with similar affinity to Rli32 as Rli31, and bound to Rli109 two-fold stronger than Rli31 (kD of 130 nM). Small migration differences between RNAs in lanes with high concentrations of SpoVG are typical of EMSA reactions and were likely due to non-specific complex formation and dissociation (163).

RNA binding was competed away using 65:1 molar ratio of cold RNA competitor, while 750:1 molar ratio of cold DNA competitor did not affect RNA binding (Figure 4.4B). To assess where SpoVG bound Rli31, Rli31 mutants were assayed for binding. Mutation of the Rli31 hairpin (Mutants A and B) did not affect binding, while mutation of the apical loop (Mutant E) resulted in 2-4 fold loss of binding (Figure 4.4C). These results suggested that *L. monocytogenes* SpoVG is a site-specific RNA binding protein that interacts with the Rli31 5' apical loop *in vitro*.

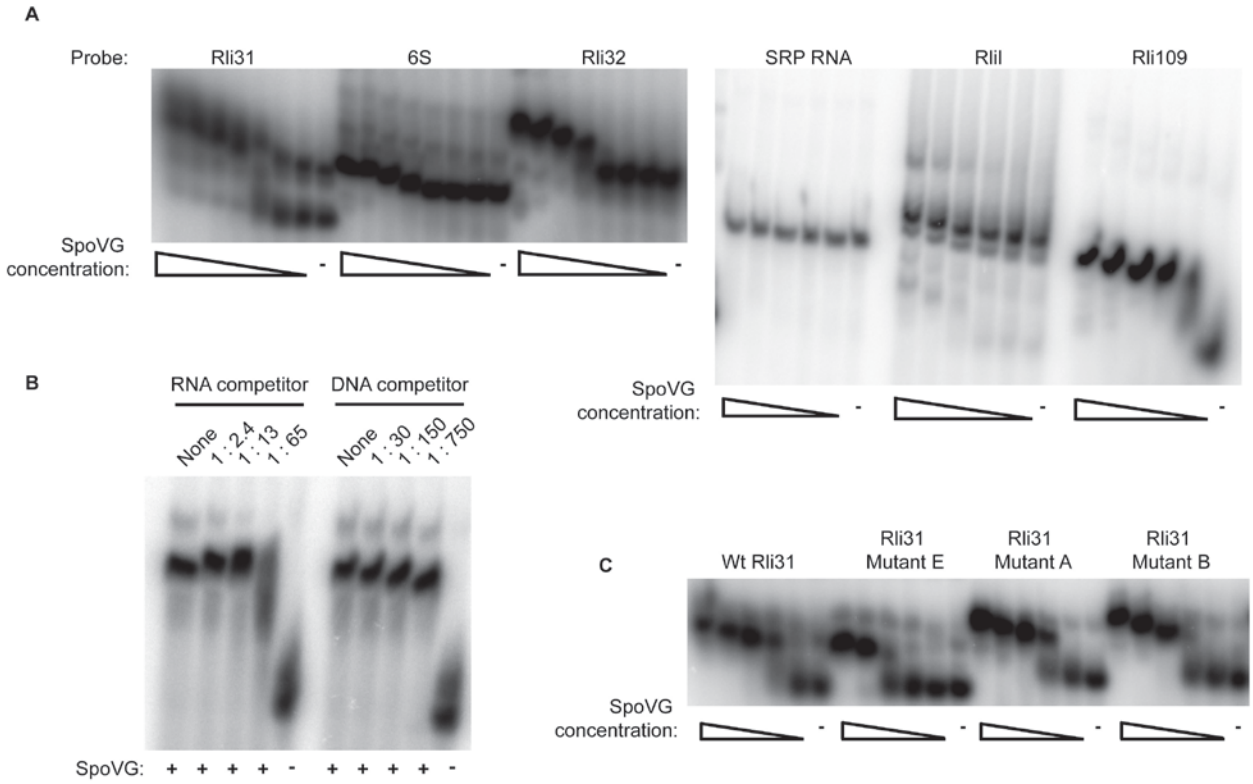

Figure 4.4 SpoVG interacts with RNA *in vitro*
A,B,C) EMSAs were performed using the indicated ^{32}P labeled, *in vitro* transcribed RNA as probes. SpoVG concentrations are represented by triangles and dashes represent no SpoVG. A) SpoVG concentrations for the Rli31, 6S, and Rli32 EMSAs were: 4.1, 2.1, 1.0, 0.52, 0.26, 0.13, 0.65 μM, and 0. SpoVG concentrations for the SRP RNA, RliI, and Rli109 EMSAs were 2.1, 1.0, 0.52, 0.26, 0.13μM, and 0. Each reaction contained 250 ng RNA B) 60 ng of Rli109 was incubated with 0.26 μM SpoVG for thirty minutes with the indicated molar ratio of competitor RNA (Rli109) or DNA (Cap1). The fifth and tenth lanes contained no SpoVG and no competitor. C) EMSA reactions were performed with 250 ng of Wt Rli31 and the indicated Rli31 mutants, where the SpoVG concentrations were: 2.1, 1.0, 0.52, 0.26, 0.13 μM, and 0.

4.2.4 Purification of SpoVG and identification of SpoVG post-translational modifications

To better understand how SpoVG bound RNA, we sought to identify proteins that interacted with SpoVG in *L. monocytogenes*, to identify SpoVG-RNA interactions in *L. monocytogenes*, and to confirm SpoVG post-translational modifications (144). Attempts were made to clone SpoVG with a 6-His epitope tag into the site specific integration vector pPL2; however, leaky expression of SpoVG was toxic to *E. coli* (data not shown). To circumvent this, a 6His epitope was chromosomally fused the C-terminus of *spoVG I* at the gene's native locus, and the protein was affinity purified from *L. monocytogenes* lysate. Eluates were concentrated, separated by gel-electrophoresis, and visualized by coomassie staining (Figure 4.5). Purification of SpoVG revealed that only one other protein co-eluted with SpoVG I, which was identified by mass-spectrometry as SpoVG II. This suggested that the two SpoVG paralogs interact in *L. monocytogenes*. High resolution mass spectrometry of these peptides confirmed previous data

that serine 66 was phosphorylated and additionally identified 5 methyl glutamate modifications on residues 2, 12, 41, 56, and 74.

Attempts were made to isolate RNA that co-purified with SpoVG from *L. monocytogenes* lysates. These studies are ongoing, as the procedure is complicated by 1) the sonication required to lyse high numbers of the bacteria, which shears nucleotides, 2) the impurity obtained from the resin (Figure 4.5), and 3) the inability to easily clone other affinity epitope tags onto SpoVG. Attempts are currently being made to chromosomally add other epitope tags to SpoVG in an effort to obtain more pure elutions to identify interacting RNAs.

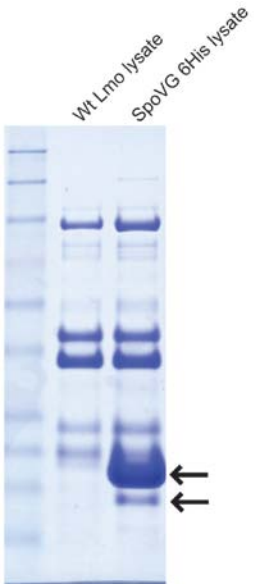

Figure 4.5 Purification of SpoVG and identification of post-translational modifications
A 6-histidine epitope was chromosomally added to SpoVG I and bacterial lysates were collected from mid-exponential phase bacteria in BHI. Wt bacteria were grown alongside SpoVG I:6His bacteria. Lysates were passed over Ni-affinity resin, eluted with imidazole, concentrated, separated by denaturing gel electrophoresis, and stained with coomassie R-250. Arrows indicate SpoVG I:6His (top arrow) and SpoVG II (bottom arrow), as identified by mass spectrometry.

Identification of putative RNA-binding grooves on SpoVG by modeling charged residues

Phosphorylation of serine results in a negatively charged species, while methylation of glutamate alters the negatively charged residue to a neutral charge (209). To understand how charges were dispersed around the protein, the positive and negative charged residues were modeled onto the SpoVG structure from *B. subtilis* (PDB entry 2IA9 (142)), as determined by X-ray crystallography. Based on the modeling of negatively charged residues, two grooves were apparent that lacked any negative charges (Figure 4.6A). Annotation of the positively charged residues determined that the grooves were highly positively charged (Figure 4.6B). Measurements of the positively charged grooves' widths varied from approximately 8 to 16A^{o} (Figure 4.6C). Given that the diameter of single-stranded RNA is approximately 10 A^{o} (210), these findings are in-line with a model whereby SpoVG binds single-stranded RNA. Similar results were obtained upon modeling charges onto the SpoVG structure from *Staphylococcus epidermidis* (PDB entry 2I9X, data not shown (143)).

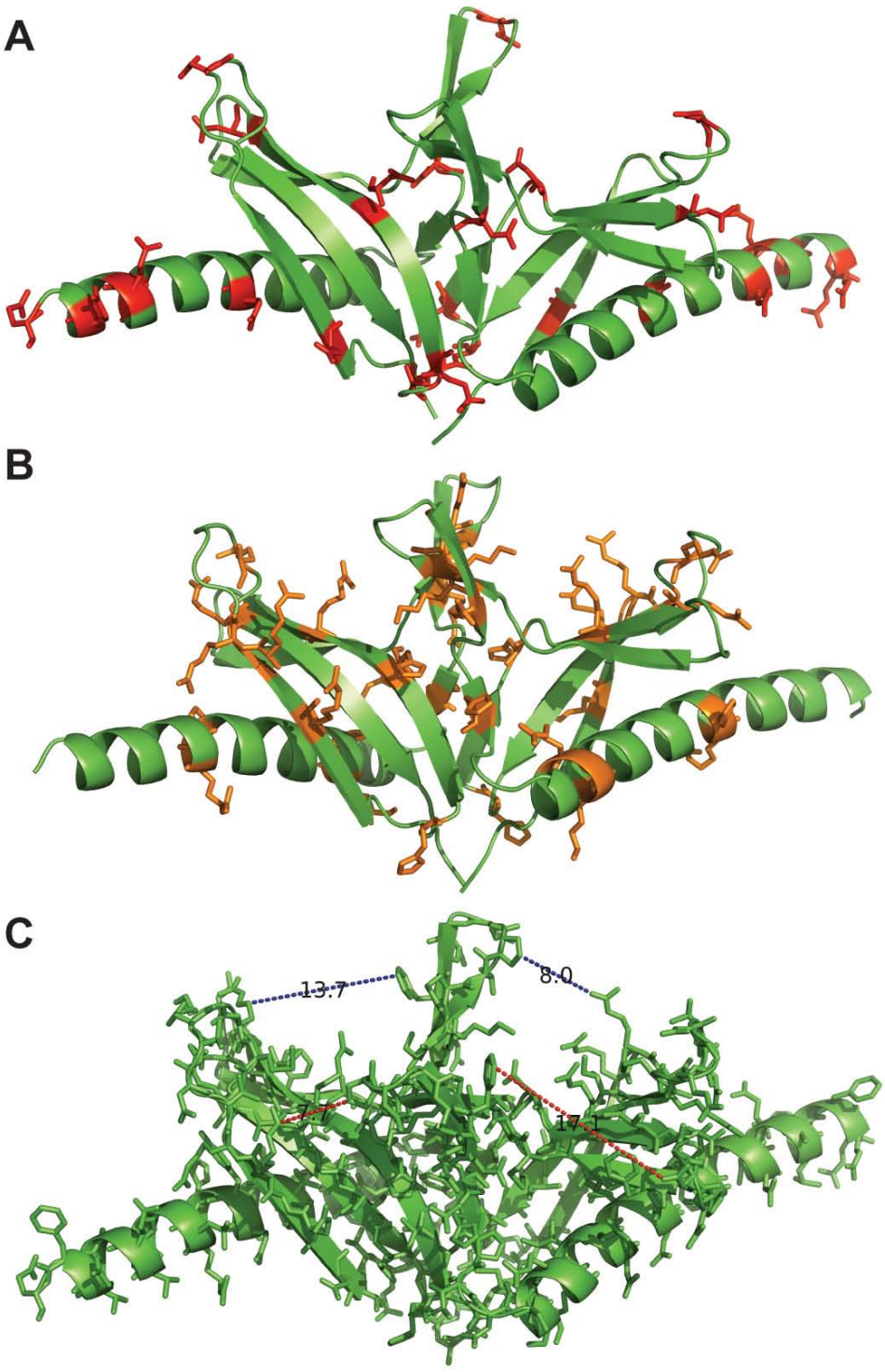

Figure 4.6 Two positively-charged grooves in the SpoVG dimer
A,B,C) The crystal structure of SpoVG, chains A and B, from *B. subtilis* (PDB entry 2IA9), with the peptide chain annotated in green. A) Negatively charged side-chains are annotated and colored red. B) Positively charged side-chains are annotated and colored in orange. (C) All side-chains are annotated and colored in green. Dotted lines are representative measurements in A^{o} of

the two positively-charged grooves, and read 13.7 (top left), 8.0 (top right), 7.7 (bottom left), and 17.1 (bottom right).

4.3 Discussion

This study sought to better characterize SpoVG in *L. monocytogenes* and determined that it was a methylated, RNA-binding protein required for swarming motility. SpoVG bound with high affinity to multiple sRNAs *in vitro* and did not interact with sRNAs that have known protein binding partners. The data suggest that SpoVG may represent a class of RNA-binding proteins that function analogously to, or alternatively to, Hfq. The following discussion aims to compare and contrast the similarities and dissimilarities between the two proteins in terms of their mutant phenotypes, their structural characteristics, and their intimate relationships with sRNAs. We conclude that the Gram-negative Hfq may share more functional similarities to SpoVG than it does to the actual Hfq homolog in Gram-positive bacteria.

hfq mutants in Gram-negative bacteria often display pleiotropic phenotypes, which are surprisingly similar to *spoVG* mutants phenotypes observed in firmicutes. *hfq* mutants of *Burkholderia cepacia* are defective for capsule formation (211), and *hfq* mutants in *E. coli* are less prone to form biofilms (212). *spoVG* mutants in *S. aureus* are defective for capsule formation (135) and mutants in *L. monocytogenes* bind poorly to congo red, suggesting a defect in biofilm formation (Figure 3.4). *hfq* mutants have reduced motility in a number of Gram-negative organisms, including *E.coli* (212), *Pseudomonas* (213), and *Salmonella* (214), and this study reports that *spoVG* mutants are non-motile (Figure 4.1). Hfq is required for sRNA mediated regulation of central metabolism genes, including carbohydrate metabolism genes (186), and purine/pyrimidine metabolism (119). SpoVG was shown in this study to regulate the chitobiose import gene *lmo0901* (Figure 3.6), and *spoVG* mutants rescue ppGpp-related defects in *L. monocytogenes* (138). In *B. subtilis*, deletion of isocitrate dehydrogenase arrests sporulation, and deletion of *spoVG* restores sporulation (134). Given the abundance of defects exhibited by the *spoVG* mutant, however, the mutant displayed no detectable virulence defect (Figure 3.3D) and was viable in nutrient-limiting growth mediums (data not shown).

SpoVG shares many structural features with Hfq but may differ from Hfq in its oligomerization state. SpoVG from *L. monocytogenes* and Hfq from *E. coli* are both exactly 102 amino acids in length and both contain a single terminal α-helix that is overlaid by 4-5 β-strands (215, 216). Hfq oligomerizes into a homohexamer, while SpoVG oligomerizes into a dimer (217) that may then heterooligomerize into a tetramer (139, 217) or possibly a hexamer (142). The RNA binding surface of SpoVG likely varies from Hfq, as the Hfq β-strands form the core of the protein, while the loops and α-helices interact with RNA (218). Modeling charges on SpoVG led us to predict that RNA binding is principally mediated by residues located in the β-strands of the protein (Figure 4.6). Further investigation is needed to better understand the oligomerization state of SpoVG and determine if it forms a ring-shaped oligomer similar to Hfq.

SpoVG and Hfq both appear intricately related to sRNAs, to RNAses, and to the transcription termination machinery. Hfq has been well-established as a mediator of sRNA:mRNA interactions and also functions with RNAse E to target RNAs for degradation. Hfq can also protect RNA from RNAse mediated degradation (118). Hfq directly interacts with Rho to inhibit Rho-dependent transcription termination, yet addition of NusG displaced antitermination by Hfq (206). The data presented here and elsewhere suggest that SpoVG may share all of these characteristics with Hfq. SpoVG is intimately related to Rli31, as these sRNAs

regulate the same target genes, interact *in vitro*, and the SpoVG mRNA contains 14/14 nucleotides of perfect complementarity to the apical loop of Rli31, suggesting that the SpoVG mRNA may regulate Rli31. SpoVG is translationally regulated by the sRNA SprX in *S. aureus* (140), and SpoVG protein abundance is increased in mutants of *rsaA*, another sRNA (141). SpoVG interacted with numerous sRNAs *in vitro* but did not interact with sRNAs that have known protein binding partners, perhaps suggesting specificity for unstructured or single-stranded RNA. *spoVG* mutants were non-motile in semisolid agar and mutation of RNAse J1, Rho, and NusG restored mRNA abundance of flagellar genes and restored motility. This data suggests that some form of cross-talk exists between SpoVG and the major RNA regulatory machinery, and that SpoVG may protect flagellar mRNAs from RNAse mediated degradation.

Mutation of Rho, NusG, and RNAse J1 restored swarming motility to *spoVG* mutants yet did not alter the Δ*spoVG* lysozyme resistance phenotype (Figure 4.2). This suggested that two *spoVG* mutant phenotypes could be dissected, whereby one was rescued by Rho/NusG/RNAse J1, while another was not. Similarly, some *hfq* phenotypes are dependent on RNAse E, while others are not (118, 119, 205). This data may suggest that SpoVG retains multiple functionalities, such as protecting RNA from degradation and, separately, regulating sRNAs.

Multiple methyl-glutamate residues were identified on SpoVG, and methylation of glutamate is well-described in bacteria as a mechanism to regulate chemotaxis. Methyl-accepting chemotaxis proteins (MCPs) are methylated on glutamates in response to certain stimuli, such as detection of extracellular sugars, and methylation signals for flagellar rotation and swarming motility (219-222). Multiple similarities exist between MCPs and SpoVG, which regulates expression of the sugar import gene *lmo0901*, is required for motility in soft agar, and contains multiple methyl glutamate modifications. The similarities between SpoVG and MCPs may be coincidental, or perhaps protein methylation plays a universal role in regulating motility in response to environmental stimuli.

In conclusion, SpoVG is a methylated RNA binding protein required for flagellar motility, which has many similarities to Hfq, as described in Gram-negative bacteria. Further investigation of the biochemical and functional properties of SpoVG are required to determine what RNAs it interacts with and how it regulates their activities in *L. monocytogenes*.

Table 4.2, bacterial strains used in Chapter 4
L. monocytogenes 10403S, Δ*spoVG*
Δ*spoVG* swarmer #1
Δ*spoVG* swarmer #2
Δ*spoVG* swarmer #3
Δ*spoVG* swarmer #4
Δ*spoVG* swarmer #5
Δ*spoVG* swarmer #6
Δ*spoVG* swarmer #1 + *pgdA*::Tn
Δ*spoVG* swarmer #2 + pgdA::Tn
Δ*spoVG* swarmer #3 + pgdA::Tn
Δ*spoVG* swarmer #4 + pgdA::Tn
Δ*spoVG* swarmer #5 + pgdA::Tn
Δ*spoVG* swarmer #6 + pgdA::Tn
Δ*pgdA*
Δ*spoVG* + *pgdA*::Tn
Chromosomal *spoVG I*: 6-His
E. coli - BL21, pLysS - SpoVG C-terminal 6His

Table 4.3, oligonucleotides used in Chapter 4	
TB122, DegU qPCR F	gaggcgcgtatattcatccacgtgta
TB123, DegU qPCR R:	aagaagttgcaatacctcgcactctc
TB471: FliN qPCR F	Gaaaaacaagcaagcgaatc
TB472: FliN qPCR Rev	Gtaattctcggaaaagtgcttc
TB473: FliP qPCR F	Tttcgttggttgtttttggcc
TB474: FliP qPCR Rev	ggacgataatacagtaggtaaag
TB475: GmaR qPCR F	agcgattgatgcagatgaatgtt
TB476: GmaR qPCR Rev	Gaagcaaattgtgccgtcatt
TB477: FlaA qPCR F	GCAAGAACGTTTAGCATCTGGT
TB478: FlaA qPCR Rev	TGACGCATACGTTGCAAGATTG
TB463: mogR qPCR F	Atccaagtagaagatattccg
TB464: mogR qPCR R	Caaccaggttttttcgcgtgat
TB379: pgdA promoter 1 F, for EMSAs	acaaaaactagaaacttgccttttttcatgtataattgtttataagaa
TB381: pgdA promoter 2 F, for EMSAs	tttgttaagaaatcgttggtccttttttcctattttagtacaaaaacta
TB383: pgdA promoter 3 F, for EMSAs	cggtaaaagctcccactttatccgtgtctttttgtgacatttgttaag
TB389: pgdA ORF, F, for EMSAs	gtcgcgcaacaaagtaataatgcagatggacagactaatgaaagaccag
TB391: scrambled 1 F, for EMSAs	AATTCGATATATGATTTTGAAAATGAATTTCATA

	ACTTTTAAATTGCGT
TB393: scrambled 2 F, for EMSAs	GCCGAGCGGGTACGCCGTGCGGTATGGGCCCAC GCTCCGTGGCGTGCCG
TB395: Scrambled 3 F, for EMSAs	ATTTTTTAGCGCTATAAAAAAGCTATTTTTTAAA AAAGTACTTTTTTGA
TB377: cap1 probe F, for EMSAs	GAGTATAATTATTTTTAATTTACATATAAATAAA AAGGCGAAAATAATGCGGTTTAAAAGTAATTAA T
TB378: cap1 probe Rev, for EMSAs	ATTAATTACTTTTAAACCGCATTATTTTCGCCTTT TTATTTATATGTAAATTAAAAATAATTATACTC
TB149: rli31 F with T7 promoter for IVT	Ccaagtaatacgactcactata gg tatcccatagagattgtcatttgaaataag
TB150: rli31 R, no rest site, for IVT	taattatagcacagaatctgggaaattctg
TB403: 6S RNA, with T7, for IVT	Ccaagtaatacgactcactata gg gaaaagaaaccctaatgtattcg
TB404: 6S RNA, Reverse, for IVT	caaaaaagaaaccccaatcgtaccg
TB401: rli32 F with T7 promoter for IVT	Ccaagtaatacgactcactata gg gtggagagctttcatttttccc
TB402: rli32 R, for IVT	caaaaaaataaccgcaccagggg
TB413: Rli31 Forward with T7 and mut9 mutation	Ccaagtaatacgactcactata gg tatcccatagagattgtcaGGG
TB455: SRP, Forw, with T7 for IVT	Ccaagtaatacgactcactata gg ttgtcgtgctagacggggaggta
TB456: SRP Rev, for IVT	ttagtgtcgcgcacctcacatcga
TB457: Rli109, Forw, with T7 for IVT	Ccaagtaatacgactcactata gg gcagtggaattaaaggcatctaag
TB458: Rli109, Rev for IVT	tgtcactcgcaaaagcattgc
TB447: RliI, with T7, Forward, for IVT	Ccaagtaatacgactcactata gg tgagatgacatgtttcttttgaatg
TB448: RliI, reverse, for IVT	ttttttcagacaacaaaaaagcg
TB254, SpoVG I F w Nde1 for pET20b	GCGC CATATG atggagattacagatgtgagattacgac
TB255, SpoVG I R w Xho1, no stop, for pET20b	tata ctcgag gttttcttctacaatactttcgtctgc
TB274: SpoVG Rev from stop, to add His tag	gttttcttctacaatactttcgtctgc
TB275: SpoVG For from stop, with His tag	catcatcatcatcatcat taaaaaatcctcggttagggagaacg
TB258: lmo0196/7 Forw from mid I with BamHI, for pKSV7	tcat ggatcc gggattgttcgtagctatgcctagtaa
TB259: lmo0196/7 Rev from mid II, with SalI, for pKSV7	gttac gtcgac cggaattaattgggtgagcgatatcac

Chapter 5

Conclusions and future perspectives

5.1 Summary of results and conclusions

This study defined the molecules required for lysozyme resistance of *L. monocytogenes* and subsequently sought to characterize how these molecules regulated one another. In total, 14 genes were required for lysozyme resistance in this organism, including many cell wall enzymes, multiple two-component systems, and many regulators of gene expression. The screen for lysozyme-sensitive mutants provided an answer for a question originally proposed by Fleming nearly 100 years ago, which was: how are pathogens so lysozyme-resistant? The answer is not merely via the acquisition of *pgdA* or *oatA* genes, as previously suggested (89, 93), because these enzymes are found ubiquitously among bacteria. Instead, our data suggests that lysozyme resistance of pathogens is achieved via upregulation of common cell wall modifying enzymes. This logic provides an alternative example of how virulence phenotypes are acquired by bacteria, many of which are thought to originate via horizontal gene transfer (56). We propose that pathogen-specific regulation of broadly distributed genes represents another mechanism by which pathogens acquire virulence.

Subsequent investigations sought to better characterize the abundant non-coding RNA Rli31. It was determined that Rli31 maintains a complex, multifaceted, and still poorly understood relationship with the SpoVG mRNA and protein. The data suggest that Rli31 and SpoVG independently and oppositely regulate expression of the same target genes, and that they may regulate one another by two separate mechanisms. SpoVG was characterized as an RNA binding protein, and we propose that this molecule may function similarly to, or as an alternative to, the RNA chaperone Hfq. While the original goal of these investigations to identify the lysozyme resistance gene regulated by Rli31 has not yet been realized, many other aspects of *L. monocytogenes* physiology and pathogenesis have been discovered. As Alexander Fleming famously once wrote, “One sometimes finds what one is not looking for” (71).

5.2 Remaining questions and future directions

Lysozyme resistance

The major remaining question in regards to lysozyme resistance in *L. monocytogenes* is: what is the lysozyme resistance protein regulated by Rli31 and SpoVG? Despite exhaustive attempts to identify the lysozyme resistance gene(s) regulated by Rli31, we are only left with clues as to its identity. We predict that the gene will be oppositely regulated in *rli31/spoVG* mutants and will remain at Wt levels of expression in the *rli31 spoVG* double mutant. Based on the TEM and congo red data, this gene is likely either a glycosyltransferase responsible for EPS production or a peptidoglycan carboxypeptidase responsible for peptide cross-linking of the cell wall. As we were unable to identify this gene by genetic approaches (either forward screening or suppressor analysis), this may signify that the gene is either essential for viability or possibly redundantly expressed. At this point, the best method to identify this gene will be to identify SpoVG interacting RNAs or to comprehensively mutate genes with predicted complementarity to Rli31.

It is satisfying to reflect on the screen for lysozyme-sensitive mutants, knowing that one major question was answered, yet this screen has raised an abundance of questions that we have not even begun to explore. A few of these questions are: how does PbpX modify the cell wall and how does this confer lysozyme resistance? What are the functions of *lmo2473* and *lmo2768*? Does DegU bind the *pgdA* promoter directly and how is DegU regulated post-translationally?

Does post-translational regulation of DegU reduce expression of flagellar genes inside cells, and if so, does it reduce lysozyme resistance inside cells? What lysozyme resistance genes does the *vir* operon regulate and is this phenotype dependent on *pgdA*? Why is the *dltA* mutant lysozyme-resistant and CAMP sensitive, while *dltB* and *dltD* mutants are sensitive to both CAMPs and lysozyme? Is lysozyme resistance detrimental to fitness in lysozyme-free environments? Are CAMP-resistance genes regulated by such complex mechanisms as lysozyme resistance genes?

SpoVG

The relationship between SpoVG and Rli31 remains unclear. If the Rli31/SpoVG regulatory system functions analogously to ChiP/ChiX, we would hypothesize that chitobiose or another sugar stimulates transcription of SpoVG mRNA, yet we did not observe any such upregulation (data not shown). We are convinced that the 5' UTR of SpoVG functions as a decoy that regulates Rli31 activity, but it remains unclear when this decoy is active, and what stimulates its transcription. Once the expression of the *spoVG* UTR is better understood, it will be intriguing to observe whether this is sufficient to reduce lysozyme resistance. It also remains unclear how sugar import genes are connected to lysozyme resistance. Given that chitobiose directly inhibits lysozyme activity by serving as a competitive inhibitor (223), it seems unlikely that the sugar import and lysozyme resistance phenotypes are coincidental.

Finally and perhaps most obviously, a multitude of questions remain in regards to SpoVG. Mainly, what RNA does it interact with in *L. monocytogenes*? Future experiments using purified SpoVG:RNA complexes and high-throughput sequencing will determine if SpoVG interacts with sRNAs, which would solidify our hypothesis that this protein is functionally similar to Hfq. This approach may determine whether SpoVG has a characteristic RNA binding motif, which may lend insight into its target RNAs in other bacteria. Secondly, the oligomerization state of SpoVG remains unclear. It will be worthwhile to understand how this protein forms a tetramer/hexamer in solution and how this affects RNA-binding. Lastly, it remains unclear how SpoVG exerts gene regulation upon RNA binding. As indicated by the mutations identified in RNAse J1, perhaps SpoVG protects mRNA from degradation.

5.3 Speculation into the future

The future of lysozyme resistance

My predictions for future endeavors into the field of lysozyme resistance are rather pessimistic, and are in fact aligned with Alexander Fleming himself, who wrote the following introduction to his Presidential Address to the Royal Society of Medicine in 1932 (68):

> *I choose lysozyme as the subject for this address for two reasons, firstly because I have a fatherly interest in the name, and, secondly, because its importance in connection with natural immunity does not seem to be generally appreciated.*

To date, it appears that Fleming's words have remained accurate. It was not until this study that we were able to provide a conclusive explanation to answer Fleming's original observation in the 1920s that pathogens were more lysozyme-resistant than non-pathogens. Despite being absolutely essential for pathogenesis of all bacteria, lysozyme resistance remains a remarkably underappreciated phenomenon. Only 3 genes (*pgdA, oatA*, and *prsA2*) were

previously observed to confer lysozyme resistance to *L. monocytogenes* (92, 154), yet this organism was probably the best studied of all bacteria in terms of lysozyme resistance. Given the history of disinterest that Fleming and I both seem to observe, I foresee a slow rate of progress in this field despite the innumerable questions that remain to be answered. It would be exciting to screen for lysozyme-sensitive mutants in other organisms, especially *S. aureus*, where *oatA* has been well studied. Will a similarly complex mechanism of regulation be identified? What transcription factor or sRNA is responsible for upregulation of *oatA* in pathogenic *S. aureus*? Are *spoVG* mutants in *S. aureus* (which have reduced capsule formation (135)) more lysozyme-resistant than Wt bacteria? I am excited to follow this field throughout the course of my career and am curious to observe whether important questions relating to lysozyme resistance will continue to be asked.

The future of sRNAs and SpoVG

My pessimism of the lysozyme resistance field is mirrored by a hopeful optimism regarding SpoVG, as non-coding RNA biology has become more appreciated than ever. Over the past six years, numerous studies have comprehensively identified the sRNAs in *L. monocytogenes* (123-125, 201, 224), and the first wave of characterizing these RNAs has begun over the past few years (123, 199, 202-204). Over the next decade we will certainly learn many new mechanisms by which sRNAs can regulate gene expression and we may learn that these gene regulators play a much more significant role in bacterial physiology and pathogenesis than previously imagined. Indeed, the interest in bacterial sRNAs led to the revolutionary discovery of Cas9 as a gene-editing tool (225, 226).

The future of *Listeria monocytogenes* biology

I feel fortunate to have been at ground-zero for a number of exciting discoveries in the field of *L. monocytogenes* biology over the past six years. From the discovery of c-di-AMP as the IFN-β stimulatory molecule (17), to the discovery that glutathione is an allosteric regulator of PrfA (55), to the exciting work being done at Aduro Biotech in Berkeley, where *L. monocytogenes* is being used as an anti-cancer therapy (35) and, where c-di-nucleotides are being applied as anti-tumor therapies (227).

The use of attenuated *L. monocytogenes* and c-di-nucleotides as successful cancer therapies would bring much attention to the use of bacterial pathogens as tools to cure disease. Indeed, if the results from mouse studies (227) are recapitulated in humans, these tools would undoubtedly be considered by many as a long-sought magical anti-cancer drug. If true, these discoveries would surely be deserving of international recognition and credit. Whether or not this prediction becomes reality, the studies on *L. monocytogenes* biology over the past two decades has provided a textbook example for how basic biology can be translated into medicinal benefit.

The Golden Age of molecular biology

During the course of human history we have experience many golden ages. From the golden age of exploration, when the Americas were discovered, to the golden age of painting in the Dutch Republic in the 17th century, to the golden age of piracy in the 18th century. In retrospect, we look back on these times and deem them golden ages, but at the time the people in these eras may not have recognized their fortune.

Over the past twenty years, molecular biology has transformed from an era where DNA sequencing gels were analyzed by hand, to a time where ribosome profiling can use millions of

nucleotide reads to examine the activities of an entire cell. Whereas twenty years ago, histology and light microscopy were fundamental techniques to assess the cell types found in an organ, today flow cytometry coupled with dozens of fluorescently tagged antibodies can assess the cellular landscape of an entire organism. Thirty years ago, we did not even know that bacterial pathogens induced interferon. Today, the ligands, receptors, host factors, and bacterial enzymes for producing interferon and nearly every other PAMP are mostly known and characterized. These remarkable advances, and many more, have provided the knowledge and the tools to build powerful drugs and to combat disease. Without a doubt, we are currently living in the golden age of molecular biology.

What discoveries await us in the future? Perhaps we will develop cheap, effective vaccines and treatments for infectious diseases such as tuberculosis and HIV. Perhaps we will be able to diagnose and prevent genetic diseases, and develop effective therapies for cancer. What advances will science make in the future? Perhaps we will chemically recreate a cell or synthetically create human organs. The current rate of progress suggests that these discoveries may occur sooner rather than later. I cannot help but speculate on how long our golden age will last. It is hard to imagine the advancement of technology will slow down, but history would suggest that all golden ages must end. If molecular biology is anything like piracy, our age may only last another 60 years. I wonder what the field of molecular biology will look like in 40 years (when I'm hopefully still around) or in 1,000 years (when humanity will hopefully still be around). I hope that our knowledge produces fruitful results and useful technology that advance health and science for the ages to come.

Materials and Methods

Ethics Statement

This study was carried out in strict accordance with the recommendations in the Guide for the Care and Use of Laboratory Animals of the National Institutes of Health. All protocols were reviewed and approved by the Animal Care and Use Committee at the University of California, Berkeley (MAUP# R235-0815B).

Bacterial strains

All strains of *L. monocytogenes* used in this study were in the 10403S background and cultured in brain heart infusion media (BHI), unless otherwise noted. Construction of Δ*rli31* was performed by amplifying neighboring regions of *rli31* with oligonucleotide pairs TB7 and TB8, and TB9 and TB10, then combining them via splice overlap extension PCR. This product was then introduced into *L. monocytogenes* by allelic exchange using pKSV7 (59). A similar process was performed to construct Δ*spoVG* and Δ*lmo0901*, using their respective oligonucleotides. Constructs in pPL2 or pAM401 were cloned by amplifying the indicated region with primers found in oligonucleotides Tables, digested with the respective nuclease, and ligated into the respective plasmid as described (58, 228).

Transductions were performed using U153 phage as previously described (229). Briefly, 10^7 phage were grown in the donor strain, incubated with 10^8 recipient bacteria, and selected for on BHI erythromycin plates. For construction of the *pgdA pbpX rli31* triple mutant, the *rli31::*Tn917 transposon was transduced into Δ*pgdA pbpX*::Tn and selected for on BHI chloramphenicol plates.

Lysozyme assays

Hen egg-white lysozyme (Sigma) was used for all lysozyme assays. For measurements by CFU, bacteria were grown in 15 ml volumes shaking at 37^o C in BHI until an OD_{600} of 0.5 and lysozyme was added to the indicated concentration. For assays measuring OD_{600}, bacteria were grown in 200 µl volume in BHI at 37^o shaking in a 96-well plate reader 340PC (Molecular Devices). For disk diffusion assays, 10^8 bacteria were spread on BHI agar plates and lysozyme disks containing 1 mg lysozyme were added. Plates were incubated at 37^o for 12 h and zones of clearance were measured.

In vivo infections and assays in blood

All *in vivo* infections in Chapter 2 were performed with Crl:CD1(ICR) (CD-1) or C57BL/6J (B6) mice from Charles River and The Jackson Laboratory, respectively. All *in vivo* infections performed in Chapter 3 used CD-1 mice. Mice were infected i.v. with 10^5 logarithmically growing bacteria and indicated organs were harvested at 48 hours/30 minutes postinfection. Organs were homogenized with 0.1% NP-40 and indicated dilutions were plated onto LB-agar. For competitive index experiments, 10^5 total bacteria at a 1:1 ratio of each mutant was used for infection and organ homogenates were plated onto both LB and LB containing erythromycin to determine ratios between the two strains.

For assays in blood, strains were grown to mid-exponential phase in BHI, washed with PBS, and diluted 1:100 into defibrinated sheep or horse blood (Hemostat). For assays using bentonite treated blood, 5 mg of bentonite (Sigma) was added to 1ml of blood and incubated at

4^{o} for 30 minutes. Bentonite was then removed from blood by two centrifugation steps, at 5,000 rpm and then 12,000 rpm.

Northern blots and qPCR

RNA was purified from 20 ml of logarithmically grown bacteria by phenol/chloroform extraction and ethanol precipitation. 20 μg per sample was then loaded onto a 6% urea-polyacyrlamide gel and separated by electrophoresis. Gels were stained with a 1:10,000 dilution of SYBR Gold (Invitrogen) and imaged using Typhoon (GE). For northern analysis, nucleotides were transferred to a nylon membrane, probed using ^{32}P labeled oligonucleotides, and imaged with Typhoon. For qPCR analysis, 4.4 μg of RNA was DNAse treated and reverse transcribed with iScript (BioRad). cDNA levels were measured using SYBR Fast (KAPA) and DNA oligonucleotides specific for the target gene (listed in Tables above).

Sequencing of transposon insertions

Flanking regions of transposon insertions were amplified using two rounds of PCR and a hot-start polymerase (Takara). For each colony, a small amount of bacteria was resuspended in 100 μl water and 1μl was used for the first PCR reaction. This reaction amplified the flanking regions of the *Himar1* transposon by using the TN1 primer that was specific to the transposon and the Arb1 primer that contained random nucleotides (Table 2.5). The second reaction used 1.5 μl of the previous PCR reaction and primers TN2 and Arb2, which were specific to the previously amplified PCR product. The product of this reaction was then treated with 5 μl of ExoSAP-IT (Affymetrix) and sequenced using primer TNSEQ.

Intracellular growth curves

Bone marrow-derived macrophages (3×10^{6}) from B6 mice were plated onto TC coverslips, incubated for at least 12h, and infected with the indicated strains at time zero. Bacteria were washed at 30 minutes postinfection, gentomycin was added at 1h post infection, and bacteria were plated for CFU on LB agar at the given intervals.

Whole genome sequencing

Genomic DNA was isolated from stationary phase cultures of *L.monocytogenes* grown in BHI broth using the MasterPure DNA purification kit (Epicentre). DNA was then fragmented using Covaris S22 (Covaris Inc.), libraries were constructed using Apollo 324 (IntegenX Inc.), PCR amplified, and multiplexed at the QB3 Functional Genomics Laboratory at UC Berkeley (http://qb3.berkeley.edu/qb3/fgl/). The resulting libraries were sequenced using single-end reads with a Hiseq 2000 Illumina platform. Sequence data were aligned to the *L.monocytogenes* 10403S reference genome CP002002.1 using Bowtie 2 (230) and SNPs were identified using SAMtools (231) and CLC Genomics Workbench (CLC bio). Approximately 93% of all reads aligned to the reference, resulting in an average of greater than 50-fold coverage of the genome. Annotated mutations were identified in >80% of all reads.

Cell wall purification and muropeptide analysis

Peptidoglycan was purified from mid-exponential phase cultures as described previously (232). For extracted cell walls, incubation in 48% hydrofluoric acid was omitted to retain the wall teichoic acids. Chromatograms corresponded to previously published data (105); however, muropeptide identity assignments were further confirmed by mass spectrometry (MS). MS

analysis was carried out by the Unité de Spectrométrie de Masse Structurale et Protéomique at Institut Pasteur.

Precipitation of secreted proteins

Wt and *spoVG* mutant bacteria were grown to mid-exponential phase in BHI and bacteria were removed by centrifugation. Supernatants were treated with 10% TCA for 1h on ice. Precipitated proteins were then pelleted by centrifugation at 13,000 RPM for 30 minutes at 4^{o} C. Pellets were washed with acetone and resuspended in loading buffer. Proteins were then separated by denaturing gel electrophoresis, stained with coomassie R-250, and the appropriate band was gel-excised and identified by mass spectrometry, as described below.

Electron microscopy

Bacteria were high pressure frozen in a Bal-Tec HPM 010 (Bal-Tec AG, Liechenstein) high pressure freezer and freeze substituted in 1% osmium tetroxide and 0.1% uranyl acetate in acetone over a period of 2 hours by the SQFS method of McDonald and Webb [45]. Infiltration of Epon epoxy resin was carried out by 15 minute incubations in 25, 50, and 75% acetone-resin mixtures on a rocker, then three 15 minute incubations in pure resin. Polymerization of resin was for 2 hours in a 100°C oven (233). Sections of 70 nm thickness were post-stained with aqueous 2% uranyl acetate for 4 minutes and lead citrate for 2 minutes. Images were viewed on a Tecnai 12 (FEI Inc., Hillsboro, OR, USA) transmission electron microscope operating at 120 kV, and images recorded with a Gatan Ultrascan 1000 CCD camera (Gatan Inc., Pleasanton, CA, USA). Electron microscopy was performed at the Electron Microscope Lab at UC Berkeley.

Purification of SpoVG from *E. coli*

spoVG I was amplified using primers TB254 and TB255, digested, ligated into pET20b, and transformed into BL21 cells containing pLysS. 1.4L of bacteria was grown shaking at 37^{o}C until an $_{600}$OD of 0.4, and production of SpoVG was induced with 1 mM IPTG (Sigma) for 2h. Bacteria were then concentrated by centrifugation, flash frozen, and eventually lysed by sonication in buffer A (300 mM NaCl, 50 mM Tris, 25 mM imidazole, 0.5 mM TCEP, 20% glycerol, pH 8.0). Cell wall debris was removed by centrifugation and the resulting lysate was incubated with Ni-affinity resin (Thermo Scientific). The resin was washed with a minimum of 40 mL NiA followed by elution with increasing concentrations of imidazole (50, 75, 100, 125, 300 mM). Elutions 3-5 were pooled dialyzed into the following buffer overnight (100mM DTT, 50 mM Tris-HCl, 25 mM KCl, 2 mM $MgCl_2$, 10% glycerol, 0.01% tween-20, 1 mM PMSF, pH 8.0)(139). Proteins were then concentrated using spin concentrators (Millipore) to a final concentration of 500 μg/ml, as determine by Bradford assay (Bio-Rad).

Purification of SpoVG from *L. monocytogenes*

A truncation of the SpoVG operon was amplified using primers TB258 and TB259, digested, and ligated into pKSV7. Inverse PCR was then used with primers TB274 and TB275 to add a 6His epitope tag to the C-terminus of SpoVG I. Colonies that underwent homologous recombination were screened for losing the pKSV7 plasmid and by sequencing to confirm integration of the 6His epitope tag. 2.8 L of this strain was then grown alongside Wt *L. monocytogenes*

EMSAs and preparation of nucleotide probes

EMSA reactions were performed with the indicated amounts of SpoVG in either 25 or 30 µl volume. Unless otherwise stated, between 250 and 500 ng of ^{32}P labeled DNA/RNA was used for each reaction. All reactions contained 2X EMSA buffer (40 mM Tris HCl, 2 mM $MgCl_2$, 20% glycerol, 300 mM NaCl, 5 mM DTT, pH 8.0), 5 µg yeast tRNA, 1 µg BSA, and 100 ng dI-dC. Reactions were incubated at room-temperature for 30 minutes upon addition of protein before being separated by 6% native-PAGE.

For *in vitro* transcription reactions, the indicated RNAs were amplified by primers listed in Table 4.3 containing T7 promoters and *in vitro* transcribed using α-^{32}P ATP (Perkin Elmer) and a MEGAscript T7 transcription kit (Life Technologies). *In vitro* transcribed RNAs were diluted in TE buffer and purified using MicroSpin G-25 columns (GE Life Sciences). ^{32}P labeling of DNA oligonucleotides was performed using T4 PNK kinase (NEB) and γ-^{32}P ATP (Perkin Elmer).

Motility assays

Motility assays were performed as previously described (234). Briefly, bacterial cultures were grown to stationary phase overnight at 30^o C and 1 µl (approximately 10^7 bacteria) was inoculated into semisolid BHI agar plates contained 0.35% agarose. Plates were incubated at 30^o C for between 3 and 5 days before imaging.

Western blot analysis

For GFP Western blot analysis, 30 ml of the indicated strains were grown to mid-exponential phase shaking at 37^o C in LB media, collected by centrifugation, and lysed by bead-beating and boiling in buffer containing SDS. Protein abundance was normalized to OD_{600} and soluble proteins were separated by denaturing gel electrophoresis. Membranes were probed using anti-GFP (Roche), washed, probed using the appropriate secondary antibodies (LI-COR), and fluorescence was visualized using an Odyssey imaging system (LI-COR). For SpoVG Western blot analysis, 10 ml of bacteria growing in BHI at 37^o C were collected and analyzed similarly but used a SpoVG specific antibody generated against *B. subtilis* SpoVG (a generous gift from Linc Sonenshein, Tufts University) and anti-LLO as a loading control.

Mass spectrometry

Purified SpoVG protein was in-gel digested with Trypsin Gold (Promega), peptides were extracted, and mass spectrometry was performed as described (235). Briefly, peptides were analyzed using a Thermo Dionex UltiMate3000 RSLCnano liquid chromatograph that was connected in-line with a Thermo LTQ-Orbitrap-XL mass spectrometer equipped with a nanoelectrospray ionization source. This instrument is located in the QB3/Chemistry Mass Spectrometry Facility at UC Berkeley.

Modeling of SpoVG

SpoVG from *B. subtilis* (PDB Accession 2IA9) was manipulated using PyMol (The PyMOL Molecular Graphics System, Version 1.7.4 Schrödinger, LLC.) to annotate positively charged residues (R/K/H) and negatively charged residues (E/D).

References

1. **Botzler RG, Cowan AB, Wetzler TF.** 1974. Survival of Listeria monocytogenes in soil and water. J Wildl Dis **10:**204-212.
2. **Welshimer HJ, Donker-Voet J.** 1971. Listeria monocytogenes in nature. Appl Microbiol **21:**516-519.
3. **Weis J, Seeliger HP.** 1975. Incidence of Listeria monocytogenes in nature. Appl Microbiol **30:**29-32.
4. **Botzler RG, Wetzler TF, Cowan AB.** 1973. Listeria in aquatic animals. J Wildl Dis **9:**163-170.
5. **Carpentier B, Cerf O.** 2011. Review--Persistence of Listeria monocytogenes in food industry equipment and premises. Int J Food Microbiol **145:**1-8.
6. **Pearson LJ, Marth EH.** 1990. Listeria monocytogenes--threat to a safe food supply: a review. J Dairy Sci **73:**912-928.
7. **Ferreira V, Barbosa J, Stasiewicz M, Vongkamjan K, Moreno Switt A, Hogg T, Gibbs P, Teixeira P, Wiedmann M.** 2011. Diverse geno- and phenotypes of persistent Listeria monocytogenes isolates from fermented meat sausage production facilities in Portugal. Appl Environ Microbiol **77:**2701-2715.
8. **Vazquez-Boland JA, Kuhn M, Berche P, Chakraborty T, Dominguez-Bernal G, Goebel W, Gonzalez-Zorn B, Wehland J, Kreft J.** 2001. Listeria pathogenesis and molecular virulence determinants. Clin Microbiol Rev **14:**584-640.
9. **Mead PS, Slutsker L, Dietz V, McCaig LF, Bresee JS, Shapiro C, Griffin PM, Tauxe RV.** 1999. Food-related illness and death in the United States. Emerg Infect Dis **5:**607-625.
10. **Hoffmann S, Batz MB, Morris JG, Jr.** 2012. Annual cost of illness and quality-adjusted life year losses in the United States due to 14 foodborne pathogens. J Food Prot **75:**1292-1302.
11. **Jiang L, Olesen I, Andersen T, Fang W, Jespersen L.** 2010. Survival of Listeria monocytogenes in simulated gastrointestinal system and transcriptional profiling of stress- and adhesion-related genes. Foodborne Pathog Dis **7:**267-274.
12. **Nikitas G, Deschamps C, Disson O, Niault T, Cossart P, Lecuit M.** 2011. Transcytosis of Listeria monocytogenes across the intestinal barrier upon specific targeting of goblet cell accessible E-cadherin. J Exp Med **208:**2263-2277.
13. **Corr S, Hill C, Gahan CG.** 2006. An in vitro cell-culture model demonstrates internalin- and hemolysin-independent translocation of Listeria monocytogenes across M cells. Microb Pathog **41:**241-250.
14. **Melton-Witt JA, Rafelski SM, Portnoy DA, Bakardjiev AI.** 2012. Oral infection with signature-tagged Listeria monocytogenes reveals organ-specific growth and dissemination routes in guinea pigs. Infect Immun **80:**720-732.
15. **Hardy J, Francis KP, DeBoer M, Chu P, Gibbs K, Contag CH.** 2004. Extracellular replication of Listeria monocytogenes in the murine gall bladder. Science **303:**851-853.
16. **O'Riordan M, Yi CH, Gonzales R, Lee KD, Portnoy DA.** 2002. Innate recognition of bacteria by a macrophage cytosolic surveillance pathway. Proc Natl Acad Sci U S A **99:**13861-13866.
17. **Woodward JJ, Iavarone AT, Portnoy DA.** 2010. c-di-AMP secreted by intracellular Listeria monocytogenes activates a host type I interferon response. Science **328:**1703-1705.
18. **Vance RE, Isberg RR, Portnoy DA.** 2009. Patterns of pathogenesis: discrimination of pathogenic and nonpathogenic microbes by the innate immune system. Cell Host Microbe **6:**10-21.
19. **Witte CE, Whiteley AT, Burke TP, Sauer JD, Portnoy DA, Woodward JJ.** 2013. Cyclic di-AMP is critical for Listeria monocytogenes growth, cell wall homeostasis, and establishment of infection. MBio **4:**e00282-00213.
20. **Sauer JD, Sotelo-Troha K, von Moltke J, Monroe KM, Rae CS, Brubaker SW, Hyodo M, Hayakawa Y, Woodward JJ, Portnoy DA, Vance RE.** 2011. The N-ethyl-N-nitrosourea-

induced Goldenticket mouse mutant reveals an essential function of Sting in the in vivo interferon response to Listeria monocytogenes and cyclic dinucleotides. Infect Immun **79:**688-694.
21. **Burdette DL, Vance RE.** 2013. STING and the innate immune response to nucleic acids in the cytosol. Nat Immunol **14:**19-26.
22. **Burdette DL, Monroe KM, Sotelo-Troha K, Iwig JS, Eckert B, Hyodo M, Hayakawa Y, Vance RE.** 2011. STING is a direct innate immune sensor of cyclic di-GMP. Nature **478:**515-518.
23. **Sauer JD, Witte CE, Zemansky J, Hanson B, Lauer P, Portnoy DA.** 2010. Listeria monocytogenes triggers AIM2-mediated pyroptosis upon infrequent bacteriolysis in the macrophage cytosol. Cell Host Microbe **7:**412-419.
24. **Sun L, Wu J, Du F, Chen X, Chen ZJ.** 2013. Cyclic GMP-AMP synthase is a cytosolic DNA sensor that activates the type I interferon pathway. Science **339:**786-791.
25. **Hornung V, Ablasser A, Charrel-Dennis M, Bauernfeind F, Horvath G, Caffrey DR, Latz E, Fitzgerald KA.** 2009. AIM2 recognizes cytosolic dsDNA and forms a caspase-1-activating inflammasome with ASC. Nature **458:**514-518.
26. **Burckstummer T, Baumann C, Bluml S, Dixit E, Durnberger G, Jahn H, Planyavsky M, Bilban M, Colinge J, Bennett KL, Superti-Furga G.** 2009. An orthogonal proteomic-genomic screen identifies AIM2 as a cytoplasmic DNA sensor for the inflammasome. Nat Immunol **10:**266-272.
27. **Fernandes-Alnemri T, Yu JW, Datta P, Wu J, Alnemri ES.** 2009. AIM2 activates the inflammasome and cell death in response to cytoplasmic DNA. Nature **458:**509-513.
28. **Chavarria-Smith J, Vance RE.** 2015. The NLRP1 inflammasomes. Immunol Rev **265:**22-34.
29. **Vance RE.** 2015. The NAIP/NLRC4 inflammasomes. Curr Opin Immunol **32:**84-89.
30. **Kofoed EM, Vance RE.** 2012. NAIPs: building an innate immune barrier against bacterial pathogens. NAIPs function as sensors that initiate innate immunity by detection of bacterial proteins in the host cell cytosol. Bioessays **34:**589-598.
31. **Kofoed EM, Vance RE.** 2011. Innate immune recognition of bacterial ligands by NAIPs determines inflammasome specificity. Nature **477:**592-595.
32. **Sauer JD, Pereyre S, Archer KA, Burke TP, Hanson B, Lauer P, Portnoy DA.** 2011. Listeria monocytogenes engineered to activate the Nlrc4 inflammasome are severely attenuated and are poor inducers of protective immunity. Proc Natl Acad Sci U S A **108:**12419-12424.
33. **Harty JT, Schreiber RD, Bevan MJ.** 1992. CD8 T cells can protect against an intracellular bacterium in an interferon gamma-independent fashion. Proc Natl Acad Sci U S A **89:**11612-11616.
34. **Archer KA, Durack J, Portnoy DA.** 2014. STING-dependent type I IFN production inhibits cell-mediated immunity to Listeria monocytogenes. PLoS Pathog **10:**e1003861.
35. **Le DT, Wang-Gillam A, Picozzi V, Greten TF, Crocenzi T, Springett G, Morse M, Zeh H, Cohen D, Fine RL, Onners B, Uram JN, Laheru DA, Lutz ER, Solt S, Murphy AL, Skoble J, Lemmens E, Grous J, Dubensky T, Jr., Brockstedt DG, Jaffee EM.** 2015. Safety and Survival With GVAX Pancreas Prime and Listeria Monocytogenes-Expressing Mesothelin (CRS-207) Boost Vaccines for Metastatic Pancreatic Cancer. J Clin Oncol **33:**1325-1333.
36. **Geoffroy C, Gaillard JL, Alouf JE, Berche P.** 1987. Purification, characterization, and toxicity of the sulfhydryl-activated hemolysin listeriolysin O from Listeria monocytogenes. Infect Immun **55:**1641-1646.
37. **Mengaud J, Chenevert J, Geoffroy C, Gaillard JL, Cossart P.** 1987. Identification of the structural gene encoding the SH-activated hemolysin of Listeria monocytogenes: listeriolysin O is homologous to streptolysin O and pneumolysin. Infect Immun **55:**3225-3227.
38. **Mengaud J, Vicente MF, Chenevert J, Pereira JM, Geoffroy C, Gicquel-Sanzey B, Baquero F, Perez-Diaz JC, Cossart P.** 1988. Expression in Escherichia coli and sequence analysis of the listeriolysin O determinant of Listeria monocytogenes. Infect Immun **56:**766-772.

39. **Cossart P.** 1988. The listeriolysin O gene: a chromosomal locus crucial for the virulence of Listeria monocytogenes. Infection **16 Suppl 2:**S157-159.
40. **Parrisius J, Bhakdi S, Roth M, Tranum-Jensen J, Goebel W, Seeliger HP.** 1986. Production of listeriolysin by beta-hemolytic strains of Listeria monocytogenes. Infect Immun **51:**314-319.
41. **Jacobs T, Darji A, Frahm N, Rohde M, Wehland J, Chakraborty T, Weiss S.** 1998. Listeriolysin O: cholesterol inhibits cytolysis but not binding to cellular membranes. Mol Microbiol **28:**1081-1089.
42. **Shatursky O, Heuck AP, Shepard LA, Rossjohn J, Parker MW, Johnson AE, Tweten RK.** 1999. The mechanism of membrane insertion for a cholesterol-dependent cytolysin: a novel paradigm for pore-forming toxins. Cell **99:**293-299.
43. **Tweten RK, Parker MW, Johnson AE.** 2001. The cholesterol-dependent cytolysins. Curr Top Microbiol Immunol **257:**15-33.
44. **Morgan PJ, Hyman SC, Byron O, Andrew PW, Mitchell TJ, Rowe AJ.** 1994. Modeling the bacterial protein toxin, pneumolysin, in its monomeric and oligomeric form. J Biol Chem **269:**25315-25320.
45. **Portnoy DA, Tweten RK, Kehoe M, Bielecki J.** 1992. Capacity of listeriolysin O, streptolysin O, and perfringolysin O to mediate growth of Bacillus subtilis within mammalian cells. Infect Immun **60:**2710-2717.
46. **Brunt LM, Portnoy DA, Unanue ER.** 1990. Presentation of Listeria monocytogenes to CD8+ T cells requires secretion of hemolysin and intracellular bacterial growth. J Immunol **145:**3540-3546.
47. **Cossart P, Vicente MF, Mengaud J, Baquero F, Perez-Diaz JC, Berche P.** 1989. Listeriolysin O is essential for virulence of Listeria monocytogenes: direct evidence obtained by gene complementation. Infect Immun **57:**3629-3636.
48. **Tilney LG, Connelly PS, Portnoy DA.** 1990. Actin filament nucleation by the bacterial pathogen, Listeria monocytogenes. J Cell Biol **111:**2979-2988.
49. **Kocks C, Gouin E, Tabouret M, Berche P, Ohayon H, Cossart P.** 1992. L. monocytogenes-induced actin assembly requires the actA gene product, a surface protein. Cell **68:**521-531.
50. **Cameron LA, Footer MJ, van Oudenaarden A, Theriot JA.** 1999. Motility of ActA protein-coated microspheres driven by actin polymerization. Proc Natl Acad Sci U S A **96:**4908-4913.
51. **Welch MD, Rosenblatt J, Skoble J, Portnoy DA, Mitchison TJ.** 1998. Interaction of human Arp2/3 complex and the Listeria monocytogenes ActA protein in actin filament nucleation. Science **281:**105-108.
52. **Welch MD, Iwamatsu A, Mitchison TJ.** 1997. Actin polymerization is induced by Arp2/3 protein complex at the surface of Listeria monocytogenes. Nature **385:**265-269.
53. **Tilney LG, Portnoy DA.** 1989. Actin filaments and the growth, movement, and spread of the intracellular bacterial parasite, Listeria monocytogenes. J Cell Biol **109:**1597-1608.
54. **Mitchell G, Ge L, Huang Q, Chen C, Kianian S, Roberts MF, Schekman R, Portnoy DA.** 2015. Avoidance of autophagy mediated by PlcA or ActA is required for Listeria monocytogenes growth in macrophages. Infect Immun.
55. **Reniere ML, Whiteley AT, Hamilton KL, John SM, Lauer P, Brennan RG, Portnoy DA.** 2015. Glutathione activates virulence gene expression of an intracellular pathogen. Nature **517:**170-173.
56. **Hacker J, Blum-Oehler G, Muhldorfer I, Tschape H.** 1997. Pathogenicity islands of virulent bacteria: structure, function and impact on microbial evolution. Mol Microbiol **23:**1089-1097.
57. **Groisman EA, Ochman H.** 1996. Pathogenicity islands: bacterial evolution in quantum leaps. Cell **87:**791-794.
58. **Lauer P, Chow MY, Loessner MJ, Portnoy DA, Calendar R.** 2002. Construction, characterization, and use of two Listeria monocytogenes site-specific phage integration vectors. J Bacteriol **184:**4177-4186.

59. **Smith K, Youngman P.** 1992. Use of a new integrational vector to investigate compartment-specific expression of the Bacillus subtilis spoIIM gene. Biochimie **74:**705-711.
60. **Zemansky J, Kline BC, Woodward JJ, Leber JH, Marquis H, Portnoy DA.** 2009. Development of a mariner-based transposon and identification of Listeria monocytogenes determinants, including the peptidyl-prolyl isomerase PrsA2, that contribute to its hemolytic phenotype. J Bacteriol **191:**3950-3964.
61. **Sun AN, Camilli A, Portnoy DA.** 1990. Isolation of Listeria monocytogenes small-plaque mutants defective for intracellular growth and cell-to-cell spread. Infect Immun **58:**3770-3778.
62. **Portnoy DA, Jacks PS, Hinrichs DJ.** 1988. Role of hemolysin for the intracellular growth of Listeria monocytogenes. J Exp Med **167:**1459-1471.
63. **Bakardjiev AI, Stacy BA, Fisher SJ, Portnoy DA.** 2004. Listeriosis in the pregnant guinea pig: a model of vertical transmission. Infect Immun **72:**489-497.
64. **Bakardjiev AI, Stacy BA, Portnoy DA.** 2005. Growth of Listeria monocytogenes in the guinea pig placenta and role of cell-to-cell spread in fetal infection. J Infect Dis **191:**1889-1897.
65. **Bakardjiev AI, Theriot JA, Portnoy DA.** 2006. Listeria monocytogenes traffics from maternal organs to the placenta and back. PLoS Pathog **2:**e66.
66. **Bou Ghanem EN, Jones GS, Myers-Morales T, Patil PD, Hidayatullah AN, D'Orazio SE.** 2012. InlA promotes dissemination of Listeria monocytogenes to the mesenteric lymph nodes during food borne infection of mice. PLoS Pathog **8:**e1003015.
67. **Callewaert L, Michiels CW.** 2010. Lysozymes in the animal kingdom. J Biosci **35:**127-160.
68. **Fleming A.** 1932. Lysozyme: President's Address. Proc R Soc Med **26:**71-84.
69. **Fleming A.** 1922. On a Remarkable Bacteriolytic Element found in Tissues and Secretions. Proceedings of the Royal Society of London B: Biological Sciences **93:**306-317.
70. **Fleming A, Allison VD.** 1927. On the development of strains of bacteria resistant to lysozyme action and the relation of lysozyme action to intracellular digestion. British Journal of experimental pathology **8:**214-218.
71. **Wennergren G, Lagercrantz H.** 2007. "One sometimes finds what one is not looking for" (Sir Alexander Fleming): the most important medical discovery of the 20th century. Acta Paediatr **96:**141-144.
72. **Meyer K, Thompson R, Palmer JW, Khorazo D.** 1934. The Nature of Lysozyme Action. Science **79:**61.
73. **Meyer K, Hahnel E.** 1946. Lysozyme as a mucolytic enzyme. Fed Proc **5:**147.
74. **Epstein LA, Chain E.** 1940. Some observations on the preparation and properties of the substrate of lysozyme. The British Journal of Experimental Pathology **21:**339-355.
75. **Ghuysen JM.** 1960. Acetylhexosamine compounds enzymically released from Micrococcus lysodeikticus cell walls. II. Enzymic sensitivity of purified acetylhexosamine and acetylhexosamine-peptide complexes. Biochim Biophys Acta **40:**473-480.
76. **Ghuysen JM, Salton MR.** 1960. Acetylhexosamine compounds enzymically released from Micrococcus lysodeikticus cell walls. I. Isolation and composition of acetylhexosamine and acetylhexosamine-peptide complexes. Biochim Biophys Acta **40:**462-472.
77. **Salton MR, Ghuysen JM.** 1960. Acetylhexosamine compounds enzymically released from Micrococcus lysodeikticus cell walls. III. The structure of DI- and tetra-saccharides released from cell walls by lysozyme and Streptomyces F1 enzyme. Biochim Biophys Acta **45:**355-363.
78. **Salton MR, Ghuysen JM.** 1959. The structure of di- and tetrasaccharides released from cell walls by lysozyme and Streptomyces F 1 enzyme and the beta(1 to 4) N-acetylhexos-aminidase activity of these enzymes. Biochim Biophys Acta **36:**552-554.
79. **Saari KM, Aine E, Posz A, Klockars M.** 1983. Lysozyme content of tears in normal subjects and in patients with external eye infections. Graefes Arch Clin Exp Ophthalmol **221:**86-88.
80. **Aine E, Morsky P.** 1984. Lysozyme concentration in tears--assessment of reference values in normal subjects. Acta Ophthalmol (Copenh) **62:**932-938.

81. **Hankiewicz J, Swierczek E.** 1974. Lysozyme in human body fluids. Clin Chim Acta **57:**205-209.
82. **Ganz T, Lehrer RI.** 1997. Antimicrobial peptides of leukocytes. Curr Opin Hematol **4:**53-58.
83. **Gordon S, Todd J, Cohn ZA.** 1974. In vitro synthesis and secretion of lysozyme by mononuclear phagocytes. J Exp Med **139:**1228-1248.
84. **Blake CC, Koenig DF, Mair GA, North AC, Phillips DC, Sarma VR.** 1965. Structure of hen egg-white lysozyme. A three-dimensional Fourier synthesis at 2 Angstrom resolution. Nature **206:**757-761.
85. **Kendrew JC, Dickerson RE, Strandberg BE, Hart RG, Davies DR, Phillips DC, Shore VC.** 1960. Structure of myoglobin: A three-dimensional Fourier synthesis at 2 A. resolution. Nature **185:**422-427.
86. **Vollmer W, Joris B, Charlier P, Foster S.** 2008. Bacterial peptidoglycan (murein) hydrolases. FEMS Microbiol Rev **32:**259-286.
87. **Vollmer W, Blanot D, de Pedro MA.** 2008. Peptidoglycan structure and architecture. FEMS Microbiol Rev **32:**149-167.
88. **Sauvage E, Kerff F, Terrak M, Ayala JA, Charlier P.** 2008. The penicillin-binding proteins: structure and role in peptidoglycan biosynthesis. FEMS Microbiol Rev **32:**234-258.
89. **Bera A, Herbert S, Jakob A, Vollmer W, Gotz F.** 2005. Why are pathogenic staphylococci so lysozyme resistant? The peptidoglycan O-acetyltransferase OatA is the major determinant for lysozyme resistance of Staphylococcus aureus. Mol Microbiol **55:**778-787.
90. **Burke TP, Loukitcheva A, Zemansky J, Wheeler R, Boneca IG, Portnoy DA.** 2014. Listeria monocytogenes is resistant to lysozyme through the regulation, not the acquisition, of cell wall-modifying enzymes. J Bacteriol **196:**3756-3767.
91. **Vollmer W, Tomasz A.** 2000. The pgdA gene encodes for a peptidoglycan N-acetylglucosamine deacetylase in Streptococcus pneumoniae. J Biol Chem **275:**20496-20501.
92. **Rae CS, Geissler A, Adamson PC, Portnoy DA.** 2011. Mutations of the Listeria monocytogenes Peptidoglycan N-Deacetylase and O-Acetylase Result in Enhanced Lysozyme Sensitivity, Bacteriolysis, and Hyperinduction of Innate Immune Pathways. Infect Immun **79:**3596-3606.
93. **Bera A, Biswas R, Herbert S, Gotz F.** 2006. The presence of peptidoglycan O-acetyltransferase in various staphylococcal species correlates with lysozyme resistance and pathogenicity. Infect Immun **74:**4598-4604.
94. **Herbert S, Bera A, Nerz C, Kraus D, Peschel A, Goerke C, Meehl M, Cheung A, Gotz F.** 2007. Molecular basis of resistance to muramidase and cationic antimicrobial peptide activity of lysozyme in staphylococci. PLoS Pathog **3:**e102.
95. **Bera A, Biswas R, Herbert S, Kulauzovic E, Weidenmaier C, Peschel A, Gotz F.** 2007. Influence of wall teichoic acid on lysozyme resistance in Staphylococcus aureus. J Bacteriol **189:**280-283.
96. **Wichgers Schreur PJ, van Weeghel C, Rebel JM, Smits MA, van Putten JP, Smith HE.** 2012. Lysozyme resistance in Streptococcus suis is highly variable and multifactorial. PLoS One **7:**e36281.
97. **Coulon J, Houles A, Dimopoulou M, Maupeu J, Dols-Lafargue M.** 2012. Lysozyme resistance of the ropy strain Pediococcus parvulus IOEB 8801 is correlated with beta-glucan accumulation around the cell. Int J Food Microbiol **159:**25-29.
98. **Callewaert L, Aertsen A, Deckers D, Vanoirbeek KG, Vanderkelen L, Van Herreweghe JM, Masschalck B, Nakimbugwe D, Robben J, Michiels CW.** 2008. A new family of lysozyme inhibitors contributing to lysozyme tolerance in gram-negative bacteria. PLoS Pathog **4:**e1000019.
99. **Vanderkelen L, Van Herreweghe JM, Vanoirbeek KG, Baggerman G, Myrnes B, Declerck PJ, Nilsen IW, Michiels CW, Callewaert L.** 2011. Identification of a bacterial inhibitor against g-type lysozyme. Cell Mol Life Sci **68:**1053-1064.

100. **Deckers D, Masschalck B, Aertsen A, Callewaert L, Van Tiggelen CG, Atanassova M, Michiels CW.** 2004. Periplasmic lysozyme inhibitor contributes to lysozyme resistance in Escherichia coli. Cell Mol Life Sci **61:**1229-1237.
101. **Monchois V, Abergel C, Sturgis J, Jeudy S, Claverie JM.** 2001. Escherichia coli ykfE ORFan gene encodes a potent inhibitor of C-type lysozyme. J Biol Chem **276:**18437-18441.
102. **Ho TD, Hastie JL, Intile PJ, Ellermeier CD.** 2011. The Bacillus subtilis extracytoplasmic function sigma factor sigma(V) is induced by lysozyme and provides resistance to lysozyme. J Bacteriol **193:**6215-6222.
103. **Flores AR, Parsons LM, Pavelka MS, Jr.** 2005. Characterization of novel Mycobacterium tuberculosis and Mycobacterium smegmatis mutants hypersusceptible to beta-lactam antibiotics. J Bacteriol **187:**1892-1900.
104. **Aubry C, Goulard C, Nahori MA, Cayet N, Decalf J, Sachse M, Boneca IG, Cossart P, Dussurget O.** 2011. OatA, a Peptidoglycan O-Acetyltransferase Involved in Listeria monocytogenes Immune Escape, Is Critical for Virulence. J Infect Dis **204:**731-740.
105. **Boneca IG, Dussurget O, Cabanes D, Nahori MA, Sousa S, Lecuit M, Psylinakis E, Bouriotis V, Hugot JP, Giovannini M, Coyle A, Bertin J, Namane A, Rousselle JC, Cayet N, Prevost MC, Balloy V, Chignard M, Philpott DJ, Cossart P, Girardin SE.** 2007. A critical role for peptidoglycan N-deacetylation in Listeria evasion from the host innate immune system. Proc Natl Acad Sci U S A **104:**997-1002.
106. **Fittipaldi N, Sekizaki T, Takamatsu D, de la Cruz Dominguez-Punaro M, Harel J, Bui NK, Vollmer W, Gottschalk M.** 2008. Significant contribution of the pgdA gene to the virulence of Streptococcus suis. Mol Microbiol **70:**1120-1135.
107. **Kaoukab-Raji A, Biskri L, Bernardini ML, Allaoui A.** 2012. Characterization of SfPgdA, a Shigella flexneri peptidoglycan deacetylase required for bacterial persistence within polymorphonuclear neutrophils. Microbes Infect **14:**619-627.
108. **Nash JA, Ballard TN, Weaver TE, Akinbi HT.** 2006. The peptidoglycan-degrading property of lysozyme is not required for bactericidal activity in vivo. J Immunol **177:**519-526.
109. **Thedieck K, Hain T, Mohamed W, Tindall BJ, Nimtz M, Chakraborty T, Wehland J, Jansch L.** 2006. The MprF protein is required for lysinylation of phospholipids in listerial membranes and confers resistance to cationic antimicrobial peptides (CAMPs) on Listeria monocytogenes. Mol Microbiol **62:**1325-1339.
110. **Abachin E, Poyart C, Pellegrini E, Milohanic E, Fiedler F, Berche P, Trieu-Cuot P.** 2002. Formation of D-alanyl-lipoteichoic acid is required for adhesion and virulence of Listeria monocytogenes. Mol Microbiol **43:**1-14.
111. **Mandin P, Fsihi H, Dussurget O, Vergassola M, Milohanic E, Toledo-Arana A, Lasa I, Johansson J, Cossart P.** 2005. VirR, a response regulator critical for Listeria monocytogenes virulence. Mol Microbiol **57:**1367-1380.
112. **Guariglia-Oropeza V, Helmann JD.** 2011. Bacillus subtilis sigma(V) confers lysozyme resistance by activation of two cell wall modification pathways, peptidoglycan O-acetylation and D-alanylation of teichoic acids. J Bacteriol **193:**6223-6232.
113. **Tucker BJ, Breaker RR.** 2005. Riboswitches as versatile gene control elements. Curr Opin Struct Biol **15:**342-348.
114. **Storz G, Vogel J, Wassarman KM.** 2011. Regulation by small RNAs in bacteria: expanding frontiers. Mol Cell **43:**880-891.
115. **Frohlich KS, Vogel J.** 2009. Activation of gene expression by small RNA. Curr Opin Microbiol **12:**674-682.
116. **Wassarman KM, Storz G.** 2000. 6S RNA regulates E. coli RNA polymerase activity. Cell **101:**613-623.
117. **Liu MY, Gui G, Wei B, Preston JF, 3rd, Oakford L, Yuksel U, Giedroc DP, Romeo T.** 1997. The RNA molecule CsrB binds to the global regulatory protein CsrA and antagonizes its activity in Escherichia coli. J Biol Chem **272:**17502-17510.

118. **Vogel J, Luisi BF.** 2011. Hfq and its constellation of RNA. Nat Rev Microbiol **9:**578-589.
119. **Chao Y, Vogel J.** 2010. The role of Hfq in bacterial pathogens. Curr Opin Microbiol **13:**24-33.
120. **Nielsen JS, Lei LK, Ebersbach T, Olsen AS, Klitgaard JK, Valentin-Hansen P, Kallipolitis BH.** 2010. Defining a role for Hfq in Gram-positive bacteria: evidence for Hfq-dependent antisense regulation in Listeria monocytogenes. Nucleic Acids Res **38:**907-919.
121. **Bohn C, Rigoulay C, Bouloc P.** 2007. No detectable effect of RNA-binding protein Hfq absence in Staphylococcus aureus. BMC Microbiol **7:**10.
122. **Toledo-Arana A, Dussurget O, Nikitas G, Sesto N, Guet-Revillet H, Balestrino D, Loh E, Gripenland J, Tiensuu T, Vaitkevicius K, Barthelemy M, Vergassola M, Nahori MA, Soubigou G, Regnault B, Coppee JY, Lecuit M, Johansson J, Cossart P.** 2009. The Listeria transcriptional landscape from saprophytism to virulence. Nature **459:**950-956.
123. **Mraheil MA, Billion A, Mohamed W, Mukherjee K, Kuenne C, Pischimarov J, Krawitz C, Retey J, Hartsch T, Chakraborty T, Hain T.** 2011. The intracellular sRNA transcriptome of Listeria monocytogenes during growth in macrophages. Nucleic Acids Res **39:**4235-4248.
124. **Behrens S, Widder S, Mannala GK, Qing X, Madhugiri R, Kefer N, Mraheil MA, Rattei T, Hain T.** 2014. Ultra Deep Sequencing of Listeria monocytogenes sRNA Transcriptome Revealed New Antisense RNAs. PLoS One **9:**e83979.
125. **Wurtzel O, Sesto N, Mellin JR, Karunker I, Edelheit S, Becavin C, Archambaud C, Cossart P, Sorek R.** 2012. Comparative transcriptomics of pathogenic and non-pathogenic Listeria species. Mol Syst Biol **8:**583.
126. **Izar B, Mraheil MA, Hain T.** 2011. Identification and Role of Regulatory Non-Coding RNAs in Listeria monocytogenes. Int J Mol Sci **12:**5070-5079.
127. **Tjaden B.** 2012. Computational identification of sRNA targets. Methods Mol Biol **905:**227-234.
128. **Eggenhofer F, Tafer H, Stadler PF, Hofacker IL.** 2011. RNApredator: fast accessibility-based prediction of sRNA targets. Nucleic Acids Res **39:**W149-154.
129. **Gopel Y, Gorke B.** 2014. Lies and deception in bacterial gene regulation: the roles of nucleic acid decoys. Mol Microbiol **92:**641-647.
130. **Overgaard M, Johansen J, Moller-Jensen J, Valentin-Hansen P.** 2009. Switching off small RNA regulation with trap-mRNA. Mol Microbiol **73:**790-800.
131. **Figueroa-Bossi N, Valentini M, Malleret L, Fiorini F, Bossi L.** 2009. Caught at its own game: regulatory small RNA inactivated by an inducible transcript mimicking its target. Genes Dev **23:**2004-2015.
132. **Rosenbluh A, Banner CD, Losick R, Fitz-James PC.** 1981. Identification of a new developmental locus in Bacillus subtilis by construction of a deletion mutation in a cloned gene under sporulation control. J Bacteriol **148:**341-351.
133. **Zuber P, Losick R.** 1983. Use of a lacZ fusion to study the role of the spoO genes of Bacillus subtilis in developmental regulation. Cell **35:**275-283.
134. **Matsuno K, Sonenshein AL.** 1999. Role of SpoVG in asymmetric septation in Bacillus subtilis. J Bacteriol **181:**3392-3401.
135. **Meier S, Goerke C, Wolz C, Seidl K, Homerova D, Schulthess B, Kormanec J, Berger-Bachi B, Bischoff M.** 2007. sigmaB and the sigmaB-dependent arlRS and yabJ-spoVG loci affect capsule formation in Staphylococcus aureus. Infect Immun **75:**4562-4571.
136. **Schulthess B, Bloes DA, Francois P, Girard M, Schrenzel J, Bischoff M, Berger-Bachi B.** 2011. The sigmaB-dependent yabJ-spoVG operon is involved in the regulation of extracellular nuclease, lipase, and protease expression in Staphylococcus aureus. J Bacteriol **193:**4954-4962.
137. **Schulthess B, Meier S, Homerova D, Goerke C, Wolz C, Kormanec J, Berger-Bachi B, Bischoff M.** 2009. Functional characterization of the sigmaB-dependent yabJ-spoVG operon in Staphylococcus aureus: role in methicillin and glycopeptide resistance. Antimicrob Agents Chemother **53:**1832-1839.

138. **Whiteley AT, Pollock AJ, Portnoy DA.** 2015. The PAMP c-di-AMP is essential for Listeria growth in macrophages and rich but not minimal media, due to a toxic increase in (p)ppGpp. Cell Host Microbe **(In Press)**.
139. **Jutras BL, Chenail AM, Rowland CL, Carroll D, Miller MC, Bykowski T, Stevenson B.** 2013. Eubacterial SpoVG homologs constitute a new family of site-specific DNA-binding proteins. PLoS One **8:**e66683.
140. **Eyraud A, Tattevin P, Chabelskaya S, Felden B.** 2014. A small RNA controls a protein regulator involved in antibiotic resistance in Staphylococcus aureus. Nucleic Acids Res **42:**4892-4905.
141. **Romilly C, Lays C, Tomasini A, Caldelari I, Benito Y, Hammann P, Geissmann T, Boisset S, Romby P, Vandenesch F.** 2014. A non-coding RNA promotes bacterial persistence and decreases virulence by regulating a regulator in Staphylococcus aureus. PLoS Pathog **10:**e1003979.
142. **Tan K, Borovilos M, Abdullah J, Joachimiak A.** 2006. The Structure of SpoVG from Bacillus subtilis, PDB, ID 2IA9.
143. **Tan K, Matlseva N, Bargassa M, Joachimiak A.** 2006. The crystal structure of SpoVG from Staphylococcus epidermidis, PDB, entry 2I9X.
144. **Misra SK, Milohanic E, Ake F, Mijakovic I, Deutscher J, Monnet V, Henry C.** 2011. Analysis of the serine/threonine/tyrosine phosphoproteome of the pathogenic bacterium Listeria monocytogenes reveals phosphorylated proteins related to virulence. Proteomics **11:**4155-4165.
145. **Premaratne RJ, Lin WJ, Johnson EA.** 1991. Development of an improved chemically defined minimal medium for Listeria monocytogenes. Appl Environ Microbiol **57:**3046-3048.
146. **Phan-Thanh L, Gormon T.** 1997. A chemically defined minimal medium for the optimal culture of Listeria. Int J Food Microbiol **35:**91-95.
147. **Barabote RD, Saier MH, Jr.** 2005. Comparative genomic analyses of the bacterial phosphotransferase system. Microbiol Mol Biol Rev **69:**608-634.
148. **Stoll R, Goebel W.** 2010. The major PEP-phosphotransferase systems (PTSs) for glucose, mannose and cellobiose of Listeria monocytogenes, and their significance for extra- and intracellular growth. Microbiology **156:**1069-1083.
149. **Vogel J.** 2009. An RNA trap helps bacteria get the most out of chitosugars. Mol Microbiol **73:**737-741.
150. **Yu C, Lee AM, Bassler BL, Roseman S.** 1991. Chitin utilization by marine bacteria. A physiological function for bacterial adhesion to immobilized carbohydrates. J Biol Chem **266:**24260-24267.
151. **Davis KM, Weiser JN.** 2011. Modifications to the peptidoglycan backbone help bacteria to establish infection. Infect Immun **79:**562-570.
152. **Vollmer W.** 2008. Structural variation in the glycan strands of bacterial peptidoglycan. FEMS Microbiol Rev **32:**287-306.
153. **Camilli A, Portnoy A, Youngman P.** 1990. Insertional mutagenesis of Listeria monocytogenes with a novel Tn917 derivative that allows direct cloning of DNA flanking transposon insertions. J Bacteriol **172:**3738-3744.
154. **Forster BM, Zemansky J, Portnoy DA, Marquis H.** 2011. Posttranslocation chaperone PrsA2 regulates the maturation and secretion of Listeria monocytogenes proprotein virulence factors. J Bacteriol **193:**5961-5970.
155. **Alonzo F, 3rd, Xayarath B, Whisstock JC, Freitag NE.** 2011. Functional analysis of the Listeria monocytogenes secretion chaperone PrsA2 and its multiple contributions to bacterial virulence. Mol Microbiol **80:**1530-1548.
156. **Dubrac S, Bisicchia P, Devine KM, Msadek T.** 2008. A matter of life and death: cell wall homeostasis and the WalKR (YycGF) essential signal transduction pathway. Mol Microbiol **70:**1307-1322.

157. **Dubrac S, Msadek T.** 2008. Tearing down the wall: peptidoglycan metabolism and the WalK/WalR (YycG/YycF) essential two-component system. Adv Exp Med Biol **631:**214-228.
158. **Bisicchia P, Noone D, Lioliou E, Howell A, Quigley S, Jensen T, Jarmer H, Devine KM.** 2007. The essential YycFG two-component system controls cell wall metabolism in Bacillus subtilis. Mol Microbiol **65:**180-200.
159. **Howell A, Dubrac S, Andersen KK, Noone D, Fert J, Msadek T, Devine K.** 2003. Genes controlled by the essential YycG/YycF two-component system of Bacillus subtilis revealed through a novel hybrid regulator approach. Mol Microbiol **49:**1639-1655.
160. **Ng WL, Kazmierczak KM, Winkler ME.** 2004. Defective cell wall synthesis in Streptococcus pneumoniae R6 depleted for the essential PcsB putative murein hydrolase or the VicR (YycF) response regulator. Mol Microbiol **53:**1161-1175.
161. **Steen A, Palumbo E, Deghorain M, Cocconcelli PS, Delcour J, Kuipers OP, Kok J, Buist G, Hols P.** 2005. Autolysis of Lactococcus lactis is increased upon D-alanine depletion of peptidoglycan and lipoteichoic acids. J Bacteriol **187:**114-124.
162. **Gueriri I, Bay S, Dubrac S, Cyncynatus C, Msadek T.** 2008. The Pta-AckA pathway controlling acetyl phosphate levels and the phosphorylation state of the DegU orphan response regulator both play a role in regulating Listeria monocytogenes motility and chemotaxis. Mol Microbiol **70:**1342-1357.
163. **Gueriri I, Cyncynatus C, Dubrac S, Arana AT, Dussurget O, Msadek T.** 2008. The DegU orphan response regulator of Listeria monocytogenes autorepresses its own synthesis and is required for bacterial motility, virulence and biofilm formation. Microbiology **154:**2251-2264.
164. **Knudsen GM, Olsen JE, Dons L.** 2004. Characterization of DegU, a response regulator in Listeria monocytogenes, involved in regulation of motility and contributes to virulence. FEMS Microbiol Lett **240:**171-179.
165. **Mauder N, Williams T, Fritsch F, Kuhn M, Beier D.** 2008. Response regulator DegU of Listeria monocytogenes controls temperature-responsive flagellar gene expression in its unphosphorylated state. J Bacteriol **190:**4777-4781.
166. **Williams T, Joseph B, Beier D, Goebel W, Kuhn M.** 2005. Response regulator DegU of Listeria monocytogenes regulates the expression of flagella-specific genes. FEMS Microbiol Lett **252:**287-298.
167. **Williams T, Bauer S, Beier D, Kuhn M.** 2005. Construction and characterization of Listeria monocytogenes mutants with in-frame deletions in the response regulator genes identified in the genome sequence. Infect Immun **73:**3152-3159.
168. **Cross M, Mangelsdorf I, Wedel A, Renkawitz R.** 1988. Mouse lysozyme M gene: isolation, characterization, and expression studies. Proc Natl Acad Sci U S A **85:**6232-6236.
169. **Wehkamp J, Chu H, Shen B, Feathers RW, Kays RJ, Lee SK, Bevins CL.** 2006. Paneth cell antimicrobial peptides: topographical distribution and quantification in human gastrointestinal tissues. FEBS Lett **580:**5344-5350.
170. **Milani CJ, Aziz RK, Locke JB, Dahesh S, Nizet V, Buchanan JT.** 2010. The novel polysaccharide deacetylase homologue Pdi contributes to virulence of the aquatic pathogen Streptococcus iniae. Microbiology **156:**543-554.
171. **Conlan JW, North RJ.** 1991. Neutrophil-mediated dissolution of infected host cells as a defense strategy against a facultative intracellular bacterium. J Exp Med **174:**741-744.
172. **Glynn AA, Milne CM.** 1967. A kinetic study of the bacteriolytic and bactericidal action of human serum. Immunology **12:**639-653.
173. **Feingold DS, Goldman JN, Kuritz HM.** 1968. Locus of the action of serum and the role of lysozyme in the serum bactericidal reaction. J Bacteriol **96:**2118-2126.
174. **Prixova J.** 1975. Serum lysozyme in mice subjected to combined immunosuppression with 6-mercaptopurine and hydrocortisone. Folia Microbiol (Praha) **20:**509-512.
175. **Murray EJ, Kiley TB, Stanley-Wall NR.** 2009. A pivotal role for the response regulator DegU in controlling multicellular behaviour. Microbiology **155:**1-8.

176. **Kobayashi K, Sudiarta IP, Kodama T, Fukushima T, Ara K, Ozaki K, Sekiguchi J.** 2012. Identification and characterization of a novel polysaccharide deacetylase C (PdaC) from Bacillus subtilis. J Biol Chem **287:**9765-9776.
177. **Ogura M, Yamaguchi H, Yoshida K, Fujita Y, Tanaka T.** 2001. DNA microarray analysis of Bacillus subtilis DegU, ComA and PhoP regulons: an approach to comprehensive analysis of B.subtilis two-component regulatory systems. Nucleic Acids Res **29:**3804-3813.
178. **Derbise A, Pierre F, Merchez M, Pradel E, Laouami S, Ricard I, Sirard JC, Fritz J, Lemaitre N, Akinbi H, Boneca IG, Sebbane F.** 2013. Inheritance of the lysozyme inhibitor Ivy was an important evolutionary step by Yersinia pestis to avoid the host innate immune response. J Infect Dis **207:**1535-1543.
179. **Austin CM, Maier RJ.** 2013. Aconitase-mediated posttranscriptional regulation of Helicobacter pylori peptidoglycan deacetylase. J Bacteriol **195:**5316-5322.
180. **Vanderkelen L, Ons E, Van Herreweghe JM, Callewaert L, Goddeeris BM, Michiels CW.** 2012. Role of lysozyme inhibitors in the virulence of avian pathogenic Escherichia coli. PLoS One **7:**e45954.
181. **Markart P, Faust N, Graf T, Na CL, Weaver TE, Akinbi HT.** 2004. Comparison of the microbicidal and muramidase activities of mouse lysozyme M and P. Biochem J **380:**385-392.
182. **Berche P.** 1995. Bacteremia is required for invasion of the murine central nervous system by Listeria monocytogenes. Microb Pathog **18:**323-336.
183. **Wang G, Lo LF, Forsberg LS, Maier RJ.** 2012. Helicobacter pylori peptidoglycan modifications confer lysozyme resistance and contribute to survival in the host. MBio **3:**e00409-00412.
184. **Balomenou S, Fouet A, Tzanodaskalaki M, Couture-Tosi E, Bouriotis V, Boneca IG.** 2013. Distinct functions of polysaccharide deacetylases in cell shape, neutral polysaccharide synthesis and virulence of Bacillus anthracis. Mol Microbiol **87:**867-883.
185. **Walter P, Blobel G.** 1982. Signal recognition particle contains a 7S RNA essential for protein translocation across the endoplasmic reticulum. Nature **299:**691-698.
186. **Gorke B, Vogel J.** 2008. Noncoding RNA control of the making and breaking of sugars. Genes Dev **22:**2914-2925.
187. **Gruber AR, Lorenz R, Bernhart SH, Neubock R, Hofacker IL.** 2008. The Vienna RNA websuite. Nucleic Acids Res **36:**W70-74.
188. **Geissmann T, Chevalier C, Cros MJ, Boisset S, Fechter P, Noirot C, Schrenzel J, Francois P, Vandenesch F, Gaspin C, Romby P.** 2009. A search for small noncoding RNAs in Staphylococcus aureus reveals a conserved sequence motif for regulation. Nucleic Acids Res **37:**7239-7257.
189. **Papenfort K, Pfeiffer V, Lucchini S, Sonawane A, Hinton JC, Vogel J.** 2008. Systematic deletion of Salmonella small RNA genes identifies CyaR, a conserved CRP-dependent riboregulator of OmpX synthesis. Mol Microbiol **68:**890-906.
190. **Tjaden B.** 2008. TargetRNA: a tool for predicting targets of small RNA action in bacteria. Nucleic Acids Res **36:**W109-113.
191. **Dubrac S, Msadek T.** 2004. Identification of genes controlled by the essential YycG/YycF two-component system of Staphylococcus aureus. J Bacteriol **186:**1175-1181.
192. **Koseoglu VK, Heiss C, Azadi P, Topchiy E, Guvener ZT, Lehmann TE, Miller KW, Gomelsky M.** 2015. Listeria monocytogenes exopolysaccharide: origin, structure, biosynthetic machinery and c-di-GMP-dependent regulation. Mol Microbiol.
193. **Chen LH, Koseoglu VK, Guvener ZT, Myers-Morales T, Reed JM, D'Orazio SE, Miller KW, Gomelsky M.** 2014. Cyclic di-GMP-dependent signaling pathways in the pathogenic Firmicute Listeria monocytogenes. PLoS Pathog **10:**e1004301.
194. **Ross P, Mayer R, Benziman M.** 1991. Cellulose biosynthesis and function in bacteria. Microbiol Rev **55:**35-58.

195. **Cywes-Bentley C, Skurnik D, Zaidi T, Roux D, Deoliveira RB, Garrett WS, Lu X, O'Malley J, Kinzel K, Rey A, Perrin C, Fichorova RN, Kayatani AK, Maira-Litran T, Gening ML, Tsvetkov YE, Nifantiev NE, Bakaletz LO, Pelton SI, Golenbock DT, Pier GB.** 2013. Antibody to a conserved antigenic target is protective against diverse prokaryotic and eukaryotic pathogens. Proc Natl Acad Sci U S A **110:**E2209-2218.
196. **Benachour A, Ladjouzi R, Le Jeune A, Hebert L, Thorpe S, Courtin P, Chapot-Chartier MP, Prajsnar TK, Foster SJ, Mesnage S.** 2012. The lysozyme-induced peptidoglycan N-acetylglucosamine deacetylase PgdA (EF1843) is required for Enterococcus faecalis virulence. J Bacteriol **194:**6066-6073.
197. **Plumbridge J, Bossi L, Oberto J, Wade JT, Figueroa-Bossi N.** 2014. Interplay of transcriptional and small RNA-dependent control mechanisms regulates chitosugar uptake in Escherichia coli and Salmonella. Mol Microbiol **92:**648-658.
198. **Feng DF, Cho G, Doolittle RF.** 1997. Determining divergence times with a protein clock: update and reevaluation. Proc Natl Acad Sci U S A **94:**13028-13033.
199. **Nielsen JS, Larsen MH, Lillebaek EM, Bergholz TM, Christiansen MH, Boor KJ, Wiedmann M, Kallipolitis BH.** 2011. A small RNA controls expression of the chitinase ChiA in Listeria monocytogenes. PLoS One **6:**e19019.
200. **Miyakoshi M, Chao Y, Vogel J.** 2015. Cross talk between ABC transporter mRNAs via a target mRNA-derived sponge of the GcvB small RNA. EMBO J.
201. **Mellin JR, Cossart P.** 2012. The non-coding RNA world of the bacterial pathogen Listeria monocytogenes. RNA Biol **9:**372-378.
202. **Quereda JJ, Ortega AD, Pucciarelli MG, Garcia-Del Portillo F.** 2014. The Listeria Small RNA Rli27 Regulates a Cell Wall Protein inside Eukaryotic Cells by Targeting a Long 5'-UTR Variant. PLoS Genet **10:**e1004765.
203. **Kun X, Qingling M, Qiao J, Yelong P, Tianli L, Cheng C, Yu M, Zhengxiang H, Xuepeng C, Chuangfu C.** 2014. Impact of rli87 gene deletion on response of Listeria monocytogenes to environmental stress. FEMS Microbiol Lett **359:**50-54.
204. **Peng YL, Meng QL, Qiao J, Xie K, Chen C, Liu TL, Hu ZX, Ma Y, Cai XP, Chen CF.** 2014. The roles of noncoding RNA Rli60 in regulating the virulence of Listeria monocytogenes. J Microbiol Immunol Infect.
205. **Valentin-Hansen P, Eriksen M, Udesen C.** 2004. The bacterial Sm-like protein Hfq: a key player in RNA transactions. Mol Microbiol **51:**1525-1533.
206. **Rabhi M, Espeli O, Schwartz A, Cayrol B, Rahmouni AR, Arluison V, Boudvillain M.** 2011. The Sm-like RNA chaperone Hfq mediates transcription antitermination at Rho-dependent terminators. EMBO J **30:**2805-2816.
207. **Christiansen JK, Larsen MH, Ingmer H, Sogaard-Andersen L, Kallipolitis BH.** 2004. The RNA-binding protein Hfq of Listeria monocytogenes: role in stress tolerance and virulence. J Bacteriol **186:**3355-3362.
208. **Sittka A, Lucchini S, Papenfort K, Sharma CM, Rolle K, Binnewies TT, Hinton JC, Vogel J.** 2008. Deep sequencing analysis of small noncoding RNA and mRNA targets of the global post-transcriptional regulator, Hfq. PLoS Genet **4:**e1000163.
209. **Sherris D, Parkinson JS.** 1981. Posttranslational processing of methyl-accepting chemotaxis proteins in Escherichia coli. Proc Natl Acad Sci U S A **78:**6051-6055.
210. **Tanaka Y, Fujii S, Hiroaki H, Sakata T, Tanaka T, Uesugi S, Tomita K, Kyogoku Y.** 1999. A'-form RNA double helix in the single crystal structure of r(UGAGCUUCGGCUC). Nucleic Acids Res **27:**949-955.
211. **Sousa SA, Ramos CG, Moreira LM, Leitao JH.** 2010. The hfq gene is required for stress resistance and full virulence of Burkholderia cepacia to the nematode Caenorhabditis elegans. Microbiology **156:**896-908.

212. **Kulesus RR, Diaz-Perez K, Slechta ES, Eto DS, Mulvey MA.** 2008. Impact of the RNA chaperone Hfq on the fitness and virulence potential of uropathogenic Escherichia coli. Infect Immun **76:**3019-3026.
213. **Sonnleitner E, Hagens S, Rosenau F, Wilhelm S, Habel A, Jager KE, Blasi U.** 2003. Reduced virulence of a hfq mutant of Pseudomonas aeruginosa O1. Microb Pathog **35:**217-228.
214. **Sittka A, Pfeiffer V, Tedin K, Vogel J.** 2007. The RNA chaperone Hfq is essential for the virulence of Salmonella typhimurium. Mol Microbiol **63:**193-217.
215. **Schumacher MA, Pearson RF, Moller T, Valentin-Hansen P, Brennan RG.** 2002. Structures of the pleiotropic translational regulator Hfq and an Hfq-RNA complex: a bacterial Sm-like protein. EMBO J **21:**3546-3556.
216. **Sauter C, Basquin J, Suck D.** 2003. Sm-like proteins in Eubacteria: the crystal structure of the Hfq protein from Escherichia coli. Nucleic Acids Res **31:**4091-4098.
217. **Kim HH, Lee BJ, Kwon AR.** 2010. Expression, crystallization, and preliminary X-ray crystallographic analysis of putative SpoVG from Staphylococcus aureus. Arch Pharm Res **33:**1285-1288.
218. **Someya T, Baba S, Fujimoto M, Kawai G, Kumasaka T, Nakamura K.** 2012. Crystal structure of Hfq from Bacillus subtilis in complex with SELEX-derived RNA aptamer: insight into RNA-binding properties of bacterial Hfq. Nucleic Acids Res **40:**1856-1867.
219. **Kondoh H, Ball CB, Adler J.** 1979. Identification of a methyl-accepting chemotaxis protein for the ribose and galactose chemoreceptors of Escherichia coli. Proc Natl Acad Sci U S A **76:**260-264.
220. **Kehry MR, Dahlquist FW.** 1982. The methyl-accepting chemotaxis proteins of Escherichia coli. Identification of the multiple methylation sites on methyl-accepting chemotaxis protein I. J Biol Chem **257:**10378-10386.
221. **Silverman M, Simon M.** 1977. Chemotaxis in Escherichia coli: methylation of che gene products. Proc Natl Acad Sci U S A **74:**3317-3321.
222. **Lukat GS, Stock JB.** 1993. Response regulation in bacterial chemotaxis. J Cell Biochem **51:**41-46.
223. **Mink SN, Kasian K, Jacobs H, Cheng ZQ, Light RB.** 2008. N,N'-diacetylchitobiose, an inhibitor of lysozyme, reverses myocardial depression and lessens norepinephrine requirements in Escherichia coli sepsis in dogs. Shock **29:**681-687.
224. **Mraheil MA, Billion A, Kuenne C, Pischimarov J, Kreikemeyer B, Engelmann S, Hartke A, Giard JC, Rupnik M, Vorwerk S, Beier M, Retey J, Hartsch T, Jacob A, Cemic F, Hemberger J, Chakraborty T, Hain T.** 2010. Comparative genome-wide analysis of small RNAs of major Gram-positive pathogens: from identification to application. Microb Biotechnol **3:**658-676.
225. **Jinek M, Chylinski K, Fonfara I, Hauer M, Doudna JA, Charpentier E.** 2012. A programmable dual-RNA-guided DNA endonuclease in adaptive bacterial immunity. Science **337:**816-821.
226. **Qi LS, Larson MH, Gilbert LA, Doudna JA, Weissman JS, Arkin AP, Lim WA.** 2013. Repurposing CRISPR as an RNA-guided platform for sequence-specific control of gene expression. Cell **152:**1173-1183.
227. **Fu J, Kanne DB, Leong M, Glickman LH, McWhirter SM, Lemmens E, Mechette K, Leong JJ, Lauer P, Liu W, Sivick KE, Zeng Q, Soares KC, Zheng L, Portnoy DA, Woodward JJ, Pardoll DM, Dubensky TW, Jr., Kim Y.** 2015. STING agonist formulated cancer vaccines can cure established tumors resistant to PD-1 blockade. Sci Transl Med **7:**283ra252.
228. **Camilli A, Tilney LG, Portnoy DA.** 1993. Dual roles of plcA in Listeria monocytogenes pathogenesis. Mol Microbiol **8:**143-157.
229. **Hodgson DA.** 2000. Generalized transduction of serotype 1/2 and serotype 4b strains of Listeria monocytogenes. Mol Microbiol **35:**312-323.

230. **Langmead B, Salzberg SL.** 2012. Fast gapped-read alignment with Bowtie 2. Nat Methods **9:**357-359.
231. **Li H, Handsaker B, Wysoker A, Fennell T, Ruan J, Homer N, Marth G, Abecasis G, Durbin R.** 2009. The Sequence Alignment/Map format and SAMtools. Bioinformatics **25:**2078-2079.
232. **Girardin SE, Boneca IG, Viala J, Chamaillard M, Labigne A, Thomas G, Philpott DJ, Sansonetti PJ.** 2003. Nod2 is a general sensor of peptidoglycan through muramyl dipeptide (MDP) detection. J Biol Chem **278:**8869-8872.
233. **McDonald KL.** 2014. Out with the old and in with the new: rapid specimen preparation procedures for electron microscopy of sectioned biological material. Protoplasma **251:**429-448.
234. **Durack J, Burke TP, Portnoy DA.** 2015. A prl Mutation in SecY Suppresses Secretion and Virulence Defects of Listeria monocytogenes secA2 Mutants. J Bacteriol **197:**932-942.
235. **Carlson HK, Kuehl JV, Hazra AB, Justice NB, Stoeva MK, Sczesnak A, Mullan MR, Iavarone AT, Engelbrektson A, Price MN, Deutschbauer AM, Arkin AP, Coates JD.** 2014. Mechanisms of direct inhibition of the respiratory sulfate-reduction pathway by (per)chlorate and nitrate. ISME J.